A gene regulatory network of vertebrate retina development

by

Maryam Hejazi

A thesis submitted in partial fulfillment of the requirements for the degree of

Doctor of Philosophy

Medical Sciences - Medical Genetics
University of Alberta

Abstract

Gene regulatory networks (GRN) play a central role in the specification, differentiation and function of the central nervous system (CNS) during development. During vertebrate retinal development, six types of neural cells and one type of glial cell are specified in a temporal order from a pool of multipotent retinal progenitor cells (RPC). There has been extensive research on the competence model of retinal development. An attractive hypothesis explains that RPCs follow through a series of competent states, which are intrinsically regulated, and thus cell fate choices are intrinsically defined. There are transcriptional and translational differences between progenitor cells at different stages of development, which make RPC populations heterogeneous at different time points of development. Transcription factors (TFs) are one of the intrinsic factors that drive the RPC towards various cell fates. TFs regulate each other in a transcriptional regulatory network to alter RPC competency and drive them towards becoming various specialized cell types (Cepko et al., 2014).

We were interested in GRN of the *distal-less* homedomain TF DLX family in the development of the vertebrate retina. *Dlx1/Dlx2* double knock out (DKO) mice die at birth with multiple congenital anomalies (Anderson, Qiu, et al., 1997). We have assessed the retinal phenotype in the *Dlx1/Dlx2* DKO mice. At post-natal day 0 (P0), there is a reduced amount of retinal ganglion cells (RGCs) (33%) and decreased *Brn3a* and *Brn3b* (RGC markers) expression in the ganglion cell layer (GCL) (de Melo et al., 2005). Of significance, there is increased and ectopic expression of *Crx,* supporting an alternative cell fate in the *Dlx1/Dlx2* null retina (de Melo et al., 2005). In addition, *Dlx2* expression is highest in early differentiation (embryonic day 13/E13) and later during adulthood (de Melo et al., 2003). This might explain the involvement of *Dlx2* in early RPC fate specification and later for RGC maintenance. Based on my results, I suggested a possible GRN of *Dlx2/Crx/miR-124* in the determination of RGC cell fate with

concomitant repression of photoreceptor (PR) differentiation at E18. I also suggested, that *Dlx2* may have a temporal function working with *Otx2* in retinal progenitor cells (RPC) at E13.

Unlike the mouse, there have not been any studies on the expression and function of *dlx* genes in the zebrafish eye during development or in adulthood. Based on our lab's preliminary data, we did not find *dlx* gene family expression in the zebrafish eye, limiting further study of their role in zebrafish eye development. During evolution of the zebrafish, *dlx* gene orthologue expression appears to be lost in the zebrafish retina, but their expression and function is conserved in the forebrain and pharyngeal arches. However, the absence or the low levels of endogenous expression of *dlx* genes might assist us in studying its function by expressing one of the mice *Dlx* genes in the zebrafish eye during embryogenesis. Thus, I investigated the role of *Dlx* genes in the eye during evolution by expressing mouse *Dlx2* in the zebrafish eye. I generated mouse *Dlx2* transgenic retina *Tg[rx3:Dlx2]* of zebrafish to further investigate *Dlx* gene expression and function in the retina during vertebrate evolution.

Retinal vasculature development is also critical for ocular development, and its developmental process is tightly connected with retinal neuronal development (Paredes et al., 2018). Neuropilin family member are critical for vascular, cardiovascular, and neuronal development (Kawasaki et al., 1999). While there have been a few reports regarding *Nrp1's* role during retinal vasculature development, very little is known about the role of *Nrp2* during eye development (Pellet-Many et al., 2008). *Nrp2* expression was observed in the choroid and hyaloid vessels starting at early retinal development, and in the RGC during later developmental stages. We demonstrated *Nrp2's* critical role in retinal neurovascular development, as retina structure and physiology of adult mice was disrupted in *Nrp2* KO mice. We also demonstrated the possible connection between neuronal and vasculature development, as retinal neuronal cell

expression was changed in *Nrp2* KO mice. Collectively, my research has contributed to a better understanding of some of the mechanisms underlying vertebrate retinal development.

Preface

Chapter 3 contains primarily original unpublished work carried out by Maryam Hejazi. The X-gal staining (Figure 3.6A-F) was performed by Mehdi Eshraghi.

Chapter 4 contains primarily original unpublished work carried out by Maryam Hejazi. This work has been done in collaboration with Dr. W. Ted Allison's lab.

Chapter 5 contains primarily original unpublished work carried out by Maryam Hejazi and Pranidhi Baddam in collaboration with Dr. Daniel Graf's lab. The H&E staining (Figure 5.3) was performed by Pranidhi Baddam and Dr. Jamie Zagozewski. The ERG data analysis was performed by Dr. Yves Sauvé (Figure 5.7).

Permissions for use of figures adapted in this thesis were obtained from the copyright clearance center and publisher for Figures 1.1 and 3.1..

Acknowledgements

Firstly, I would like to thank my supervisor Dr. David Eisenstat. Your continuous guidance and support throughout my PhD program paved the way for my success. I am extremely grateful that you gave me the chance to join your team, and I am thankful for all the training and opportunities along the way. I also would like to express my gratitude for supporting me through the hard times that I experienced a few years back. I could not have imagined a better advisor for my PhD program, and I always will be thankful to you as my first mentor in Canada. THANK YOU

Next, I would like to thank my supervisory committee. First, Dr. Fred Berry for your great scientific insights and advice whenever I asked for it. I also would like to thank Dr. Berry for challenging me throughout my PhD program, and teaching me to always reach higher. I am extremely grateful to have Dr. William Ted Allison for not just being a great scientific support but also for being an exceptional person. I am specifically thankful to him for giving me the chance to collaborate with his lab to learn new techniques and step up my science knowledge using the zebrafish model system.

Thank you to the members of my Ph.D examining committee. I am thankful to Dr. Jennifer Hocking for serving on my defense committee and challenging me during the oral defense. Thank you to my external examiner Dr. Marc Ekker from the University of Ottawa for not only serving on my defense committee but also for kindly providing me with Zebrafish *dlx* plasmids several years ago.

I would like to acknowledge my fellow labmates past and present: Jamie Zagozewski for training me during my first few years, Sara Japoni for being a great friend and support during my program, Xiaohua Song for being an exceptional technician and supporting all of us all the time, Qiang Jiang for answering my scientific questions, Hunter McColl for helping out on *Nrp2* genotyping problems, Mikaela Nevin and Zixuan Li for supporting me with all the genotyping during my PhD thesis writing and defense period, and Sara Moradipour for being my best friend in the lab. I am extremely grateful for being part of this lab with many great people, which all supported me during one of the most difficult times in my life.

Thanks to all the staff, professors and colleagues in Department of Medical Genetics for making the department a fun and safe place to spend my time every day. Special thanks to Dr. Mike Walter, chair of the department for not only being a great mentor, but also being a graduate students' friend, and someone who I could go with my problems. I am thankful to Dr. Sarah Hughes as the department's graduate student coordinator who sincerely cared about graduate student wellbeing.

I made so many best friends for life during my PhD program, and I am extremely grateful for meeting every single one of them. Thank you to Ping Wee, Fahed Ellian and Vanessa Carias for simply being my friends.

I would like to thank my parents and my only sister for always being there for me no matter what. My mom, who has always been my role model, is a lovely and kind person, and my dad, who was my cheer leader, helped to push my boundaries all the time and encouraged me to come to Canada and enter graduate school. I always keep carrying on his memories. To my sister and best friend during all of my life: I can rely on her for anything.

Lastly, I am deeply grateful to my husband and best friend. Your continuous support and love got me here. I am looking forward to achieving many successes together with you....

THANK YOU

Table of Contents

List of tables

List of figures

List of Abbreviation

AMD	Age-related macular degeneration
bHLH	Basic helix loop helix
Bp	Base pair
cDNA	Complementary deoxyribonucleic acid
cGMP	cyclic guanosine monophosphate
ChIP	Chromatin immunoprecipitation
CKO	Conditional knockout
CNS	Central nervous system
Crx	cone rod homeobox
DAPI	4′,6-diamidine-2-phenylindole
DKO	Double knockout
Dlx2	Distal-less homeobox (gene)
DLX2	Distal-less homeobox (protein)
dlx2	Distal-less homeobox (zebrafish)
DMEM	Dulbecco's modified Eagle's medium
DNA	Deoxyribonucleic acid
E-coli	Escherichia coli
EFTF	Eye field transcription factors
EMSA	Electromobility shift assay
GAD	Glutamate decarboxylase
GAPDH	Glyceraldehyde 3-phosphate dehydrogenase
GCL	Ganglion cell layer
GDF	Guanosine diphosphate
gDNA	Genomic deoxyribonucleic acid
GFP	Green fluorescent protein

GOF	Gain of function
GRN	Gene regulatory network
H&E	Hematoxylin and eosin
INL	Inner nuclear layer
IPL	Inner plexiform layer
NBL	Neuroblastic layer
Nrp1	Neuropilin-1
Nrp2	Neuropilin-2
ON	Overnight
OCT	Optical coherence tomography
OCT	Optimal cutting temperature compound
ONL	Outer nuclear layer
OPL	Outer plexiform layer
Otx2	Orthodenticle homeobox 2
PBS	Phosphate buffered saline
PCR	Polymerase chain reaction
PFA	Paraformaldehyde
PR	Photoreceptor
PTU	1-phenyl 2-thiourea
qRT-PCR	Quantitative real-time polymerase chain reaction
rDLX2	Recombinant DLX2 protein
RGC	Retina ganglion cell
RNA	Ribonucleic acid
RPC	Retinal progenitor cell
RPE	Retinal pigmented epithelium
RPM	Rotation per minute
RT	Room temperature

Shh	Sonic hedgehog
SVZ	Subventricular zone
TF	Transcription factor
VEGF	Vascular endothelial growth factor
VZ	Ventricular zone
WT	Wild type
αDLX2	High affinity polyclonal DLX2 antibody

1 Chapter 1. General Introduction

1.1 Gene Regulatory Networks

The body plan and morphology of different species are unique to that specific species, which is determined during embryonic development. Gene regulatory networks (GRNs) control various aspects of embryonic development, temporally and spatially. GRNs specify the body plan, regulate organ formation, and essentially control the entire process of development. GRNs are networks of genes and their interactions and they are composed of transcription factors (TFs), promoters, *cis*-regulatory elements, non-coding RNAs, and many other elements (Davidson et al., 2002; Yuh, Bolouri, & Davidson, 2001) Development proceeds as a progression of various states of spatially and temporally defined regulatory gene expression. Through this progression, specification occurs, and cells in various parts of the developing animal come to express a given set of genes which assign diverse cellular functions. In other words, a GRN is a set of multiple connected regulatory genes that interact with each other to perform specific operations and regulate specific cell fates, which is critical for development (Davidson et al., 2002; Yuh et al., 2001). The genomic components of GRNs are the genes encoding the effectors and regulators. Regulatory genes may play dual roles in the network; while upstream gene regulation controls the expression and transcriptional input of regulatory genes, regulatory proteins simultaneously provide regulatory input for downstream target gene expression (Zuber, Gestri, Viczian, Barsacchi, & Harris, 2003). Figure1.1 is a simple GRN with three nodes: gene 1, gene 2, and gene 3. In this network the transcription factor, “protein 1”, a product of “gene 1” binds to the regulatory target site of “gene 2” to promote its expression and produce “protein 2” (Figure 1.1). “Protein 1” in combination with “protein 2” binds to the promoter of “gene 3” to induce its expression (Figure 1.1) (Van Anh Huynh-Thu & Guido Sanguinetti, 2019). During development

thousands of GRNs work in a complex spatiotemporal patterning process to give rise to various cell types. Transcription has been known as a major control point in gene expression. Transcription factors with sequence specific binding sites play a central role in gene expression regulation and build various GRNs in a cell-type specific pattern (Wilkinson et al, 2017)

TFs are an important part of the GRN which directly or indirectly interprets, regulates and controls gene expression during development and adulthood. Genes encoding transcription factors are typically activated at various times and in many cells during the life cycle, and so the uniqueness of any given developmental GRN lies in its operative *cis*-regulatory modules. They can directly or indirectly bind to DNA regulatory elements through their sequence-specific binding domains. The DNA binding domain structure provides the TF with specific properties to interact with distinct DNA sequences on the gene promoter. For instance, the homeobox TFs canonically bind to core tetranucleotide TAAT/ATTA motifs, located at DNA promoters or DNA regulatory elements to regulate target gene expression. Initially, the study of *Hox* genes revealed the various roles of transcription factors in GRNs. It was shown that *Drosophila Hox* genes, which are located in two gene clusters, determine the identity of each segment of the *Drosophila* in the embryo's body plan, and individual mutations of *Hox* genes result in homeotic transformations (Pavlopoulos & Akam, 2007). These *Hox* genes are highly conserved throughout evolution and have a similar function in mammals. The activation of *Hox* genes in the mouse follows a temporal sequence that correlates with the gene's position within the cluster (temporal collinearity), which leads to a corresponding distribution of each gene along the body axis. They act as switches which activate or repress GRN patterning in a subset of the body plan. *Hox* gene studies revealed that TFs can regulate their own expression, and the expression of other TFs by building a complex and dynamic regulatory network.

One of the earliest examples of GRN research was on the *Endo16* gene, which encodes a polyfunctional protein that is secreted into the extracellular matrix at early stages of embryonic development in sea urchins. *Endo16* is expressed in early progenitor endomesoderm, and later becomes restricted to mid-gut cells (Turner & Cepko, 1987 Britten, & Davidson, 1994). The *Endo16* regulatory network turns out to be a precise and complex way to set the boundaries of expression. Two different regulatory modules control its early and late expression, and within these regulatory regions, several transcription binding sites have been mapped. Each module has a functional role in interacting with a specific TF (Yuh, Bolouri, & Davidson, 1998). These interactions are temporally and spatially controlled; for instance, the major early activator of the *Endo16* gene is an *Otx* family gene, which is expressed during mid-cleavage of the vegetal plate of the embryo and binds to a specific part of *Endo16* promoter (module A). However, *Endo16* gene expression has to be specified to the vegetal plate at this time, hence another TF acts as a repressor and binds to other promoter regions (module F and E) to prevent *Endo16* expression in the overlying ectodermal domains (Yuh et al., 2001). When sea urchin embryos were injected with *Endo16* morpholinos, the vegetal plate failed to invaginate during gastrulation leading to a lack of skeletal patterning, and the embryo did not survive 72 hours post fertilization (Yuh et al., 2001).

The regulatory network of the homeobox TFs is complex. For instance, *Dlx1/Dlx2* and *Brn3b* act in parallel but in a cross-regulatory pathway to determine and maintain retinal ganglion cell (RGC) fate during mouse retinogenesis. While *Atoh7* is required to initiate the RGC differentiation by activating *Dlx1/Dlx2* and *Brn3b*, *Dlx1/Dlx2* cross-regulates *Brn3b* expression to maintain the differentiation and survival of RGCs (Q. Zhang et al., 2017). Recent improvements in computational modeling of genes regulatory interactions are helping us with the

understanding of whole system operations; however, the complex nature of GRN still leave so many questions in terms of their function and regulation to be answered. This thesis contributes to further our understanding of the *Dlx* gene regulatory network to shed light on the retinal neuronal cell specification process during ocular development.

1.2 Ocular development

Ocular development is part of forebrain development. Shortly after gastrulation, the eye field starts to form in the medial anterior neural plate of the developing diencephalon. The bilateral optic vesicles then evaginate from the forebrain and extend to contact the surface ectoderm. As a result, the ectoderm and optic vesicle start to fold and invaginate to become the optic cup. The optic cup forms a bilayer structure where the inner layer gives rise to the neural retina and the outer layer becomes retinal pigment epithelium (RPE). The surface ectoderm induces the lens placode which later becomes the lens vesicle, which buds off from the rest of the ectoderm and eventually becomes the lens. Neural retinal progenitor cells give rise to all major mature retinal cell types (Jadhav, Cho, & Cepko, 2006).

A majority of TFs and signaling pathways are involved in mammalian ocular development as part of many GRNs. The establishment of the eye field requires a Wnt/β-catenin signaling gradient, by which it establishes anterior-posterior patterning of the eye field. The expression of eye field TFs establishes a genetic network which inhibits bone morphogenic protein (BMP), Nodal, and Wnt/β-catenin signaling in the anterior neural plate concomitantly (Fuhrmann, 2008). Studies showed that a network, known as the eye field transcription factors (EFTFs), which are highly conserved throughout the vertebrates, further induces eye field

formation. The EFTFs *ET, Pax6, Six3, Optx2, Lhx2*, and *Rax* (Zuber et al., 2003) are expressed in the area of the anterior neural plate where the eye field starts to form. Mutations in any of these genes leads to abnormal eye development (Martinez-De Luna, 2011; Chow et al., 1999; Porter et al.,1997; Reese, 2011; Loosli et al., 1999). Moreover, the coordinated overexpression of EFTFs in *Xenopus* embryos is sufficient to produce a secondary eye field (Zuber et al., 2003). *Otx2* and the neuronal inducer *Noggin* are the master regulators upstream of EFTFs. They initiate the whole process of neural induction and midbrain specification, which subsequently induces the EFTF network, and eye field specification. EFTFs have an extended proliferative property to produce a sufficient progenitor pool for all retina cell type differentiation. *Otx2* promotes *Rax* expression in neural ectoderm in cooperation with *Sox2* in the anterior neural ectoderm (Danno et al., 2008). *Rax* is required for *Lhx2, Pax6*, and *Six3* activation, which leads to the regionalization of optic vesicles along its axis. *Pax6* is a key regulator to establish optic cup/optic stalk boundaries during ocular development through reciprocal control of *Pax2* expression (Schwarz et al., 2000). *Pax6* null mice show a complete absence of the eyes. *Pax6* is upstream of *Atoh7* and neurogenin2 (*Ngn2)* in retinal progenitor cells, which are required for neurogenesis and specification of RGC (Wang et al., 2001). *Pax6* maintains the multipotency of RPCs, and loss of RPC competency in the absence of *Pax6* can be due to the loss of *Atoh7* and *Ngn2* expression. Along with *Pax6, Rax* is also required for maintaining RPC, and *Rax* null mouse and zebrafish *rx3* mutant do not develop eyes (Loosli et al., 2003). *Lhx2* is essential for regionalization and patterning of the optic neuroepithelium, as the loss of *Lhx2* in the eye leads to regionalization failure in the optic vesicle (Yun et al., 2009). *Lhx2* null mice eye field specification occurs, but the development of optic cup formation fails in both the optic neuroepithelium and lens ectoderm (Yun et al., 2009).

As mentioned above, both eyes arise from a single eye field that is divided into two eyes. The main players of this process are sonic hedgehog (*Shh*) and *Six3*. *Shh* is expressed in the ventral forebrain and prechordal mesoderm, *Six3* is present in the anterior neural ectoderm and later in the eye field. The expression of *Shh* in prechordal mesoderm activates *Six3* expression which inhibits the posteriorizing activity of *Wnt1* in the anterior neural ectoderm (Lagutin et al., 2003). The loss of either *Shh* or *Six3* in mice induces holoprosencephaly with cyclopia and formation of only one eye. *Vsx2* expression found in the distal optic vesicle by E9.5, promoting pattern formation in the neural retina, and the *Mitf* TF specifies the RPE. The antagonistic relation of *Mitf* and *Vsx2* leads to boundary establishment between the neural retina (NR) and the RPE. Following the expression of *Vsx2, Mitf* becomes downregulated distally in the optic vesicle. Mice with *Mitf* loss of function shows conversion from NR to RPE (Nguyen & Arnheiter, 2000). Fibroblast growth factor (FGF) signaling in the surface ectoderm also induces neural retina identity, as its removal from ectoderm results in the conversion of the eye cup to RPE in the mouse (Nguyen & Arnheiter, 2000). The lens forms simultaneously with optic vesicle formation in surface ectoderm. The thickening of surface ectoderm and its invagination forms the lens cup, and eventually the lens vesicle. *Pax6, Six3,* and *Sox2* are the master regulators of lens development. *Six3* activates *Sox2* and *Pax6* expression which leads to surface ectoderm thickening. BMP signaling gradient is present during lens development to activate downstream targets (*Pax6* and *Sox2*) (Wawersik et al., 1999). *Prox1* plays a critical role in lens development; its expression has been found in the lens placode at E9.5, and later in lens vesicles and lens fibres (Wigle, Chowdhury, Gruss, & Oliver, 1999). The *Prox1* mutant mouse dies embryonically with abnormal lens differentiation, due to downregulation of cell cycle inhibitors, *p27KIP1* and *p57KIP2*. This abnormal lens differentiation is a result of failed polarization and elongation of

the lens. Following lens formation, detachment of the surface ectoderm gives rise to the corneal epithelium. Later the outer lips of the optic cup goes through a series of transformations to form the iris and ciliary body (Davis-Silberman & Ashery-Padan, 2008).

1.3 Retinogenesis

1.3.1 Retinal Progenitor Cells

For generations, the eye has offered an easy and accessible model to study tissue development and morphogenesis of diverse cell types. The vertebrate retina has been a great tool to study the mechanism of cell fate determination during development. One of the key questions related to vision formation is how various retinal cells are generated from one type of neuronal progenitor cells during development. This process happens during retinogenesis as part of central nervous system (CNS) development. Six classes of neuronal cells and one class of glial cell form the three nuclear layers which are separated by two plexiform layers in the vertebrate retina (Zuber et al., 2003). The temporal birth order of retinal cells is highly conserved across vertebrate species. During prenatal development in mice, retinogenesis starts around E10 and RGC are the first class of neuronal cells to form, followed by horizontal cells, cones, and amacrine cells. Rods, bipolar cells, and Muller glia differentiation is initiated prenatally and continue to post-natal day 12 (P12) when all of the retinal layers are formed (Wilson & Houart, 2004). These retinal neuronal cells build a network that achieves the task of image detection, processing, and transmission in a manner similar to other parts of the CNS.

All the differentiated retinal cell types originate from retinal progenitor cells (RPC) during retina development. RPC are a multipotent group of cells which temporally become restricted by the regulatory intrinsic and extrinsic factors to give rise to various distinct type of cells. These regulatory molecules or pathways build genetic networks of particular genes to determine the fate or behaviour of RPC. Individual RPC pass through symmetric and asymmetric divisions to self-renew and generate postmitotic cells, respectively. The distinct postmitotic daughter cells designate different competence states to drive a specific type of progeny at the

next round of division (Figure 1.2). When Cepko's group labelled rat RPC with retrovirus at E13-E14.5 to trace *Olig2*-expressing clones, they found that the clones derived from *Olig2*-expressing RPC were differentiated to cones and horizontal cells, and when *Olig2*-expressing RPC were targeted at P0-P3, other than a few clones comprised of amacrine cells, most clones were comprised of rod cells. Furthermore, they demonstrated that *Olig2*-expressing cone and horizontal cells can be driven from a common RPC pool (Turner & Cepko, 1987). *Cre*-fate mapping of several basic helix-loop-helix (bHLH) genes in the mouse suggested that the expression of these bHLH varies among RPC and might be correlated with the type of daughter cells that they produce. It has been suggested that the different cell types observed in the retina could originate from a common progenitor pool (Turner & Cepko, 1987). Progenitor cells remain multipotent during neurogenesis but have a preferable fate at each time point. The preference depends on the gene expression profiles which vary in a different population of RPC at different time points; in other words, retinal progenitor cells are a heterogeneous population intrinsically different in terms of their competence to generate specific cell types (C. L. Cepko, Austin, Yang, Alexiades, & Ezzeddine, 1996). The heterogeneity of RPC is not only due to the intrinsic cues but also to extrinsic cues, which are required for proper differentiation of retinal cells at specific time points (C. Cepko, 2014). These extrinsic factors, such as signaling pathways, transduce their signal via cell surface receptors to define the properties of RPC in correlation with TFs (Livesey & Cepko, 2001).

TFs play a significant role in RPC fate determination through interaction with each other, signaling pathways, microRNAs (miRNAs), and chromatin. TFs including members of the Homeobox, bHLH and forkhead box families build various gene networks that direct RPC to differentiate or attain their competency during development. Other than the transcriptional

programming of RPC, several other mechanisms such as RPC migration behaviour along the neuroblast layer and their dividing orientation plane are involved in retinal cell fate specification (Taverna & Huttner, 2010).

At certain stages of mice development (around E8), FGF signalling which is present in the ventral midline triggers a neurogenic switch to start retina development (Martinez-Morales et al., 2005). Once FGFs have induced retinogenesis, the process propagates through the entire retina. There are several key regulators of RPC development including *Pax6, Rax* and *Otx2*. The *Rax* homeodomain TF activates *Pax6* and *Otx2* in early eye development to specify RPC. *Pax6* maintains RPCs multipotency during later development stages. Along with *Pax6*, *Sox2* -a high mobility group-containing TF- is a key regulator of progenitor cell renewal. The expression of these two genes are inversely correlated, as PAX6 expression is lower and SOX2 expression is higher in the central neural retina where neurons differentiate, and PAX6 is higher, and SOX2 is lower in the retina periphery (Matsushima, Heavner, & Pevny, 2011). Shh pathway regulates *Sox2* expression by activating *Gli* transcription factors. *Gli2* activation is related to increased *Sox2* activity and reduced *Pax6* expression, which leads to the failure of key cell fate determination expression.

Notch signaling also maintains RPCs multipotency by inducing symmetric divisions in mice (Wall et al., 2009) and zebrafish (Scheer, Groth, Hans, & Campos-Ortega, 2001) retina. Notch maintains the progenitor cells in a proliferative, undifferentiated state by regulating HES proteins. *Hes1* is initially present in the optic vesicle and later in RPCs in the NR, *Hes1*-null mice fail to maintain the RPC proliferative state which leads to reduced eye size (Tomita et al., 1996). Upon activation of *Hes1* and *Hes5*, the transcription of retina specification neuronal genes such as *Ascl1*/*Mash1* and *Math3* becomes restricted to maintain the progenitor state. *Vsx2* is

another TF that prevents progenitor cells from becoming differentiated and maintaining the RPC pool during early stages of retina development. These networks maintain the presence of some progenitor pools until complete retinal maturation. Despite all available knowledge, there are many questions left to be answered regarding RPC competency shift to generate various types of neuronal cells in the retina. Several RPC competency models have been established; however, more research is required to determine if there is one dominant RPCs competency model or whether a few of these models could be involved in cell fate decisions simultaneously. There are also many questions left to be answered on how transcription factors are regulated by extrinsic cues at various times and places during the development.

1.3.2 Retinal Ganglion Cells

Retinal ganglion cells (RGC) are the first group of neuronal cells with their initial specification at E10.5 in the mouse embryo. The RPC population that expresses Atonal Homolog bHLH Transcription Factor 7 *(Atoh7)* during early retinal development predominantly becomes RGC in mice, and the ganglion cells were largely lost when *Atoh7* was deleted from the mouse retina (Kiyama et al., 2011). Therefore, the bHLH transcription factor *Atoh7* is one of the major players for early RGC differentiation, as its expression starts from the boundary between the optic stalk and the neural retina, and expands throughout the neural retina (Kiyama et al., 2011). It has been proposed that *Atoh7* promotes RGC versus amacrine cell specification by antagonizing *NeuroD* and *Math3;* however, additional genes such as *Pax6* may be required for RGC specification (Mao et al., 2013). *Pax6* is found to be an upstream regulator of *Atoth7* since *Pax6* $^{-/-}$ mice demonstrate a significant drop in *Atoh7* expression (Riesenberg et al., 2009). The *Brn3* family (POU-domain transcription factors) are proposed to be RGC fate regulators and as well, their expression has been found in postmitotic RGC. From E15 to adulthood, both *Brn3b*

and *Brn3a* expression have been detected in the majority of RGC (Moshiri et al., 2008). *Atoh7* positively regulates *Brn3b* expression; thus the *Atoh7-Brn3b* gene regulatory network induces early RGC fate by repressing other transcription factors such as *Dlx1/Dlx2, Otx2* and *Crx* (F. Qiu, Jiang, & Xiang, 2008). *Isl1* (*Islet-1*) from the LIM-homeodomain family and *Brn3b* co-expression are found in post-mitotic RGCs, where they are regulated in parallel by *Atoh7* (Pan, Deng, Xie, & Gan, 2008). RGC axons project out of the inner neuroblastic layer (INL) laterally, and this process requires precise regulation. *Isl2* (*Islet-2*) is required for the accurate lateral projection of RGC axons (Pak, Hindges, Lim, Pfaff, & O'Leary, 2004).

Dlx1/Dlx2 appear to be other ganglion cell fate determinants and survival factors in mice. It has been speculated that *Dlx1/Dlx2* and *Brn3b* function in parallel but a cross-regulatory pathway to promote RGC fate during retina development. *Atoh7-Dlx1/Dlx2-Brn3b* regulate RGC differentiation in a parallel transcriptional pathway with the *Atoh7-Brn3b/Isl1* network (Q. Zhang et al., 2017). I further investigated the mechanism of how *Dlx1/Dlx2* promotes RGC fate during various time points of retinal development. I proposed that *Dlx2* represses *Crx* and *Otx2* expression to promote RGC fate over PR fate at E18. We found DLX2 transcriptional regulation of *Crx* but not *Otx2* at E18. We found higher *Crx*-expressing cells in *Dlx1/Dlx2* DKO mice, which could mean that the negative transcriptional regulation of *Crx* by DLX2 is sufficient to promote RGCs over PR cells at E18.

1.3.3 Amacrine and Horizontal cells

Amacrine cells are one class of neuronal cells located in the INL along with horizontal and bipolar cells; their axons are connected with RGC axons through the inner plexiform layer (IPL). Although the bHLH genes *NeuroD* and *Math3* are required for amacrine cell development, individual mutations of either gene are not sufficient for the complete absence of

amacrine cells. However, *NeuroD/Math3* double mutants result in decreased amacrine cells, along with RGC increase in the retina (Inoue et al., 2002). *Pax6* and *Six3* expression are also present in amacrine cells, but individual gene misexpression does not generate amacrine cells either. Yet, co-expression of *NeuroD* or *Math3* with *Pax6* or *Six3* increases amacrine cell genesis significantly. Thus, bHLH and homeodomain genes co-operate in a network that controls the specification of the amacrine cells. *BarhI2* (BarH-like homeobox genes) is critically involved in amacrine cell subtype specification (GABAergic and glycinergic amacrine cells), as the loss of *BarhI2* leads to both glycinergic and GABAergic amacrine cell reduction (Jusuf et al., 2012). *Lhx1* (belongs to the LIM- homeodomain (LIM-HD) subfamily of homeobox genes) is expressed in postmitotic horizontal cells. In retina lacking the Onecut1 *(Oc1)* TF, a significant number of horizontal cells are lost along with down-regulation of *Lhx1* and *Prox1* expression, indicating a genetic pathway whereby *Oc1* acts upstream of *Prox1* and *Lhx1* during horizontal cell development (Goetz, Martin, Chowdhury, & Trimarchi, 2014). *Prox1* has been characterized to regulate horizontal cell fate, as *Prox1* neural retina knockout mice lack horizontal cells and also early RPC fail to exit the cell cycle (Dyer, Livesey, Cepko, & Oliver, 2003). *Foxn4* and *Oc1* are the upstream regulators of *Prox1* in horizontal cell fate decision. *Foxn4*-null mice demonstrate a total loss of horizontal cells, decreased levels of amacrine cells and a significant reduction of *Prox1* expression. Pancreas specific transcription factor 1a (*Ptf1a*) null-mice have an identical phenotype to *Foxn4* mutant in which all horizontal cells and most amacrine cells are missing. The downregulation of *Ptf1a* in *Foxn4* null-mice indicates that it is probably downstream of *Foxn4* in the horizontal cell differentiation network (Fujitani et al., 2006). Horizontal and amacrine cells have some common regulators such as *Math3*, *Pax6,* and *Six3*, although the

presence of other intrinsic or extrinsic factors determines each cell fate during retinogenesis (Dyer et al., 2003).

1.3.4 Bipolar cells

Mash1 and *Math3* cooperatively regulate bipolar cell differentiation, since a complete loss of bipolar cells is observed in *Ascl1 (Mash1)/Math3* double mutant mice (Tomita, Moriyoshi, Nakanishi, Guillemot, & Kageyama, 2000). Bipolar cells specify in the absence of either *Mash1* or *Math3*; however, *Mash1/Math3* double knockout mice lose virtually all the bipolar cells, and some bipolar cells switch fate to glial cells. Thus, both genes cooperate to promote bipolar fate over glial fate, and each gene alone is not sufficient to drive bipolar fate.

Vsx2 (Chx10) is shown to be present in bipolar cells during late retinal development and adulthood, and its absence results in complete loss of bipolar cells. It promotes bipolar cell fate over rod cell fate by repressing photoreceptor-specific genes. *Vsx2* expression alone also is insufficient for bipolar cell specification; however, misexpression of *Vsx2* with *Mash1* or *Math3* drives bipolar cell specification (Hatakeyama, Tomita, Inoue, & Kageyama, 2001). The genes located downstream of *Vsx2*, *Mash1,* and *Math3* are responsible for the differentiation of bipolar cell subtypes. For instance, *Vsx1* deficient mice lose the OFF-bipolar subtype, although the initial generation of bipolar cells is preserved in these mice (Chow et al., 2004). In addition to RGC reduction under conditional inactivation of *Islet1* in the mouse retina, the ON-bipolar cells, cone bipolar cells, and rod bipolar cells are significantly reduced at post-natal day 27 (P27). The bHLH transcription factor *Bhlhb4* is located downstream of *Islet1*, and its expression is required for normal rod bipolar differentiation (Elshatory et al., 2007)

1.3.5 Muller Glial cells

Muller Glial cells are produced post-natally during mice retinogenesis. Muller Glial cells are among the last differentiated cells from common RPC which maintain their multipotent characteristics (Furukawa, Mukherjee, Bao, Morrow, & Cepko, 2000b). Notch signaling activation in postmitotic retinal cells promotes the formation of Glial cells in the mouse post-natal retina (Jadhav et al., 2006). Downstream components of the NOTCH1 signaling pathway, including *Hes1/Hes5,* play crucial roles in Muller glial cell differentiation, as *Hes5* deficient mice have all neuronal cell classes except for the Muller glial cells (Hojo et al., 2000). Misexpression of *Hes1/Hes5* induce glial cell fate in the post-natal retina (Furukawa, Mukherjee, Bao, Morrow, & Cepko, 2000a). *Rax* is another transcription factor that directs the formation of glial cells in the retina. Thus, *Hes1, Hes5,* and *Rax* have a dual role, maintenance of RPC and promotion of Muller glial cells, depending on the developmental stage in the retina.

1.3.6 Photoreceptor cells

The study of photoreceptor development has been in the front line of combating degenerative eye diseases. Visual acuity and colour perception depend on the variety of photoreceptor cells in the retina. Photoreceptors, consisting of rods and cones, are required to initiate a phototransduction cascade that allows for the capture of light quanta and its conversion into electrochemical output which subsequently leads to proper vision. Rods are sensitive to light and are functional under low light conditions; Cones are less sensitive to light and are required for daytime vision. In the mature retina, the nuclei of photoreceptors are located in the ONL, and the cell bodies expand toward the back of RPE.

In mammals, photoreceptor genesis happens in overlapping long temporal windows. Lineage tracing experiments reveal that photoreceptor determination appears to occur in

terminally dividing or newly postmitotic progeny. Notch signaling in RPC determines when progenitor cells exit a proliferative state and enter a differentiation state at an early stage of retinal development. In mice with conditional ablation of *Notch1* in postmitotic cells, almost all newly post-mitotic cells from which *Notch1* was deleted adopt a rod photoreceptor fate (Mizeracka, DeMaso, & Cepko, 2013). Also, genetic deletion of *Notch1* or *Hes1* during early retinal development lead to less ganglion and horizontal cells, and over-expression of cone photoreceptor cells (Jadhav et al., 2006). During later stages of retinal development, blocking Notch1 signaling leads only to over-production of rods rather than cones, at the expense of the other cell types within the competency window. It has been proposed that Notch-induced *HES/HEY* proteins repress *Rax* expression, and in the absence of *Rax,* expression of *Otx2* is also abolished during early eye development (Muranishi et al., 2011).

Otx2 is a key regulator of photoreceptor differentiation, and its expression starts during the final mitosis of RPC. *Otx2* shows robust expression in forebrain within the optic vesicle, and in the RPE during early embryogenesis. Loss of *Otx2* at early stages of retinal development in RPC leads to mass depletion of photoreceptor and bipolar cells, with an increase in amacrine cells (Koike et al., 2007). For the RPC to adopt a rod fate over a bipolar fate, a GRN including *Otx2, Vsx2* and *Blimp1* is required. OTX2 binds to the *Blimp1* enhancer and activates its expression. High levels of expression of *Blimp1* in postmitotic cells leads to lower expression of *Vsx2*, and rod cell fate adoption. However, high levels of *Blimp1* triggers a negative feedback loop on *Otx2* and its expression to balance the proper ratio of rod and bipolar cells formation (S. Wang, Sengel, Emerson, & Cepko, 2014). Rod versus cone differentiation happens in photoreceptor precursors which still have the potency to adopt rods or cones cell fates depending on their intrinsic programming and environmental cues. One such intrinsic factor is the cone-rod

homeobox gene (*Crx)* which acts downstream of *Otx2* during neural retina development (Furukawa, Morrow, & Cepko, 1997). *Crx* lies downstream of *Otx2*, and the expression of most cone and rod-specific genes relies on its expression since *Crx* transactivates genes that are critical for terminal differentiation of photoreceptors (Furukawa et al., 1997). *Nrl* is a Maf-family neural retina leucine zipper protein which plays a major role in rod cell specification. The *Nrl* KO mice fails to produce rod cells and presents with an excessive number of S-cones replacing rods (Akimoto et al., 2006). RORβ (orphan nuclear receptor) is needed to initiate the expression of *Nrl* in a subpopulation of newly postmitotic precursors; thus, *Nrl* and *Rorβ* are two factors that control rod fate distinction (Kautzmann, Kim, Felder-Schmittbuhl, & Swaroop, 2011). *Nr2e3* (a nuclear receptor transcription factor) is a direct target of *Nrl* required to not only induce rod cell fate but also to suppress cone fate. *Thrb* (thyroid hormone receptor beta) is an early cone-specific marker in zebrafish, chicken, and mice. *Thrb2* deficient mice lack M-opsin but robustly express S-opsin, which shows that *Thrb2* is not the only regulator required for cone commitment identity. In mouse, cone cells are derived from bipotential RPC which can specify to either horizontal or cone cell types. OC1 expression promotes horizontal cell fate, and at the same time *Oc1* can bind to the *Thrb2* promoter and activate cone marker expression, so it has a dual role in horizontal/cone differentiation. *Oc1* mutant mice demonstrate *Nrl* upregulation. *Thrb2* has been demonstrated to suppress S-opsin expression in the mouse. In the presence of both *Thrb2* and *RXRg,* M-opsin fate is induced over S-opsin. Photoreceptor cells along with RGCs are two of the initial early differentiating neuronal cells and since their specification overlaps with each other, it is of importance to study RPC binary regulation of PR versus RGC fate.

1.4 Retina anatomy and function

The vertebrate retina is a layered structure with six major neuronal cells and one glial cell type which form structurally and functionally distinct circuits that work together to produce a complex visual output. The retinal cells develop as described above and are organized in three nuclear and two plexiform layers. The outermost layer of the retina is the RPE which is connected to photoreceptor outer segments and supports photoreception. Rod and cone nuclei are located in the outer nuclear layer (ONL), and their synapses are located in the outer plexiform layer (OPL). The rod and cone axons are connected to bipolar and horizontal cells. The bipolar, horizontal and amacrine cell bodies reside in the INL where their axons connect with RGC dendrites in the IPL. The cell bodies of RGC reside in the ganglion cell layer (GCL), and their axons enter the optic nerve via the nerve fiber layer.

Rods and cones are the light-sensitive cells of the eye which convert light information to chemical signals. The photoreceptors have a unique structure consisting of an elongated outer segment, connecting cilium, inner segment, cell body, and synaptic terminal. Photoreceptor nuclei form a single layer in the ONL of the retina, connecting with bipolar and horizontal synapses through the OPL to convey the electrochemical signals from the outer retina to inner retina. In the inner retina, bipolar cells form synapses with ganglion and amacrine cells. Amacrine cells modulate signals from bipolar cells by providing inhibition signals directly to RGC. The transmitted light information leaves the retina through RGC axons which collectively form the optic nerve. Muller glial cells, which span the entire retina, bring structural and functional support to the retinal neurons (Masland et al., 2012).

The murine retina is biased to generate photoreceptor population towards a rod majority and cone minority (Swaroop, Kim, & Forrest, 2010). While frogs have approximately an equal

numbers of cones and rods, zebrafish retina have a higher density of cones, as they possess tetrachromatic vision with four major cone types organized in a mosaic pattern (Chang & Harris, 1998; Raymond et al., 2014). Most vertebrates have a few different types of cones with different spectral light sensitivities, due to the expression of various light-sensitive proteins packed in the membrane discs (Masland, 2012a). The light absorbing photopigments are packed in PR outer segment disks, while rod disks are closed and cone disks are partially open. They have evolved to be able to collect light photons and convert them to electrochemical signals. Horizontal cells are among the first cells to emerge in the retina and modulate signals between PRs and bipolar cells, and they also transmit signals from bipolar cells to RGC. Most vertebrates have three major types of horizontal cells, based on the presence or absence of a short axon (axon-bearing H1, axon-less H2 and H3-H4) (Boije, Shirazi Fard, Edqvist, & Hallbook, 2016). For instance, humans have three types of the axon-bearing horizontal cell and one type of axon-less horizontal cell, whereas rats and mice only have a single type of axon-bearing horizontal cell (Shekhar et al., 2016). They provide an inhibitory feedback to the rods and cones, which helps to control PR responses to light (Muller & Peichl, 1993).

Bipolar cells are the only neurons that connect the outer retina to the inner retina; they act as intermediaries to transmit information between PR and RGC. Bipolar cells have been divided into subtypes based on morphology (dendritic branching pattern) or function (light responses). Recent studies have shown 13 morphological types of bipolar cells in mice retina (Shekhar et al., 2016), organized based on their dendritic distribution through the IPL (Tsukamoto & Omi, 2017). There are 12 types of cone bipolar cells and a single type of rod bipolar cell, each receiving inputs from cone or rod cells, respectively (Euler, Haverkamp, Schubert, & Baden,

2014). Bipolar cells transfer PR signals depending on chromatic preference, polarity (ON versus OFF) and kinetics (transient versus sustained responses) (Euler et al., 2014).

Amacrine cells mediate the signals transmitted from the bipolar cells to the RGC, which then fire an action potential upon a stimulus. Amacrine cells are an extremely diverse class with many subtypes based on morphology (dendritic branching style) or neurotransmitter phenotype (glycinergic or GABAergic). There are at least 33 morphologically defined subtypes in the mouse retina. Amacrine cells modulate visual signals by enhancing centre-surround signals, and refining the spatial and temporal information integrated by RGC, a single one of which might receive input from tens to hundreds of bipolar cells (Baden et al., 2016). Their dendritic field varies in size and architecture, and they have varied axon projection patterns as well. RGCs are functionally different in their response to the light; however; there is a close correlation between their structure and function in most vertebrates. Different species have different subclasses of RGCs, but in most studied species the IPL, where RGC form their intraretinal connections, is organized into sublaminae each with a distinct function and structure. ON and OFF RGC dendrites reside in different sublaminae irrespective of the subclass (Sernagor, Eglen, & Wong, 2001).

Muller glial cell bodies are located in the INL; however, they project radially in either direction throughout the entire retina, contacting and supporting all cell types (Masland, 2012b). Interestingly, zebrafish Muller glial cells have the ability to reprogram themselves after injury to acquire progenitor cell properties for retinal repair (Powell, Grant, Cornblath, & Goldman, 2013). They are responsible for homeostatic and metabolic support of retinal neuronal cells, and they serve as barriers to transfer nutrients from retinal vessels to neuronal cells. They also

contribute to cone outer segment assembly by phagocytosis of cone outer segments which helps cone cells to recycle retina chromophores (X. Wang, Iannaccone, & Jablonski, 2004).

1.5 Phototransduction

The process of capturing light energy and transforming it into electrochemical signals by the retina is called phototransduction. Light-absorbing pigment proteins (opsin), located in the outer segments of PRs, are structurally formed to absorb light and initiate a signaling cascade. The maximal light absorption of different pigment molecules varies within a specific wavelength based on their opsin protein. For instance; rhodopsin maximally absorbs light with a wavelength of 500 nm, and red opsin maximally absorbs 565 nm. When light enter the eyes, rhodopsin receptors absorb the photon and its retinal configuration changes from 11-*cis* to all-*trans* which trigger a cascade inside the cells. (Mannu, 2014). This process activates nucleotide exchange and allow the release of GTP from G-proteins. Activated G-protein induces cGMP phosphodiesterase, which reduces cGMP concentration in the disc. The intracellular cGMP concentration is responsible for opening or closing of sodium and calcium channels; the more cGMP in the cell, the more channels are open. Thus, in the presence of GMP the cell becomes hyperpolarized and OFF, which reduces the glutamate released from its synapses and, thus reduces the inhibition of retinal nerves, exciting the postsynaptic bipolar cells and horizontal cells. In dark conditions, PRs are in a depolarized state which means they continuously release glutamate across the synaptic cleft (Arshavsky, 2002). Horizontal and bipolar cells respond to glutamate release of PR cells with graded potentials. Bipolar cells express different receptors and the receptors determine how specific bipolar cells respond to glutamate flux. The ON bipolar cells are hyperpolarized in the dark and depolarized in the presence of light. In contrast, the OFF bipolar cells are depolarized in response to darkness and they lose excitation and become

hyperpolarized in the light (Shekhar et al., 2016). Cone-bipolar cells receive the signal from cone photoreceptor cells and may become hyperpolarized or depolarized by glutamate, while rod bipolar cells are hyperpolarized by glutamate in ON-type of bipolar cells. Horizontal cells have synaptic contact with PR cells to control responses and maintain contrast, enhance brightness and sharpen the image. Within the IPL axons of bipolar cells synapse with amacrine cells and RGC to transmit the chemical message in various forms. The depolarization of bipolar cells results in glutamate release from its axon terminals which is excitatory to some RGC. The RGC are the final neuronal transmitter of the retinal visual pathway to the brain. They possess voltage-gated channels throughout their axons to create action potentials. For instance, the ON-bipolar cells depolarize in the presence of light and release glutamate in the synapses with RGC and produce an action potential in the ON-ganglion cells. Amacrine cells provide lateral connections between bipolar cells, as well as vertical connections between bipolar and RGC. One type of amacrine cells is responsible for connecting rod-bipolar to cone-bipolar cells, which make RGC capable of responding to an entire range of light level from scotopic to photopic.

1.6 Objective

Retinal development studies have been at the forefront of embryonic development research. There are complex GRNs which guide every step of retinal development and understanding the connections and regulations of these networks may eventually open new doors, answering developmental and evolutionary questions. The focus of my project was on the *Dlx2* regulatory network during mouse retinal neuronal cell (RGC vs. PR) development at two temporal stages: E18 and E13. I tested if *Dlx2* promotes RGCs fate by blocking PR cell differentiation through repressing *Crx* and *Otx2* expression at E18 and E13. I also aimed to investigate possible *dlx* gene expression and function during zebrafish eye development as its

expression and function has been evolutionary conserved between vertebrates. I also generated *Tg[rx3:Dlx2]* zebrafish as a tool to further understand the *Dlx2* GRN in the retina. Additionally, I investigated the role of Neuropilin-2 (*Nrp2*) in mice during post-natal retinal neurovascular development as the *Nrp2* KO mouse presented with retina abnormalities. I characterized abnormal retina folding and physiology of *Nrp2* KO mice post-natally.

Providing a better understanding of retinal development may potentially help us to treat retinal degenerative diseases such as Retinitis Pigmentosa, as well as vascular diseases such as Persistent Fetal Vasculature (PFV).

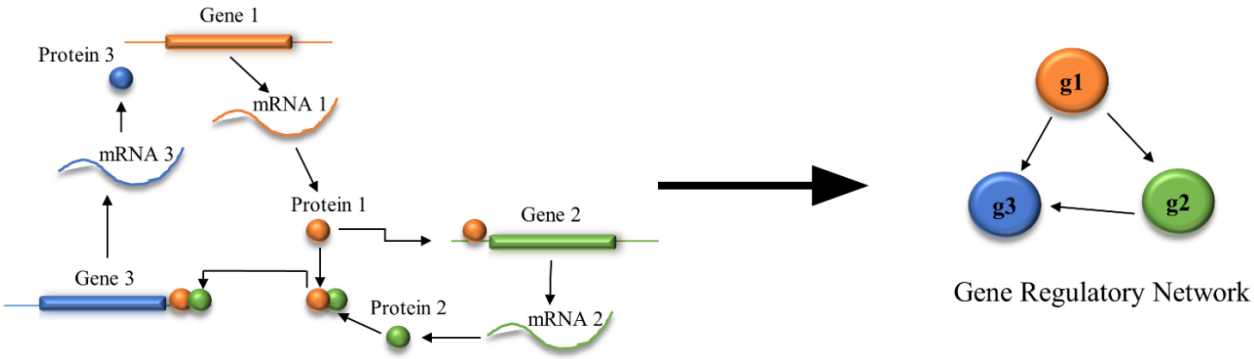

Figure 1.1 Schematic model of a Gene Regulatory Network

A schematic model of a gene regulatory network with three interacting genes. Gene 1 is a direct regulator of gene 2, and gene 3 regulation is dependent on its combinational regulation by the gene 1 and gene 2 protein complex. Adapted from Gene Regulatory Network by Van Anh Huynh-Thu & Guido Sanguinetti (Van Anh Huynh-Thu & Guido Sanguinetti, 2019). Reproduced with permission of the publisher through the Copyright Clearance Center.

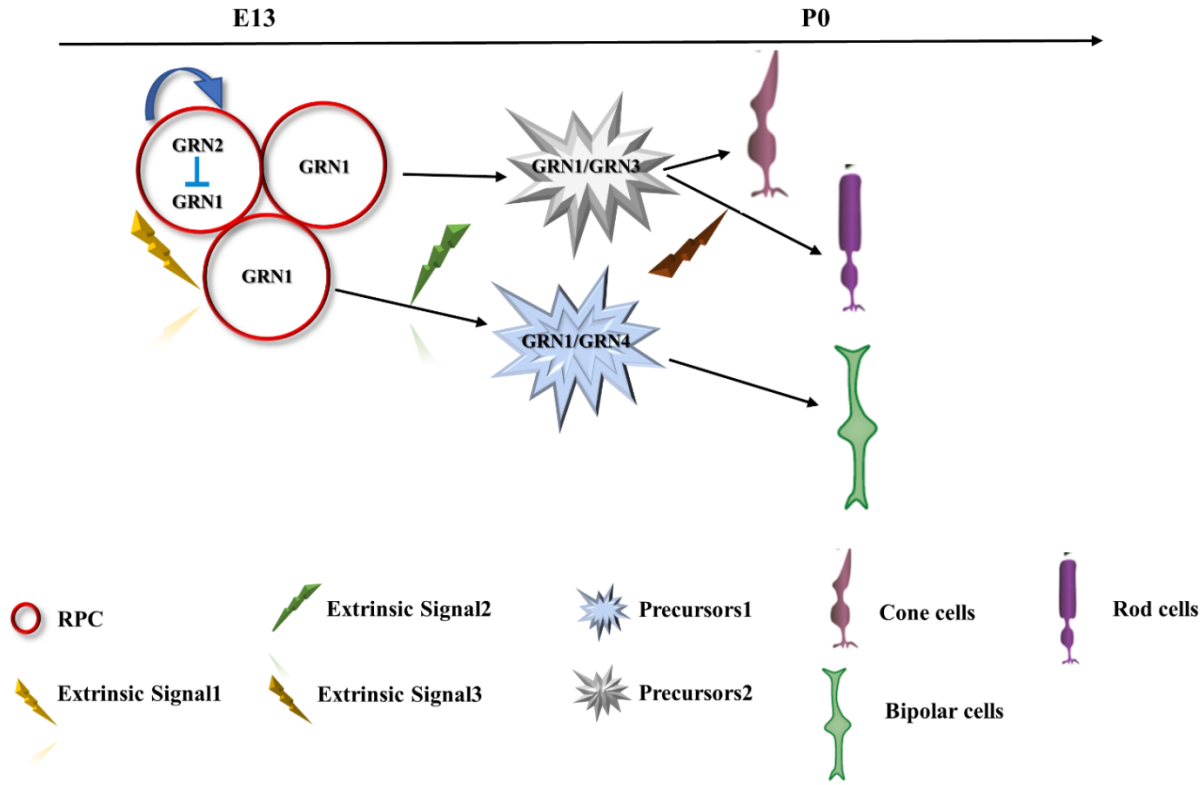

Figure 1.2. Schematic image of cell fate determination model during mouse retinogenesis

A simple schematic model of retinal progenitor cell fate determination during mouse retinal development. RPCs are a heterogenous multipotent population which go though several rounds of cell division and give rise to less potent precursor cells to possibly become a specific type of neuronal cell. RPC symmetric divisions maintain the progenitor pool, and its asymmetric divisions give rise to different precursor cell types which subsequently differentiate to various retinal neuronal cells. RPC, retinal progenitor cells; GRN, gene regulatory network; E13, embryonic day13; P0, postnatal day 0.

2 Chapter 2. Materials and Methods.

2.1 Animals

All animal protocols were carried out in accordance with the guidelines written by the Canadian Council on Animal Care and the University of Alberta. All routine colony maintenance, breeding, plug testing, and biopsy collection were carried out by Health Science Laboratory Animal Services at the University of Alberta. Timed-pregnant CD1 and C57BL/6 wild type mice were received from the Charles River Laboratories.

2.1.1 *Dlx1/Dlx2* double knockout (DKO) mice

All tissues were collected from mouse animal models with wild type mice from CD-1 BR Swiss background (Charles River Laboratories, Worcester, MA, USA), and *Dlx1/Dlx2* double heterozygous mice (Dr. John Rubenstein, University of California, San Francisco, USA) to establish the DKO colony (Anderson, Qiu, et al., 1997). Homozygous animals die at birth; thus, heterozygous animals were maintained for breeding. Ear samples were collected by animal facility staff, and genotyping was performed by phenol/chloroform gDNA extraction followed by a PCR amplification technique using *Dlx2* and *Neo* specific primers. Embryos were collected from timed pregnant mice at several time points from embryonic day 13 (E13) to adult depending on the experiments and eyes were dissected followed by tissue processing. Wild type tissues were used as controls for comparative studies (Table 1).

2.1.2 *Crx-LacZ* reporter mice

Crx-LacZ reporter mice (Furukawa et al., 1997) on a C57BL/6 background were crossed with *Dlx1/Dlx2* DKO heterozygous mice. As previously mentioned, the *Dlx1/Dlx2* heterozygotes are viable, fertile and have a normal phenotype. These heterozygotes were crossed with *Crx-*

LacZ, and the resulting F1 progeny were then crossbred. The genotyping samples were collected and genotyped with *Dlx2*, *Neo* and *LacZ* PCR primers (Table 1). The stable heterozygous colony (*Crx-LacZ* X *Dlx1/Dlx2* DKO) was maintained for breeding. The eye tissues were collected, and retinas were dissected for the various experiments at the targeted time points.

2.1.3 *Nrp2* knockout mice

Nrp2 knockout (KO) mice were provided by Dr. Marc Tessier-Lavigne (Erskine, 2011, NY, USA) and maintained on a CD1 background. Homozygous and heterozygous mice are viable and fertile, and both were retained for colony breeding (Erskine et al., 2011). The tail was collected for genotyping purposes, and whole RNA was extracted for genotyping and PCR amplification of cDNA was subsequently carried out. The cDNA was made with specific primers (*Nrp2*-RV and *Nrp2*-RC); however, three primers were applied (*Nrp2*-F, *Nrp2*-RV, and *Nrp2*-RC) for PCR amplification (Table 1).

2.1.4 *Dlx2* eye conditional knockout mice

We crossed the *Dkk3-Cre* (129.B6C3-Tg (*Dkk3-Cre*) D9TFu) (Sato et al., 2007) with *Dlx2-floxed* (C57/BL6-*Dlx2* $^{fl/fl}$) (Dr. John Rubenstein, University of California, San Francisco, USA) mice to generate a retina-specific *Dlx2* eye conditional knockout (CKO). The male *Dkk3-Cre* line was paired with *Dlx2* $^{fl/fl}$ female mice, and the resulting F1 progeny were then crossbred to produce a stable *Dkk3-Cre X Dlx2* $^{fl/fl}$ line. The ear notches were obtained, the gDNA was extracted, and PCR amplification was carried out with *LoxP*, and *Dkk3-Cre* primers (Table 1). The *Dlx2* CKO heterozygous, homozygous, and wild type mice were euthanized, and the eye samples were collected at various time points.

2.1.5 *Dlx2* transgenic zebrafish

Fish care and protocols were approved by the Animal Care and Use Committee: Biosciences at the University of Alberta. Protocols and care were in accordance with the Canadian Council on Animal Care.

Zebrafish (*Danio rerio*) were raised and maintained according to standard procedures (Westerfield, 1993). Embryos were kept in E3 media and at 28°C except where indicated in experimental procedures. Media with 0.003% PTU to prevent pigmentation was applied at 8-10hpf. A construct was designed containing the mouse *Dlx2* coding region (CDS) with a 3XFLAG tag at the N-terminus plus attl1 and attl2 sites for Gateway cloning, and a consensus Kozak sequence for translation initiation (Kwan et al., 2007). The oligos were ordered through IDT (Integrated DNA Technologies) services, and the sequence was cloned into a pDONR221 entry vector, then sub-cloned into a destination vector along with mCherry fluorescent protein CDS under the cardiac myosin light chain promoter, and an established *rx3* promoter from medaka previously used to express in the developing eye fields of zebrafish, all flanked by Tol2 sites. The final construct was verified by sequencing. The constructs were co-injected with DNA microinjection buffer (0.2 mM KCl, 0.1% phenol red), along with Tol2 transposase mRNA, into single-cell stage embryos. The transgenic fish were sorted for mCherry-heart fluorescence marker at 48hpf. Transient transgenic fish were raised to establish a stable *Dlx2* transgenic line (*Tg[rx3:Dlx2]*). Adult transgenic fish were crossed to wildtype AB fish to maintain consistency of *Dlx2* expression among embryos. Eye tissues were collected at various embryo and adult life stages.

Table 1 Genotyping primers

Primer Name	Primer Sequence (5´to 3´)
Dlx2	F- TCCGAATAGTGAACGGGAAGCCAAAG R- CAGGGTGCTGCTCGGTGGGTATCTC
Neo	F- CAAGATGGATTGCACGCAG R- CATCCTGATCGACAAGAC
LacZ	F- TGCCGGTCTGGGAGGACT R- TTCGTGATCGGGTCC
Nrp2	F- AGACTACCACCCCATATCCCATGG RV- CTTGAGCCTCTGGAGCTGCTCAGC RC- CTGCCCTGGTCCTCACGGATGAC
LoxP	F- AGT TCG TCT CCG GTC AAC AA R- GAG CGT GGA GAG GCA GAA
DKK3-Cre	F- CAGACCATACTAGTTTGGCAGTACTGG R- CTTGCGAACCTCATCACTCGTTGCA
IL2	F- GTAGGTGGAAATTCTATC R- CTAGGGCACAGAATTGAA

2.2 Statistical methods

Results are shown as the mean ± standard error of the mean. The qPCR experiments, luciferase reporter assays, and ChIP RT-PCR were performed in three biological and three technical replicates. Statistical analyses were done using the Student's t-Test, and results were statistically significant when $p < 0.05$. ERG data analysis was made using non parametric ANOVA (Kruskal-Wallis) with significance at $p < 0.05$, two tails, unequal variances.

2.3 Tissue collection and preparation

In order to collect embryonic tissues at various time points, timed-pregnant mice were obtained. The embryonic ages were determined by the presence of a vaginal plug after breeding. Pregnant females were euthanized by cervical dislocation, and embryos were sacrificed by decapitation. Eyes were dissected in cold PBS, and tails were numbered and kept in separate tubes at -20°C for future genotyping, which was accomplished via PCR with specific primers. The DNA extraction of the tails was performed according to the phenol-chloroform protocol. PCR reactions were performed using Hotstar Plus polymerase (NEB).

2.4 Tissue embedding and sectioning

The eyes were enucleated from embryos of embryonic days E15 and older, while the whole embryonic head was removed for developmental ages younger that E15. The tissues were washed in PBS and then fixed in 4% PFA for a specific time based on tissue and mouse age (E13 head/3 hour, E18 eye/45 minutes, and Adult eye/1 hour) at 4°C on rotation. Following the cross-linking step, tissues were cryopreserved by applying a sucrose gradient (10%, 20%, and 30%) at 4°C until tissues were sunk to the bottom of the tube. The eyes were placed in plastic embedding molds filled with OCT, in the correct orientation (the optic nerves facing each other and the lens facing outwards) and then placed in dry ice or liquid nitrogen until they were frozen. The blocks were stored in -80°C until used for cryosectioning. Cryosections were set at 10-12 μm on a Leica Cryostat, and tissues were sectioned. The sectioned tissues were mounted on Superfrost Plus Microscope Slides and kept at -80°C.

For post-natal paraffin tissue embedding, tissues were washed in PBS. The eyes were enucleated and fixed in Davidson's Fixative for 18 hours at room temperature. The eyes were then washed in PBS and transferred to 50% ethanol until embedding. Samples were dehydrated

in a series of graded ethanols and embedded in paraffin. Tissues blocks were embedded in a sagittal orientation and sections were cut at 7μm using an 820 Spencer Microtome.

2.5 Tissue immunofluorescence and double immunofluorescence

2.5.1 Mouse

Cryopreserved tissues were removed from -80°C and were blocked in 5% blocking buffer (0.1% bovine serum albumin (BSA), 0.2% Triton-X 100, 5% Serum in 1X PBS) for 1-2 hours at room temperature, followed by addition of the primary antibody that was diluted in the same blocking buffer. We created a humidity chamber by adding moisturized KimWipes in a slide rack and then the slides were incubated at 4°C overnight. One slide remained in blocking solution as a negative control. The following day, all slides were washed 3x for 5 minutes in 1X cold PBS/0.05 % Triton-X100. The secondary fluorescent antibody was prepared in the same blocking buffer, placed on the slides and incubated for 1-2 hours in a dark room, following 3x washed with 1X PBS/0.05 triton X-100 for 5 minutes. The slides were mounted with VectaShield mounting medium containing DAPI (VECTASHIELD), and coverslips were used and sealed with clear nail polish. The slides were kept in 4°C until they were imaged with a Nikon Eclipse TE2000 inverted epifluorescence microscope (Table 2).

2.5.2 Zebrafish

Larvae were fixed at 5dpf in 4% paraformaldehyde overnight, and wholemount immunocytochemistry was performed. Briefly, larvae underwent washes with 1XPBS +1% Tween, following 1x wash with H2O then -20°C acetone for 7 minutes. Larvae were rinsed in 1X PBS + 1% Tween+ 1% DMSO, then blocked with 10% normal goat serum/PBS for 30-90 minutes and incubated overnight at 4°C in PBS containing 2% normal goat serum (NGS) and primary antibody. Following incubation in the primary antibody, larvae were washed 3x with 1X

PBS and incubated in the secondary antibody overnight at 4°C. The larvae were mounted on slides with 70% paraffin; coverslips were used to seal the tissue. The slides were kept in 4°C until they were imaged with a Nikon Eclipse TE2000 (Table 2).

Table 2. List of Antibodies

Antibody	Source	Working concentration
Mouse/Immunostaining		
Alexa Fluor 488	Invitrogen	1/200
Alexa Fluor 595	Invitrogen	1/200
Collagen I	Millipore	1/400
Crx	A gift from Dr. C. Craft (University of Southern California)	1/1000
Dlx2	Dr. D. Eisenstat	1/200
IB4	Vector	1/400
Nrp2	R&D Systems	1/400
Otx2	Santa Cruz	1/200
Calbindin	Chemicon	1/1000
S-opsin	Santa Cruz	1/200
Recoverin	Millipore	1/500
Mouse/ChIP		
Dlx2	Dr. D. Eisenstat	10µg
H3K27me3	Millipore	10µg
Otx2	Abcam	10µg
Zebrafish/Immunostaining		

Dlx2	Dr. D. Eisenstat	1/200
FLAG	Millipore	1/400

2.6 Histological staining

The paraffin-embedded retina tissues were used for Hematoxylin and Eosin staining. The slides were placed in a 60°C oven for 10 minutes to melt the paraffin. The following procedure was performed to deparaffinize and rehydrate the sections: xylene treatment 2x for 2 minutes, one-minute treatment by decreased ethanol gradient starting from 100% ethanol, 95% ethanol, and 70% ethanol, then slides were submerged in cool running water. The slides were placed in hematoxylin staining solution, 3-5 times for one minute and washed in running water. Then 0.5% acid alcohol solution was applied three times and then rinsed in a running water bath for one minute. Slides were then submerged in a saturated lithium carbonate Bluing solution for one minute. Slides were then rinsed in running water for five minutes. Slides were next submerged in eosin staining solution for two minutes. Slides were then finally cleared and dehydrated in increasing ethanol gradients starting with 95% ethanol, and then followed by two 100% ethanol treatments. Slides were then twice submerged in xylene for three minutes each. Following clearing and dehydration, slides were mounted, and brightfield images were then captured with a Nikon Eclipse TE2000U platform and NIS Elements software.

2.7 Chromatin Immunoprecipitation

Embryonic eyes/retina were collected from WT CD-1-timed pregnant mice. Hindbrains were also collected as a negative control as Dlx2 is not expressed in the hindbrain. Tissues were manually dissociated by pipetting up and down and washed 2x in 1XPBS using a centrifuge at 2000 rpm at 4°C for 5 minutes. Supernatants were removed, and the pellet was fixed in 1% PFA

+ 1x Protease Inhibitor Cocktail (PIC) for 30 minutes at 4°C. Cross-linked tissues were spun at 2000 rpm 4°C for 5 minutes. Priming could be carried out the same day, or the pellet could be stored in -80°C until priming. Priming beads was performed as follows: 60ml of Pierce UltraLink Protein A/G beads were prepared for each sample including the controls. Beads were primed by adding dilute buffer (0.01X SDS, 1.1 X Triton X-100, 1.2 mM EDTA, 16.7 mM Tris-HCl (pH 7.0), 167 mM NaCl) to the total amount of beads to a final concentration of 1 ml, followed by centrifugation at RT 2000 rpm for 2 minutes, the supernatant was removed, and wash was repeated. Dilute buffer + 1x PIC was added to make 50% beads and leave on the ice until sonicated chromatin is ready. After the pellet was washed 2x with cold 1X PBS, 400ml of freshly made lysis buffer (1% SDS, 10mM Tris-HCl pH 8.1, 10mM EDTA) was added, and chromatin samples were sonicated on ice 10-20X, at 15 seconds intervals with 30 seconds rest period using a membrane disruptor. 1-3µl of sonicated samples were run in a 1% agarose gel to confirm that fragmented chromatin size was with 300-700bp. To preclear, 60µl of primed beads were added to the fragmented chromatin and were incubated for 1 hr at 4°C for 5 minutes, then samples were centrifuged at 2000rpm at 4°C for 5 minutes. The supernatant was transferred to a new tube, and beads were discarded, BSA and tRNA were added to the final concentration of 500µg/ml. 1-5µg of DLX2 Ab was added to the tubes designed as +Ab and incubated 4°C O/N with rotation. The IgG and -Ab tubes remained as is (retina and hindbrain) (Table 2). On the next day, BSA and tRNA with primed beads were added to all samples (including negative controls), to the final concentration of 500µg/ml, and incubated at 4°C O/N with rotation. Then the beads were pelleted with the centrifuge, and the supernatant was transferred to the new tubes, and both supernatants and beads were kept (supernatants contained unbound chromatin, which was used for qPCR analysis). The beads were washed in salt and buffer gradient in the following steps:

low salt buffer (0.1% SDS, 1% Triton, 2mM EDTA, 20 mM Tris-HCl, 150 mM NaCl) , high salt wash buffer (0.1% SDS, 1% Triton, 2mM EDTA, 20 mM Tris-HCl, 500 mM NaCl) and LiCl wash buffer (0.25M LiCl, 1% deoxycholate, 1mM EDTA, 10mM Tris-HCl, 1% NP-40). After the last wash, 250µl of preheated (65°C) elution buffer was added to samples and incubated for 15 minutes, RT with agitation. The cross-links were reversed with 5M NaCl, and extra RNA was digested with RNaseA at 65°C O/N. Finally, proteinase K was added to the samples, following with PCR cleanup (Qiagen). Purified DNA was analyzed with PCR and qPCR using primers designed to flank the putative promoter regions for target gene binding (Table 3).

Table 3. ChIP primers

Primer Name	Primer Sequence (5′ to 3′)
Crx-R1	F- GGGGCTATCTGTGTGGAGGTCT R- TGATGAAGGCTGAGAGGAAATGA
Crx-R2	F- TCTGCAGGTTGTGTTTCGT R- ACCTAACTTGGCTCTCCCTC
Crx-R3	F- CGTAGACAACTCCTCC R- GTTCTGCTTCTCTAAACACC
Crx-R4	F- TGCACGGCCCGGTGTTTAGA R- TCCTGCAATCCTTGAGCTGAAATGA
Crx-R5	F- ACCAGGGCTCCATTCTC R- GGTTCCTGGCTCTTTCCTC
Crx-R6	F- GAGGAAGTGAGGGAAGAAGGGA R- TGTGAAAGGATAGTATTGA
Otx2-R1	F- GGACTTCCGGCCACTGA R- CGCTGTTAGGTCTGGAAGC
Otx2-R2	F- CCTTCCAGACCTTAACACCG R- GCGGGCATTTGGAAAACAG

Otx2-R3	F- CTGTTTTCCAAATGCCGCG R- ATCTACCAGTTGCTGTGTCC
Otx2-R4	F- GCAAGCGGTGAAAGTTAGGT R- GAGGTCCTTCTTGGAGAGTC
Otx2-R5	F- GACTCTCCAAGAAGGACCTC R- CCCTTGGACAGTTCTGACC
Otx2-R6	F- CTGGAAGAAATCACAGCTGAA R- GGCACTTAAAGCGCTCTCTC
Otx2-R7	F- CAGCCTTACACACATTGC R- TAACCGCACTTCTCTCTGC
Otx2-R8	F- GCCCTGTGCTAGTCTTGAAG R- GGAGGAGTTTGATTACATGTG
Otx2-R9	F- CACATGTAATCAAACTCCTCC R- CTTGCTGAACAACAAACTTGTG
Otx2-R10	F- CACAAGTTTGTTGTTCAGCAAG R- GATTGGGGCCATTTGAAGAG
Dlx2-R1	F- GAGTGAAGGTTTGAGTCCAG R- CTGTCCTGGAACTCACTTTG
Dlx2-R2	F- GCAGGTAGTTCTCACAAGAC R- GGCTGGTCTGGAAGTGTG
Dlx2-R3	F- GAGTGGCTCTCCTCAGAAC R- GTGCTGGCTAGTCTGCAAC
Dlx1/Dlx2 IGE	F- CACACACTTTCGAACACACC R- CACTATTCTGAGCCTAGCTG
Dlx1-R5	F- GGTGTACCCATGAAGACTTC R- CATCCGTGAGTTAGCTC

2.8 Molecular Cloning

ChIP positive promoter regions of candidate target genes were cloned into the pGL3 basic vector for subsequent EMSA and Luciferase reporter gene assays. To clone the ChIP positive promoter regions, specific primers with the addition of restriction sites to the 5' and 3' ends were designed. Each regulatory region was PCR amplified with Phusion High-Fidelity (NEB) DNA Polymerase and purified with a QIAquick PCR Purification Kit (Qiagen). Digestion of the PCR product was performed with 1-unit NEB restriction enzymes. To create overhanging ends on an empty pGL3 plasmid, the plasmid was digested with the same restriction enzymes as before. Digested plasmid and regulatory regions were run on 1% gel electrophoresis, cut from the gel and cleaned with QIAquick Gel Extraction Kits (Qiagen). Finally, T4 DNA ligase (Invitrogen) was used to insert the regulatory region DNA into the matching pGL3 vector. Following ligation, the plasmid was used to transform competent DH5α E. coli cells for 30 minutes on ice. The bacteria were then heat shocked at 42°C for 1 minute and placed on ice for 5 minutes. These cells were added to Lysogeny Broth (LB) for 2 hours at 37°C and then plated onto LB agar plates containing 50mg/ml carbenicillin. Plates were incubated O/N at 37°C and single colonies resistant to carbenicillin were picked and grown in LB broth at 37°C O/N. Finally, QIAprep Spin Miniprep Kit (Qiagen) was used to isolate the plasmids, as per the manufacturer's instructions. Insertions of regulatory regions into the pGL3 Plasmids were first checked with restriction digestion and gel separation and then confirmed with sequencing. The clones were stored in -80°C after plasmid maxi-prep, in order to use for both EMSA and subsequent reporter gene assay (Table 4).

Table 4. Cloned regions primers

Primer Name	Primer Sequence (5′to 3′)
Crx-R6	F-GTACGCGTGAGACAGAGAATAATAGA R-CTCTCGAGGTACACTTCTTTCTGT
Otx2-R2	F-CACAGGTACCCCTTCCAGACCTAACAC R-GAGGACCTCGCGGGCATTTGGAAAACA
Otx2-R4	F-GCTCGAGGAAAGCCAGTGCCGATTT R-GAGCTAGCCTTGGAGAGTCAAAACG
Otx2-R8	F-CGGTACCATTTCTGTCAAGCCCTGTG R-CCGCTAGCAGGAGTTTGATTACATGTG
Otx2-R9	F-CGGTACCACACATGTAATCAAACTCCT R-CCTCGACCTTGCTGAACAAAC

2.9 Electrophoretic Mobility Shift Assay

To investigate direct recombinant DLX2 protein binding to candidate regulatory elements, Electrophoretic Mobility Shift Assays (EMSA) were performed. The ChIP positive promoter regions which were previously cloned and stored were digested by an appropriate restriction enzyme to create 5' overhangs. The digested plasmid was then resolved on a 1% agarose gel and the DLX2-positive DNA region was extracted and gel purified (Qiagen). These 5'overhanging DNA pieces were radiolabelled using [α-32P]-dGTP and DNA Polymerase I (Invitrogen) for 15 minutes at RT. Labeled probes were then purified with Micro-Spin G-25 columns (Healthcare Illustra). Radioactivity levels were measured using a LS 6500 scintillation counter and adjusted to 80,000 counts per million/µl. The binding reaction was set up using labeled probes, 1X binding buffer (Promega), poly(dI-dC) •poly(dI-dC), and recombinant DLX2 (rDLX2) for 1hour at RT. Controls for the experiment were included: free probe where no

rDLX2 was added to the binding solution, supershift where anti-DLX2 antibody was added to the binding solution, a non-specific antibody control where IgG antibody was added to the binding solution and cold-competition where excess unlabelled probe was added to the binding solution. The binding reaction was then run on a 4% acrylamide gel containing; 40.5ml H2O, 2.5ml 10X Tris/Borate/EDTA buffer, 1.875ml 40% Acrylamide, 3.125ml 40% Acrylamide/Bisacrylamide, 375µl 10% Ammonium Persulfate, 1.56ml 80% Glycerol, and 25µl Tetramethylethylenediamine (TEMED, Sigma) at 300V for two hours in 0.5X TBE buffer. The resolved gel then was dried onto filter paper using a gel dryer and a HydraTech vacuum pump for 2 hours at 80°C. The dried gel was exposed to X-ray film (Kodak) in Biorad autoradiography cassettes for an hour in -80°C or O/N at RT. Films were then developed in the dark using a Mini-Medical 90 film developer.

2.10 Luciferase Reporter Gene Assays

A luciferase reporter assay was conducted to explore DLX2 regulatory function on our targeted genes *in vitro*. As explained above, candidate regulatory DNA was sub-cloned into the pGL3 basic vector upstream of the luciferase gene. The *Dlx2* expression vector was also sub-cloned into a mammalian expression vector pCDNA3, placing *Dlx2* downstream of CMV (Dr. John Rubenstein, University of California, San Francisco, USA). Human embryonic kidney 293 cells (HEK293) were used as an easy to transfect cell line with no *Dlx2* endogenous expression. HEK293 cells were grown at 37°C in 75cm cell culture flasks using DMEM media (Gibco) with 10% Fetal Bovine Serum (FBS) (Gibco). Cells were maintained to reach 70% confluence, then washed with PBS, and trypsinized for 5 minutes to detach from the flasks. After counting with a hemocytometer, $2x10^5$ cells/well were seeded in a 12 well plate and incubated O/N before transfecting. Transfection mixtures per well were prepared as follows: 10µl of Lipofectamine

2000 (Invitrogen), 1µg pCDNA3-DLX2 expression vectors, 0.5µg of a pGL3 plasmid containing a specific regulatory region, 4ng β-gal vector (Promega) for transfection efficiency, and empty pGL3 and empty pCDNA3 as controls. Cells were cultured for 48 hours post-transfection in DMEM media and 10% FBS at 37°C, 5% CO2. Cells were washed with ice-cold 1X PBS, and Reporter Lysis Buffer (Promega) were applied to the cells for 15 minutes on ice. Cell lysates (20 µL) were then collected and plated in two 96 well plates. The firefly substrate (Promega) was added to one 96 well plate to measure expression levels in the presence or absence of DLX2. The firefly luminescence was measured for 1 second per well in the 1420 Victor Multilabel Counter. The β-gal assay buffer (Promega) was added to the second 96 well plate to measure the plasmid transfection efficiency, and the photometric measurement of the β-galactosidase was measured at 570 nm absorbance after one-hour incubation at 37°C.

2.11 Site-Directed Mutagenesis

The specificity of DLX2 binding site was further validated by deleting putative DLX2 binding sites of ChIP positive DNA regions. The overlap extension PCR was performed to remove TAAT/ATTA motifs within regulatory regions. For this technique, three independent PCRs with two sets of primers were carried out. For the first step, two separate PCR reactions were performed to generate two templates that overlap at the deletion site. The first two PCR products would be the template for the third PCR reaction. The first step required primers which exclude the binding motifs but include the sequence past the deletion site. The PCR products from the first step which contain a large area of overlap in the deleted region were utilized as a template for the third PCR reaction and produce a final product that contains the whole region with the desired deletions. The restriction sites were integrated into flanking primers for subsequent cloning. The PCR product containing deleted region was cloned into pGL3 basic

vector (as described), and verified by sequencing (TAGC, University of Alberta). The mutated plasmid was then maxi-prepped (Qiagen) and stored in -80°C for subsequent EMSA and Luciferase Reporter Gene Assay.

2.12 Quantitative real-time PCR

Quantitative real-time PCR measures DNA amplification during the PCR reaction. The tissue was dissected from WT and mutant mice or zebrafish. The dissected tissues were snap frozen in liquid nitrogen and stored in -80°C, until tRNA extraction using Trizol (Invitrogen). Whole RNA was used to synthesize cDNA from mRNA transcript using SuperScript III (Invitrogen) kit. First, 500ng of RNA was added to 1µl of Oligo(dT), plus 1µl d NTP, mixed and incubated 5 minutes at 65°C, followed by 1 minute's incubation on ice. Oligo(dT) was applied for whole mRNA synthesis; however, for gene specific cDNA synthesis, gene-specific primers were applied. After incubation, 4µl 5X First-Strand Buffer, 1µl RNaseOUT, 1µl DTT, and 1µl Superscript III RT were added to the mixture and incubated at 50°C for an hour, followed by 70°C for 15 minutes. Resulting cDNA was stored in -20°C, until were later applied as a template for the qRT-PCR reaction using a LightCycler 96 System (Roche) and the FastStart SYBR Green Master System (Roche). Primers were designed for exon-exon junctions, and *Gapdh* primers or other housekeeping genes were used as an internal control. Primers were optimized and validated by standard curve analysis to determine the best conditions for the development of a robust assay. Four concentrations with a dilution factor of 1:10 were tested to create a standard curve. The standard curve was analyzed with qPCR software to calculate the reaction efficiency. An efficiency range between 90 and 110% (slope curve of -3.3 for 100% efficiency) was considered as acceptable. For data analysis, the delta-delta Ct method was performed, where the difference

between the cycle of threshold (Ct) of knockout and WT samples was analyzed when both conditions were normalized to the housekeeping gene.

In order to quantify the specific microRNA expression level, sample RNA extraction was performed as described from the retina tissues. However, the final cDNA was prepared from non-coding RNA template following the Stem-Loop protocol (Kramer, 2011) (Table 5).

Table 5. qRT-PCR primers

Primer Name	Primer Sequence (5′ to 3′)
Mouse primers	
LacZ	F- AGCAGAAACAACTTTAACGCC R- CGGTCAGACGATTCATTGG
Otx2	F- GCCACCCCCCGGAAACAG R- AAACCATACCTGCACCC
Gapdh	F- ACCATCCGGGTTCCTATAAAT R- CAATACGGCCAAATCCGTT
Dlx2	F- CAAAACTCAGGTCAAAATCTG R- TTAGAAAATCGTCCCCGCG
U6	F- GCTTCGGCAGACATATACTAAAAT R- CGCTTCACGAATTTGCGTGTCAT
Mir-124	F- CGGAGAGCAGAGTCTCTGATCTTG R- TTCAAGTGCAGCCGTAGGC
Nrp2	F- GCTGGCTACATCACTTCCCC R- CAATCCACTCACAGTTCTGGTG
36b4	F- CCTAGTCCATATTTCCCGATATG R- GATACCGTTGAAGTGCTGCACC
Stx1	F- AGAGATCCGGGGCTTTATTGA R- AATGCTCTTTAGCTTGGAGCG
Calb2	F- AGTACACCCAGACCATACTACG R- GGCCAAGGACATGACACTCTT
Prox1	F- AGAAGGGTTGACATTGGAGTGA R- TGCGTGTTGCACCACAGAATA
Recoverin	F- ACGACGTAGACGGCAATGG R- CCGCTTTTCTGGGGTGTTTT
Rho	F- CCCTTCTCCAACGTCACAGG

	R- TGAGGAAGTTGATGGGGAAGC
M-opsin	F- ATGGCCCAAAGGCTTACAGG R- CCACAAGAATCATCCAGGTGC
S-opsin	F- CAGCCTTCATGGGATTTGTCT R- CAAAGAGGAAGTATCCGTGACAG
Vsx2	F- CTGAGCAAGCCCAAATCCGA R- CGCAGCTAACAAATGCCCAG
Brn3a	F- CGCGCAGCGTGAGAAAATG R- CGGGGTTGTACGGCAAAATAG
Brn3b	F- TGGACATCGTCTCCCAGAGTA R- GTGTTCATGGTGTGGTAAGTGG
Zebrafish primers	
dlx1a	F- GACCATGTCTAAATACCAGAGAG R- GAGTAATGTCCGTGGGTCATAG
dlx2a	F- TTCACTCTGTCGTTGGACTTG R- GTGGTAACTGCTGGAGGTAATC
dlx2b	F- GCGCATGGTGAATGGAAAG R- GTACTGGGTCTTCTGGAATCTG
dlx3b	F- GGCTCTGGTAGTATTCGTGATG R- GACCGATCTTTCAGGCTCTATG
FLAG	F- ATGGACTACAAGGATCACGACGG
Brn3a	F- AGAGGAGGAGAAGAGAGTCAA R- TGTGTGGTGTGTCTCTG
Brn3b	F- GAACAGCAAGCAGGCAATC R- GCGTTGGAAGTCAGAGTAGAG
Isl1	F- GAGGGAGGAGAAGAGAGTCAA R- TGTGTGGTGTGTCTCTG

2.13 Western Blotting

To detect and analyze specific proteins, immunoblotting was performed. The eye tissues were collected and homogenized in Lysis Buffer. The lysates were then collected, and the amount of protein was quantified using a BCA Protein Assay Kit on a GeneQuant Spectrophotometer. SDS buffer (4X) was then added to each sample and heated at 100°C for 5 minutes to linearize the isolated protein and ensure sample denaturation. Protein samples were separated on SDS-PAGE (Polyacrylamide Gel Electrophoresis) gel with a 10% running gel containing 1.5mM Tris-HCl pH8.8, 40% acrylamide, 10% SDS, 10% APS, TEMED and a 5% stacking gel with 40% acrylamide, 0.5 M Tris, pH 6.8, 10% SDS, 10% APS, and TEMED. After the samples were run on the gel for 55 minutes at 180V, they were transferred to nitrocellulose membranes in transfer buffer (25 mM Tris, 192 mM glycine, 10% methanol) for 3 hours at 4°C. The membrane was blocked in 3% milk in TBST for an hour at RT. Primary antibody was added and incubated at 4°C overnight. The next day, the blot was washed 3X in TBST for 5 minutes, then incubated for 1 hour at RT with secondary antibody. The membranes were washed 3x in TBST for 5 minutes. Chemiluminescence was detected using an ECL kit (GE) and developed on X-ray film (Fuji) in a film cassette for 1 to 10 minutes. Each membrane was re-probed and detected for β-actin as a loading control.

2.14 Optical Coherence Tomography

OCT is a non-invasive imaging technique used to study retina structure. The Bioptigen Envisu spectral domain ophthalmic imaging system was used. For this technique, adult mice were anesthetized by intraperitoneal injection of Ketamine and Xylazine (150mg/kg and 10mg/kg, respectively). Once the surgical plane was reached, the pupils were dilated, by applying Phenylephrine and Tropicamide (2.5% and 1%, respectively). To prevent cornea

dryness during the experiment, lubricant eye drops were applied. Mice were positioned for imaging by placing them into a stereotactic rotational cassette. The camera was focused to the retina, the retina was scanned, and a clear image was captured by InVivoVue Clinic software. The InVivoVue software was used to measure retina layer thickness.

2.15 Electroretinography (ERG)

Electroretinography (ERG) is a non-invasive test to measure retina function. Adult mice underwent bilateral full-field ERG. Dark and light-adopted ERG were performed. Prior to the experiment, for 2 hours mice became dark-adapted and they were prepared for recordings under dim red light. Mice were anesthetized and prepared for the experiment as described under OCT. Then each mouse was positioned on the ERG platform. The ground electrode needle was placed at the base of the tail, and the reference needle electrode was placed subdermally between the eyes. The contact lenses were positioned onto the cornea, and the color dome was moved so each mouse's eyes were inside the dome. Light stimulation (10 μs flashes), signal amplification (0.3–300 Hz bandpass without notch filtering) and data acquisition were provided by a commercial system (Espion E $^{2;}$ Diagnosys LLC, Littleton, MA). Dark-adapted responses were collected first, then the light-adapted responses. For each animal, only responses from the best eye were considered for analysis.

3 Chapter 3. Photoreceptor cell vs retinal ganglion cell gene regulatory networks in the retina

3.1 Chapter abstract

Dlx homeobox genes play a critical role in development of the vertebrate retina. We were interested in identifying and characterizing a DLX GRN to address retinal neural progenitor cell fate decisions. *Crx* (Cone-Rod homeobox gene) is involved in the late differentiation and maintenance of cone and rod photoreceptors (PR). *Otx2* (Orthodenticle homeobox 2 gene) is required for early specification of photoreceptors (Swaroop et al., 2010). *Dlx1/Dlx2* double knock-out (DKO) mice have a reduction of RGC numbers and increased and ectopic expression of Crx (de Melo et al., 2005). These data suggested a possible genetic network of *Dlx1* and *Dlx2* in the determination of RGC fate with concomitant repression of PR differentiation. Thus, we aimed to investigate the mechanism underlying a possible cell fate switch to PR cells from RGCs by the loss of *Dlx1* and *Dlx2*gene function. We hypothesized that *Dlx2* promotes late RGC (E18) differentiation and blocks PR specification by repressing PR-specific genes (*Crx* and *Otx2).* We characterized a negative regulatory role for DLX2 on *Crx* expression during retinal development and possibly a cell fate switch from RGC to PR in the *Dlx1/Dlx2* DKO mice. We could not confirm DLX2 functional regulation of *Otx2* expression at E18; however, DLX2 and OTX2 reciprocally occupy each other's promoter region during early retinal cell differentiation (E13). This might explain the involvement of *Dlx2* in early RPC fate specification and late RGC maintenance. Additionally, I proposed that microRNA-124 (miR-124) is an upstream regulator of *Dlx2,* and they regulate each other in a negative feedback loop at E18. We showed that DLX2 negatively regulates miR-124 expression at E18. Since *Dlx1/Dlx2* DKO mice die at birth, we generated *Dlx2* conditional knockout (CKO) mice to study *Dlx2* function in the retina after birth,

where I hypothesized that consistent with *Dlx1/Dlx2* DKO mice, PR cells would be increased at the expense of RGCs. Our CKO was viable and fertile, and the eye presented retina abnormalities including cataracts and expanded retina layers. Further phenotyping is ongoing.

3.2 Introduction

3.2.1 *Dlx* gene family

Dlx genes are the vertebrate orthologs of the *Drosophila distal-less* (*Dll*) gene which encodes the homeodomain TF required for *Drosophila* limb development. *Drosophila Dll* loss of function mutants dies embryonically, because of the absence of rudimentary larvae limbs (Cohen & Jurgens, 1989). *Dll* is also required for the development of the proximodistal axis of the antenna, and correct proximo-distal organization during early larval development. In addition to the antenna, *Dll* genes are involved in the development of the peripheral nervous system in *Drosophila*. In *Dll* loss of function, the larval antennal, maxillary and labial sense organs do not form (Panganiban & Rubenstein, 2002). The *Dll* gene targets several genes downstream during *Drosophila* leg development such as the Notch ligand Serrate (*Ser*). *Dlx* genes have a similar function repressing Notch signalling in the vertebrate central nervous system, which potentially represents a conserved genetic function between *Dll* and *Dlx* genes (Rauskolb, 2001).

Dlx genes are evolutionary conserved and consist of six family members in human and mice: *Dlx1/ Dlx2, Dlx3/Dlx7, Dlx5/Dlx6* organized in three bigenic clusters; all are homologs of the *Drosophila distal-less (Dll)* gene, and are located on mice chromosomes 2, 11 and 6, respectively (Figure 3.1). Mammalian *Dlx* genes are linked to *Hox* family genes. In mice and humans, each pair is linked to a *Hox* cluster such that in humans, *Dlx1* and *Dlx2* are linked to *Hoxd*, *Dlx3* and *Dlx4* are linked to *Hoxb*, and *Dlx5* and *Dlx6* are linked to the *Hoxa* cluster (McGuinness et al., 1996). *Dlx* genes are present in all chordate phyla, and the primitive chordate

amphioxus has one *Dlx* gene, whereas Lampreys have four *Dlx* genes. The current combination of mammalian *Dlx* genes could be the result of a neighbouring duplication of an ancestral *Dlx* gene, followed by two rounds of genome duplication and subsequent loss of a *Dlx* pair linked to the *Hoxc* cluster (Neidert, Virupannavar, Hooker, & Langeland, 2001). This theory comes from the analysis of Dlx protein and nucleotide sequence. The analysis shows that there are two types of Dlx-coding regions: *Dlx2, Dlx3* and *Dlx5* and *Dlx1, Dlx4* and *Dlx6.* In terms of function, it is not clear if there is a difference between these two groups; however, mouse *Dlx1* and *Dlx2* and zebrafish *dlx3b* and *dlx4b* are functionally redundant, suggesting that *Dlx*-coding regions share some critical features between each other (Panganiban et al., 2002). All the vertebrate *Dlx* genes have a common organization with three exons and two introns, and the homeobox sequence is split between exon 2 and 3 (Figure 3.1). Several *Dlx* genes produce various transcripts due to alternative splicing. For instance, *Dlx5* encodes an alternate protein without the homeodomain, and with nuclear localization in the forebrain; however, its functional role has not been determined (Merlo et al., 2000). There are conserved *cis*-acting enhancers within the intergenic region of *Dlx1/Dlx2* (I12a and I12b) and *Dlx5/Dlx6* (I56i and I56ii) (Poitras, Ghanem, Hatch, & Ekker, 2007). Besides, *Dlx1* holds two conserved enhancer elements in the 5′flanking region called URE1 and URE2 (Hamilton et al., 2005).

As mentioned above, *Dlx* and *Dll* encode homeodomain transcription factors which share a 60 amino acid DNA binding domain. DLX proteins are involved in the regulation (activation or repression) of various downstream target genes. In addition to the homeodomain sequence, the amino acids flanking the homeodomain are conserved in the *Dlx*1, 4, 6 and *Dlx*2, 3, 5. There are multiple conserved features in *Dll*/DLX proteins. For example, they all have two tryptophan residues at the C-terminal of the homeodomain, which may facilitate interaction with co-factors.

The proline-rich domains are involved in oligomerization and transcriptional activation (Xiao, McCarthy, Aster, & Fletcher, 2000). Many TFs collaborate with other TFs to increase their DNA binding affinity and functional activity. There have not been many studies on DLX collaborative function, although one *in-vitro* study showed DLX2 and DLX5 form a dimeric complex with the mesodermal homeodomain proteins MSX1 and MSX2 through their homeodomains, which blocks MSX DNA binding and results in the inhibition of their transcriptional activities (H. Zhang et al., 1997). There have not been many studies on post-translational modifications of DLX proteins. Protein kinase C (PKC) phosphorylates DLX3 Serine138 within the homeodomain, which reduces the DNA binding ability of the homeodomain during keratinocyte development (G. T. Park, Denning, & Morasso, 2001).

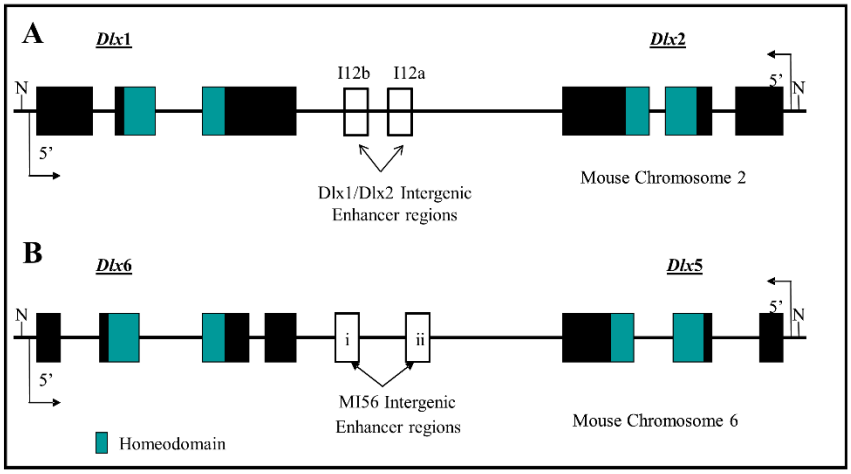

Figure 3.1. Schematic image of *Dlx1/Dlx2* and *Dlx5/Dlx6* genomic organization in the mouse

The *Dlx* gene family is organized in bigenic clusters with the genes facing each other (5′ to 3′). (A) *Dlx1* and *Dlx2* are located on chromosome 2, containing 3 exons with the homeodomain located at exons 2 and 3. There are two intergenic enhancer regions (I12b and I12a) localized between these two genes. (B) *Dlx5* and *Dlx6* are located on chromosome 6, presenting similar genomic alignment with the *Dlx1/Dlx2* genes. Modified from Zhou *et al* (Zhou et al., 2004). Reproduced with permission of the publisher through the Copyright Clearance Center.

3.2.2 Expression and function of *Dlx* genes

Dlx genes are expressed in multiple tissues during vertebrate development and in adulthood. *Dlx* genes function in the development of the apical ectodermal ridge of limb buds, which regulate the growth pattern of limbs in mice (Kraus & Lufkin, 2006). The loss of mouse single *Dlx* genes has not resulted in an obvious phenotype in the limbs; however *Dlx5/Dlx6* inactivation in mouse led to the split-hand/split-foot phenotype (Robledo, Rajan, Li, & Lufkin, 2002). *Dlx5* and *Dlx6* are the only mammalian *Dlx* family members which are expressed in the perichondral region of the embryonic axial and appendicular skeleton, since the beginning of cartilage initiation. *Dlx5/Dlx6* loss-of-function presents bone maturation abnormalities, such as a kinked tail and ossification delay in mice (Robledo et al., 2002). *Dlx5/Dlx6* has been found during endochondral bone formation, initiating at E12.5 in the axial skeleton, the clavicles and the leading edge of the calvaria. As described previously, DLX5 can form a heterodimer with MSX2 to antagonize each other's activity which is one proposed mechanism for *Dlx5's* role in osteogenesis (Newberry, Latifi, & Towler, 1998). Later on, they become expressed in the perichondral regions of ribs, as well as the digits. *Dlx5* deficient mice show delayed ossification of dermatocranial bones, and a mild defect in osteogenesis which suggests *Dlx5* role in osteoblast differentiation and bone formation (Acampora et al., 1999). *Dlx3* also plays a role in osteogenesis, as osteogenic *Dlx3* CKO mice presents a significant increase in bone mass which is associated with *Runx2* and *Dlx5* upregulation during osteoblastogenesis (Levi & Gitton, 2014). During mammalian craniofacial development, DLX family members are expressed early in the cephalic neural crest and later in the craniofacial mesenchyme, and dental mesenchyme. The branchial arches are parts of migratory hindbrain neural crest cells which eventually give rise to the craniofacial skeleton and dental mesenchyme. As early as 9.5 days of mouse development

Dlx1 and *Dlx2* genes are expressed in both the maxillary and the mandibular component of the first pharyngeal arch, whereas *Dlx3, Dlx5,* and *Dlx6* are expressed only in the mandibular portion of the first branchial arch. It has been proposed that *Dlx5/Dlx6* have an important function in the patterning of distal regions of the arches. Various mutations in *Dlx* genes lead to a diverse form of craniofacial abnormalities. For instance, *Dlx1* and *Dlx2* single knockout and *Dlx1/Dlx2* double knockout mice have defects in a subset of craniofacial bones and cartilages. The same study showed that *Dlx1* and *Dlx2* are necessary for the proximal domain of the first and second branchial arch development (M. Qiu et al., 1997). *Dlx5* is expressed in the otic cup and olfactory placode as early as E8; similarly, *Dlx5/Dlx6* are expressed in the ventral cephalic epithelium, nasal and otic placode (Acampora et al., 1999). *Dlx5* mutant mice display developmental defects in both olfactory pit and otic placode, and dysmorphogenesis of the semicircular channel (Levi et al., 2003).

Dlx1, Dlx2, Dlx5, and *Dlx6* are expressed in the CNS of mice (Eisenstat et al., 1999). Their expression is limited to the diencephalic and telencephalic parts of the forebrain, where they are expressed in a temporal order; *Dlx2, Dlx1, Dlx5,* and *Dlx6*. *Dlx2, Dlx1,* and *Dlx5* are mostly present in the subventricular zone, while *Dlx5* and *Dlx6* were found in post-mitotic neurons in the mantle zone (J. K. Liu, Ghattas, Liu, Chen, & Rubenstein, 1997). The temporal order of *Dlx* expression suggests the presence of a possible regulatory cascade among *Dlx* genes themselves. DLX1 and DLX2 subcortical telencephalon expressing cells migrate across the pallial-subpallial boundary and enter the mantle zone and subventricular zone of the cerebral cortex in the mouse embryo (Eisenstat et al., 1999). Later during CNS development *Dlx1* and *Dlx2* expression is present in interneurons of the olfactory bulb, which migrated from the SVZ. The expression of *Dlx* genes has been located in neurons producing γ-aminobutyric acid

(GABA) neurotransmitters, as *Dlx1/Dlx2* mutant mice displayed a reduction in neocortical interneurons and projection neurons (Anderson, Eisenstat, Shi, & Rubenstein, 1997).

The function of *Dlx* genes has been tested through loss and gain of function experiments in mice during the development. Interestingly, homozygous *Dlx* single knockout mice die pre-natally, or at birth; however, there has not been a significant CNS phenotype in these mice. The phenotype is more apparent in mice lacking at least two *Dlx* genes, specifically, when two genes belong to the same pair such as *Dlx1* and *Dlx2* (M. Qiu et al., 1997). As mentioned above, the *Dlx1/Dlx2* double knockout (DKO) mouse also dies at birth or a few hours after birth with severe craniofacial and CNS defects; however, the cause of death remains unknown (Cruz & Escobar, 2011). Neurogenesis within the subcortical telencephalon exhibit major blockages in *Dlx1/Dlx2* DKO mice, since the differentiation of basal ganglia late-born GABAergic (inhibitory neurotransmitter) neurons is decreased in the cerebral cortex. It has been speculated that the absence of tangentially migrating immature interneurons from the subcortical telencephalon to the cerebral cortex is the reason for this reduction (Anderson, Eisenstat, et al., 1997). It has been confirmed that *Dlx1/Dlx2* directly regulate GABAergic expression through transcriptional activation of *Gad1* and *Gad2* (glutamic acid decarboxylase isoforms) which are the main synthesizing enzyme of GABA from glutamate (Le et al., 2017). *Dlx1/Dlx2* and *Dlx5/Dlx6* (including enhancer regions) single nucleotide polymorphisms (SNPs) were found in contribution to human autism (Hamilton et al., 2005). *Dlx3* is involved during mouse placentation, and appears to play an important role in placental morphogenesis, as the mouse *Dlx3*-null embryo does not survive past midgestation due to gross vascularization of the placenta (Morasso, Grinberg, Robinson, Sargent, & Mahon, 1999). *Dlx5/Dlx6* mutant mice display split distal limb defects, comparable to ectrodactyly syndrome in humans and in humans the

Dlx5/Dlx6 deletions has been characterized with Split Hand/Foot (SHF) malformation (Filho et al., 2011). All of the foregoing suggest that the *Dlx* family of genes has multiple important functions in a variety of tissues during embryonic development.

3.2.3 Dlx1/Dlx2 expression and function in the retina

DLX2 expression has been detected as early as E11.5 in the dorsal retinal neuroepithelium in mice , and by E13.5 both DLX1 and DLX2 are expressed in the NR, with boundaries in the peripheral and central inner retina (de Melo et al., 2003). At E16, DLX1/DLX2 maintain similar expression profiles to E13 with less distinct boundaries. By E18, DLX1 and DLX2 expression is restricted to the ganglion cell layer (GCL) and the inner neuroblastic layer in mice, where they are co-expressed with markers for RGC, amacrine, and horizontal cells (de Melo, Qiu, Du, Cristante, & Eisenstat, 2003). While DLX1 expression robustly decreases after birth, DLX2 is expressed in RGCs, amacrine cells, horizontal cells and a subset of bipolar cells, but not photoreceptor cells through adulthood. Quantification of DLX2 throughout the developing retina revealed that the highest level is in the early differentiating neural retina, as well as the fully differentiated adult retina (de Melo et al., 2003). DLX2 co-localizes with syntaxin, an amacrine cell marker, at P0 with an increasing number of co-expressing cells by adulthood, suggesting that DLX2 may play a role in the terminal differentiation of amacrine cells (de Melo et al., 2003). DLX2 also co-localizes with protein kinase C (PKC), a mature rod bipolar cell marker in the ganglion cell layer (GCL) and neuroblastic layer at P0. Its expression overlaps with Calbindin (horizontal marker) in the NBL at P0. BRN3b is expressed in differentiating RGC, mostly localizing to the central inner retina and with a lesser extent in the outer retina at E13. Using BRN3b as an RGC marker, DLX2 is not co-expressed with BRN3b at E13. However, after E16 DLX2 and BRN3b expression overlaps, supporting the hypothesis that *Dlx2*

is required for differentiation and maintenance of late-born RGC cells (de Melo et al., 2003). DLX2 and VSX2 (formerly Chx10) are highly co-expressed throughout the retina with the boundary of expression at the inner central retina at E13, which could support DLX2 expression in RPCs as VSX2 is expressed in RPCs at this age.

The role of *Dlx* genes in retinal development has been the subject of a few studies. In *Dlx1/Dlx2* double knockout mice, RGC are decreased by approximately one-third due to enhanced apoptosis of RGCs, causing optic nerve thickness to be reduced compared to wild type at E18 (de Melo et al., 2005). This study suggested that *Dlx1/Dlx2* function is required for the terminal differentiation of RGCs (de Melo et al., 2005). *Brn3a* and *Brn3b* (RGC markers) expression are also decreased in the GCL of *Dlx1/Dlx2* DKO (de Melo et al., 2005). Unlike *Atoh7, Dlx1/Dlx2* is not required for the initiation of RGCs specification; however, *Dlx1/Dlx2* and *Brn3b* may act downstream of *Atoh7* to induce RGCs terminal differentiation. *Dlx1/Dlx2/Brn3b* TKO mice show dramatic loss of RGCs in the retina at both E13 and E18 (Zhang et al., 2017). These data support the possible presence of a *Dlx1/Dlx2* regulatory network to promote RGC fate during ganglion cell specification. DLX2 binds to the proximal promoter of *TrkB* -a member of the neurotrophin receptor family- which plays a role in the transcriptional regulation of *TrkB* which contributes to *Dlx1/Dlx2* dependent survival of RGC (de Melo et al., 2008). DLX2 is also co-expressed with GAD1 and GAD2 during retina development; however, unlike the forebrain, there have not been any defects in GABAergic interneuron differentiation in *Dlx1/Dlx2* null mice retina (Zhang et al., 2017). The role of *Dlx5* and *Dlx6* in the retina has not been rigorously studied. Although the expression of *Dlx5* mRNA has been detected at E16.5 in the GCL and INL, its function during retinogenesis remains unclear (Zhou et al., 2004). The

Dlx5 and *Dlx6* intergenic enhancer co-expresses with DLX1, DLX2, and DLX5 in RGC, amacrine and horizontal cells (Zhou et al., 2004).

There have been several studies on *Dlx* retinal expression in other animal models, for instance, *Dlx3* is expressed in the optic cup and neural retina during chicken retinal development (Dhawan, Schoen, & Beebe, 1997). Our lab could not detect the expression of *dlx* during zebrafish larvae retinal development or mature retina (unpublished data). Despite, all available research, still there has not been a clear image of *Dlx1/Dlx2* GRN and its downstream and upstream players in the retina.

3.2.4 Regulation of Dlx gene expression

There have been some efforts to identify dynamic upstream regulation of *Dll* and Dlx genes. The embryonic activation of *Dll* genes in *Drosophila* requires regulation by Wingless (*Wg*), a protein of the Wnt family. *Dll* transcriptional repression is controlled by the bone morphogenic protein homologue, and Decapentaplegic (*Dpp*) (Goto & Hayashi, 1997). In *Drosophila, Dll* expression is blocked in the abdomen by Ultrabithorax (*Ubx*) and abdominal-A (*abdA*), products of *Hox* genes (Vachon et al., 1992). It has been demonstrated that the *Shh* pathway can induce *Dlx2* expression in the mouse forebrain, as mice lacking *Shh* reveals lower *Dlx2* expression in the forebrain (Y. Ohkubo, K. Yun and J. L. R. Rubenstein, unpublished). Other signaling pathways such as BMP2 induces *Dlx2* in chondrocytes (Xu, Harris, Rubenstein, Mundy, & Harris, 2001) and BMP4 activates *Dlx5* in osteoblasts, as well as *Dlx1* and *Dlx2* expression in dental mesenchyme (Miyama et al., 1999). The FGF signaling pathway positively regulates *dlx2b* through its enhancer region in zebrafish during tooth development (Jackman & Stock, 2006). There have been a few studies on other TFs which can regulate *Dlx* gene

expression; for instance, *Msx1* is required to maintain *Dlx2* expression in branchial arche mesenchyme during mouse embryonic development (Chung et al., 2010).

Several *cis*-elements regulatory regions of *Dlx* genes have been identified, and it has been proposed that the *Dlx* pairs regulate each other via these shared enhancers. These regions include the intergenic region of *Dlx5/Dlx6* genes (I56i and I56ii) and *Dlx1/Dlx2* (I12a, and I12b), which are conserved between zebrafish, mouse and human. These regulatory elements are important for *Dlx* gene cross-regulatory interactions. For instance, *Dlx1/Dlx2* activates *Dlx5/Dlx6* expression by directly binding to the I56i enhancer region (Zhou et al., 2004). They also bind targets of other TFs; for example, *Mash1(Ascl1a)* binds to the I12b enhancer and activates *Dlx1/Dlx2* expression in mouse forebrain (Poitras et al., 2007). A somewhat similar network has been observed in zebrafish where *ascl1* activates expression of *dlx1a*, *dlx2a* and *dlx5a* in the pre-thalamus and hypothalamus via the I12b element during early forebrain development (MacDonald et al., 2013).

The regulatory role of microRNA (miRNAs) in various genetic networks during development has long been identified. miRNAs negatively control their target gene expression by binding to the mRNA untranslated region (UTR) and blocking its protein translation. A number of studies revealed that *Dlx* gene expression is regulated by various miRNAs in several tissues during embryonic development. Based on one of these studies, the muscle-specific miRNA, miR-133 downregulates the expression of *Dlx3* during myogenic differentiation *in-vitro*. miR-124 inhibits osteogenic differentiation by targeting several DLX transcription factors, including *Dlx5*, *Dlx3*, and *Dlx2* genes in mesenchymal stem cells (Qadir et al., 2015). However, there has not been any research on microRNA-mediated upstream regulation of *Dlx* gene expression during retina development.

3.2.5 The cone-rod homeobox (CRX)

The cone-rod homeobox (*Crx*) containing gene belongs to the mammalian orthodenticle (*Otd*) family including *Otx1*, *Otx2* and *Crx*. Original studies were from the *Drosophila Otd* homeodomain transcription factor, which is involved in the development of anterior brain, antenna, and eye. Later studies demonstrated that *Otd* plays a critical role in photoreceptor specification via regulation of Opsin expression (Tahayato et al., 2003). The *Crx* member of the family is expressed in rod and cone photoreceptors in mouse retina. The CRX protein has 299 amino acids, with an *Otd/Otx*-like paired homeodomain (HD) near the N-terminus and OTX-tail domains that share homology with OTX1 and OTX2. The CRX homeodomain shares 86% homology with the OTX2 homeodomain and 44% homology with the overall OTX2 protein (Martinez-Morales et al., 2001).

Crx controls the specification and maintenance of retinal photoreceptors and pineal gland pineocytes during circadian regulation in mice (Furukawa et al., 1997). *Crx* expression starts at E12.5 in mice retina; it is localized in the outer NBL near the RPE, and it is required for the differentiating retinal progenitors into rods or cones and their maintenance throughout the adulthood in the ONL (Furukawa et al., 1997). *Crx* peak expression is at P6, the same time point as rod photoreceptors specification and maturation. The *Crx* expressing cells are post-mitotic photoreceptor precursors, and they come from progenitor cells which express *Otx2* but not *Pax6*. It is possible that *Crx* also plays a role in rod bipolar cells differentiation (X. Wang et al., 2002). *Crx* deficient mice fail to form outer photoreceptor segments after P14, which results in disrupted cone and rod activities in electroretinogram (ERG) tests. The expression of several of the photoreceptor specifying genes (*Nrl, Nr2e3*, and *NeuroD1*) is significantly disrupted in $Crx^{-/-}$ mice. Over-expression of *Crx* in the mouse retina demonstrates an increased number of clones

with rods and decreased number of clones with amacrine and Muller glial cells (Furukawa et al., 1997). *Otx2* is upstream of *Crx* whereby *Otx2* is critical for photoreceptor cell fate specification, and subsequently activates *Crx* expression. Unlike *Otx2, Crx* is not required for early PR cell differentiation but rather for the development and maintenance of PR cells (Corbo et al., 2010). CRX itself controls downstream regulation of photoreceptor-specific genes, such as Rhodopsin, cone opsin, *Nrl*, and *Nr2e3*. CRX activates and synergizes the *Nrl* transcription factor to induce the rod differentiation lineage. In addition to PR specific genes, *Crx* binds to its own promoter to autoregulate its own expression in a dose-dependent manner (Hennig, Peng, & Chen, 2008). Interestingly, *Crx* also binds to the *Otx2* promoter and represses its expression, since in $Crx^{-/-}$ mice, *Otx2* expression increased by greater than two-fold in the retina. This shows a network whereby *Otx2* is first essential for inducing PR fate by activating *Crx* in precursor cells. Increased *Crx* expression leads to *Otx2* repression and PR specific gene (*Nrl* and *Nr2e3*) activation required for the terminal differentiation and survival of rod and cone photoreceptors (Blackshaw, Fraioli, Furukawa, & Cepko, 2001). It appears that *Otx2* and *Crx* have redundant but necessary roles in photoreceptor development and maintenance (Hennig et al., 2008).

CRX dominant mutations, whether frameshift or missense, have been linked to degenerative disorders such as cone-rod dystrophy and retinitis pigmentosa in humans (den Hollander, Roepman, Koenekoop, & Cremers, 2008). There is increased and ectopic expression of CRX in the *Dlx1/Dlx2* double knock out mice implicating *Dlx* genes in the regulation of the photoreceptor cell fate (de Melo et al., 2005). This suggests that either DLX1 and/or DLX2 play a direct or indirect repressive role in *Crx* expression. Based on previous findings we hypothesized that the *Dlx2* homeobox genes restrict the expression of *Crx* spatially and temporally during retinal development.

3.2.6 Orthodenticle Homeobox 2 (OTX2)

The mammalian orthologs of the *Drosophila* orthodenticle family, *Otd* (orthodenticle-like homeobox gene) genes encode paired-class homeodomain proteins, and they are expressed throughout the developing nervous system and required for proper anterior-posterior patterning of the brain. The vertebrate ortholog to *Otd* is comprised of three family members: *Otx1, Otx2*, and *Crx* as described earlier (Simeone et al., 1993). *Otx1* expression starts early in the developing mouse embryo throughout the presumptive forebrain and midbrain epithelium, and its expression is maintained in the VZ up to mid-late gestation stages (Simeone et al., 1993). In mouse, *Otx2* expression has been found in the epiblast, distal/anterior visceral endoderm, anterior mesendoderm, anterior neuroectoderm, forebrain/midbrain and cephalic mesenchyme. Early expression of *Otx2* is required for normal gastrulation and anterior neural plate induction. Both *Otx1* and *Otx2* are expressed in developing sensory organs, including olfactory placodes, otic and optic vesicles (Acampora, Gulisano, Broccoli, & Simeone, 2001). *Otx2* knockout mice are embryonic lethal with severe defects in gastrulation, the formation of axial mesoderm and the loss of anterior neural tissues (Ang et al., 1996). *Otx2* expression in retina initiates at E11.5 strongly in RPE and weakly in NBL of the neural retina. *Otx2* is required for the development and maintenance of RPE, by transactivation of genes encoding melanosome glycoproteins (Martinez-Morales et al., 2003). In mice, *Otx2* and *Mitf* are both necessary for RPE development, while in zebrafish *otx1a* and *otx2* play a major role in RPE development. During early retinogenesis, *Otx2* is expressed in postmitotic progenitor cells, which have the potential to develop into various retinal cell types (Baas et al., 2000). *Otx2* expression increases in the neural retina at E12.5 and it becomes localized in the outer NBL during late retinogenesis. *Otx2* expression significantly decreases in both RPE and the outer NBL after birth. Conversely, *Otx1*

maintains its appearance throughout the iris, ciliary process, and lachrymal gland after birth (Acampora et al., 2001). Mice with an *Otx2* conditional knockout in the eye resulted in microphthalmia with more amacrine-like cells and fewer photoreceptor cells (Nishida et al., 2003), and *Otx2* overexpression leads to excess photoreceptors and reduced numbers of amacrine cells (Wang et al., 2014). Thus, it was concluded that *Otx2* is necessary and sufficient for photoreceptor cell fate determination. Microarray analysis of an *Otx2* eye conditional knockout demonstrated a significant decrease in a number of photoreceptor specification genes such as *Crx, Nrl* and *Nr2e3* (Omori et al., 2011). As mentioned previously, *Otx2* is a positive upstream regulator of *Crx*, by directly binding to its promoter (M. Hejazi, Z. Li and D. Eisenstat, unpublished data).

It has been suggested that *Otx2*-expressing RPCs harbor the potential to differentiate to bipolar or horizontal cells depending on the intrinsic profile of the progenitor cell (C. L. Cepko, 2015). For instance; in the presence of *Vsx2, Otx2*-expressing progenitor cells may become bipolar cells. *Otx2* has been implicated in a number of eye disorders including microphthalmia, optic nerve hypoplasia, and optic nerve aplasia (Chatelain, Fossat, Brun, & Lamonerie, 2006). In addition to ocular disorders, *Otx2* overexpression has been found in a malignant childhood brain tumour (medulloblastoma) (Boon, Eberhart, & Riggins, 2005). We hypothesized that *Dlx2* negatively regulates *Otx2* expression to induce RGC fate over PR fate. It is possible that DLX2 repression of *Otx2* expression is an additional mechanism by which *Crx* expression is repressed in a subset of RPCs, which supports the requirement of DLX2 in RPC fate decisions.

3.2.7 MicroRNA-124

Not much is known about the microRNA-mediated regulation of the *Dlx1/Dlx2* genes in vertebrates. miRNAs are endogenous, small, non-coding, regulatory RNAs, 18-22 nucleotides in

size. MicroRNAs bind to target sites in the 3' UTR region of mRNAs and negatively regulate gene expression post-transcriptionally. MicroRNAs have been largely found during neurogenesis and neuronal progenitor cell specification in the CNS (Coolen et al., 2009). MiR-132 regulates the differentiation of dopaminergic neurons by directly regulating a principal dopamine neuron determining factor called *Nurr1* in mice (Yang et al., 2012). MiR-9 is involved in establishing a distinct type of motor neuron by regulating its target protein *FoxP1*, which specifies distinct motor neuron subtypes in the chick spinal cord (Otaegi, Pollock, Hong, & Sun, 2011). These observations suggest that miRNA expression in GRNs may contribute to defining neuronal identity. The miRNAs are involved in many aspects of retinal development, including establishing distinct cell fate. There have been several *Dicer* retina conditional knockout mouse studies to determine the role of miRNAs in retinogenesis. *Cre*-mediated *Dicer* excision in RPC have severe phenotypes in the eye. For instance, in *Pax6-Cre* (*Pax6* is expressed in RPCs at E10) *Dicer* CKO mice, the generation of early cell types such as RGC and horizontal cells was increased, and the production of later cell types like PR cells were decreased indicating the role of miRNAs in RPC competence shift over time (Georgi & Reh, 2010). *Dicer* CKO using *Rx-Cre* (expressed in mice RPC) caused massive cell death in the eye and overall eye size reduction (Pinter & Hindges, 2010). miR-124 is a highly conserved miRNA from worms to human, and it has been estimated to be the most abundant miRNA in the brain (Sun, Luo, Guo, Su, & Liu, 2015). It is almost exclusively expressed in the subventricular zone and neural retina during CNS development (Andreeva & Cooper, 2014). In *Xenopus*, miR-124 regulates the proper pathfinding of retinal cone photoreceptor, and the miR-124a isoform is essential for cone maturation by *Lhx2* transcriptional repression (Sanuki et al., 2011). miR-124 knockout mice show newly differentiated cone apoptosis, which means miR-124 may control PR cell identity (Sanuki et al.,

2011). MiR-124 is expressed in the GCL at E13.5, later at P1 in photoreceptor cells, and maintains its expression throughout adulthood in the inner segment of PR cells (Sanuki et al., 2011). *Dlx* genes were reported as a target of miR-124 in several tissues. miR-124 enhances neuronal differentiation in the subventricular zone (SVZ) by regulating *Dlx2* during mouse neurogenesis (Cheng, Pastrana, Tavazoie, & Doetsch, 2009). Furthermore, miR-124 blocks myogenic differentiation while promoting adipogenic cell fate by targeting the 3´UTR of *Dlx5* in mouse mesenchymal stem cells (Qadir et al., 2014). As mentioned previously, *Dlx5/Dlx3* genes have been postulated to be involved in osteogenesis and chondrogenesis. Later studies revealed that miR-124 endogenously reduces *Dlx3, Dlx5* and *Dlx2* expression by targeting their 3´UTR to inhibits osteoblast differentiation (Shea, Edgar, Einhorn, & Gerstenfeld, 2003).

Our further analysis of the *Dlx2* gene 3´UTR by a target prediction algorithm demonstrated that there is a single binding site for a miR-124 seed sequence, which is highly conserved in most vertebrates. Additionally, based on our lab's previous studies, using combined DLX2 immunohistochemistry and *in-situ hybridization* with a miR-124 probe, we demonstrated that *Dlx2* and miR124 are co-expressed in the same retinal cell population from E13.5 to P14. Thus, we predicted that there is a reciprocal negative feedback loop between miR-124 and *Dlx2* expression during murine retina development.

3.3 Results

3.3.1 DLX2 occupies the *Crx* promoter at E18 *in-vivo*

Dlx1/Dlx2 DKO mice show 33% RGC reduction, in addition to decreased optic nerve thickness (Zhou et al., 2004). *Crx* expression is increased in the ONL and ectopically expressed in the GCL in the *Dlx1/Dlx2* DKO implicating that *Dlx* genes might be involved in the regulation of photoreceptor cell fate (de Melo et al., 2008). To explore the regulatory function of DLX2 on *Crx* expression, the first step was to investigate if DLX2 is bound to *Crx* regulatory elements. To this end, I performed *in-vivo* chromatin immunoprecipitation (ChIP) analysis using embryonic retina as input tissue. TFs interact with chromatin at specific binding motifs to influence gene expression. The 3 kilobase pair (kbp) *Crx* proximal promoter contains 17 potential binding sites (ATTA/TAAT) for DLX2 as a homeodomain TF. DLX2 potentially can bind to these sequence specific sites; however, the ability of binding is also regulated by multiple factors such as histone marks and other TFs. In order to test all the potential binding sites for DLX2 binding, the promoter was arbitrarily divided into 6 regions to make them more convenient to characterize (Figure 3.2A). To determine which, if any, of these putative binding sites, are occupied by DLX2 *in situ*, ChIP-PCR assays were performed. We chose to isolate CD1 timed pregnant mice at E18 since it was previously shown that *Crx* is involved in later photoreceptor differentiation and maintenance. Using an in house previously characterized polyclonal antibody specific for DLX2 (Eisenstat et al., 1999), we were able to isolate DLX2 protein-DNA complexes. As DLX2 is not expressed in the embryonic hindbrain, this tissue was used as a negative control. Following the reverse cross-linking and PCR amplification, region six (R6) was determined as one region which DLX2 occupies (Figure 3.2B). This result suggested that DLX2 occupies the *Crx* promoter at the most proximal region to the transcriptional start site.

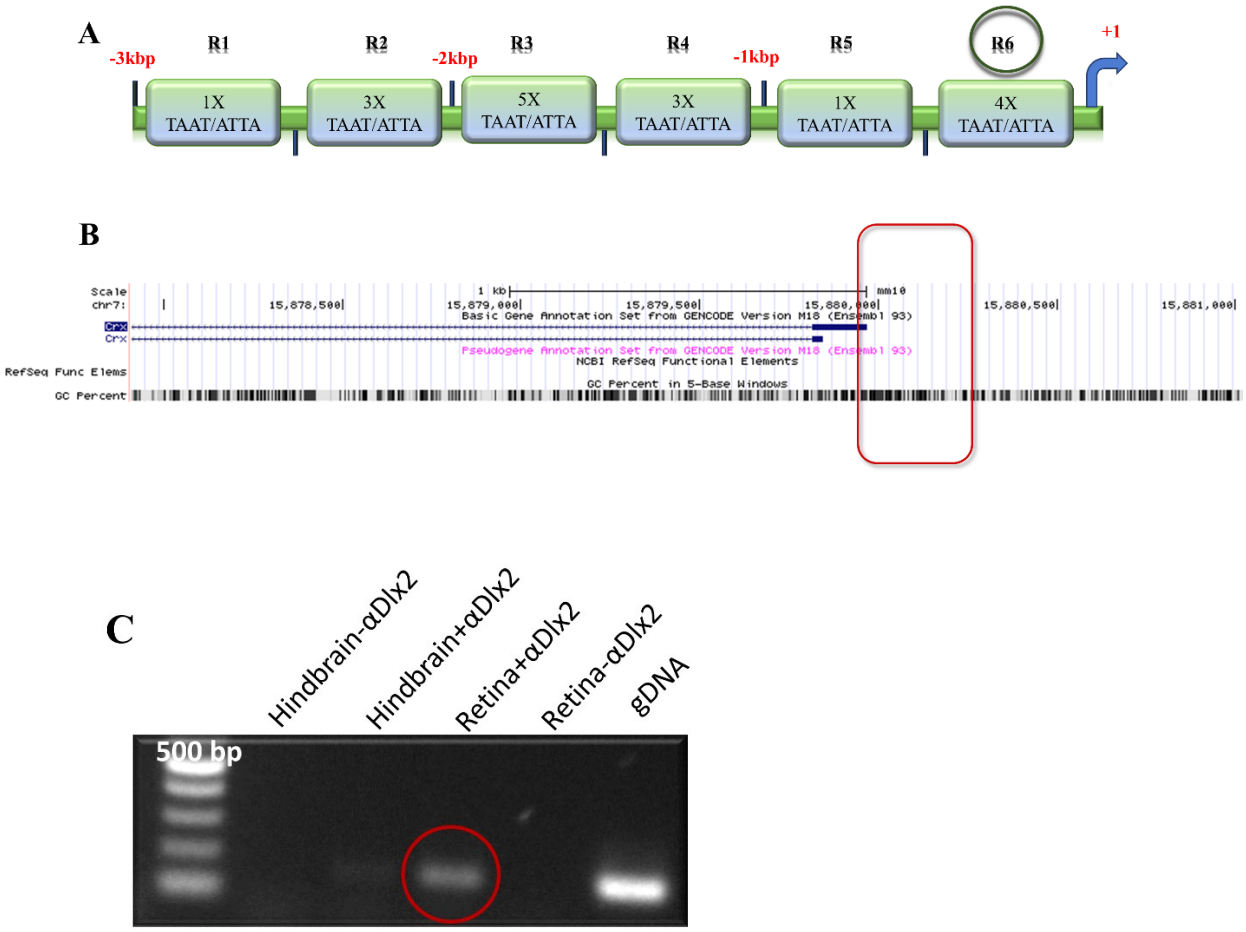

Figure 3.2. Schematic diagram of the *Crx* promoter

(A) Schematic diagram of the *Crx* promoter with potential homeodomain binding sites. *Crx* promoter map with 17 potential DLX binding sites. The promoter was divided to 6 regions (R1-R6); each of the regions has at least one potential binding site (1X). Encircled region 6 (R6) was positive for DLX2 binding. (B) Genome browsers were used to assess the entire *Crx* gene including the promoter region. (C) Using a DLX2 specific antibody (Ab), promoter occupation by DLX2 was observed at *Crx* promoter region 6 (R6) *in-vivo* in E18.5 retina as indicated by the encircled bands (red circle). DLX2 is not expressed in the hindbrain which is used as a negative tissue control. gDNA (genomic DNA) was used as a PCR positive control. Hindbrain (HB), Retina (R), Genomic DNA (gDNA), DLX2 antibody (αDLX2), base pair (bp).

3.3.2 DLX2 directly binds to the *Crx* promoter region *in-vitro*

The interaction between protein and DNA is critical for TFs to control many cellular processes. In addition to the ChIP experiment, electrophoretic mobility shift assay (EMSA) is another technique to identify sequence-specific, direct DNA-binding. Thus, to determine the direct binding of DLX2 protein to the *Crx*-R6 promoter region, which was pulled down by ChIP, recombinant DLX2 protein was radiolabelled with α-32P and analyzed with EMSA. The EMSA assay exploits relative migration rates through a polyacrylamide gel based on the complex size. The labeled probe (*Crx*-R6) incubated with DLX2 recombinant antibody demonstrated a gel shift (Figure 3.3B). To further confirm DLX2 binding specificity, DLX2/*Crx* complexes were incubated with DLX2 antibody to build a larger molecular weight complex, and a supershift was observed (Figure 3.3B). The shifted band supports the direct binding of DLX2 to the *Crx* promoter which further implicates the role of DLX2 in regulation of *Crx* expression.

Furthermore, site-directed mutagenesis experiments were carried out to identify the essential binding sequences within this region. *Crx*-R6 contains four TAAT/ATTA sites; thus, initially the most proximal ATTA motif to the transcriptional start site of the *Crx*-R6 promoter region was mutated. The most distal A was altered to G by the PCR SOE method (Splicing by overlap extension), and the mutated-*Crx*-R6 (m-*Crx*-R6) was sub-cloned into the pGL3 basic vector (Figure 3.3A). The mutated probe was resolved on an acrylamide gel along with wild-type probe in the presence of recombinant DLX2 (rDLX2). A shift and supershift were observed in both mutant and wild-type probe, which suggests that DLX2 can still bind to m-*Crx*-R6 in spite of one nucleotide change (Figure3.3B). Next, the entire ATTA binding site was deleted (D-*Crx*-R6) to find out if DLX2 can still recognize the *Crx* promoter and occupy it in this region. After the binding site deletion, we did not find a shift compared to wild *Crx*-R6 clones (Figure 3.3C).

Altogether, these results confirm that DLX2 binds to the *Crx*-R6 region of the *Crx* promoter *in vitro*, which indicates that this binding site may be critical for DLX2 binding, as one binding sequence deletion is sufficient to disrupt rDLX2 binding to this region.

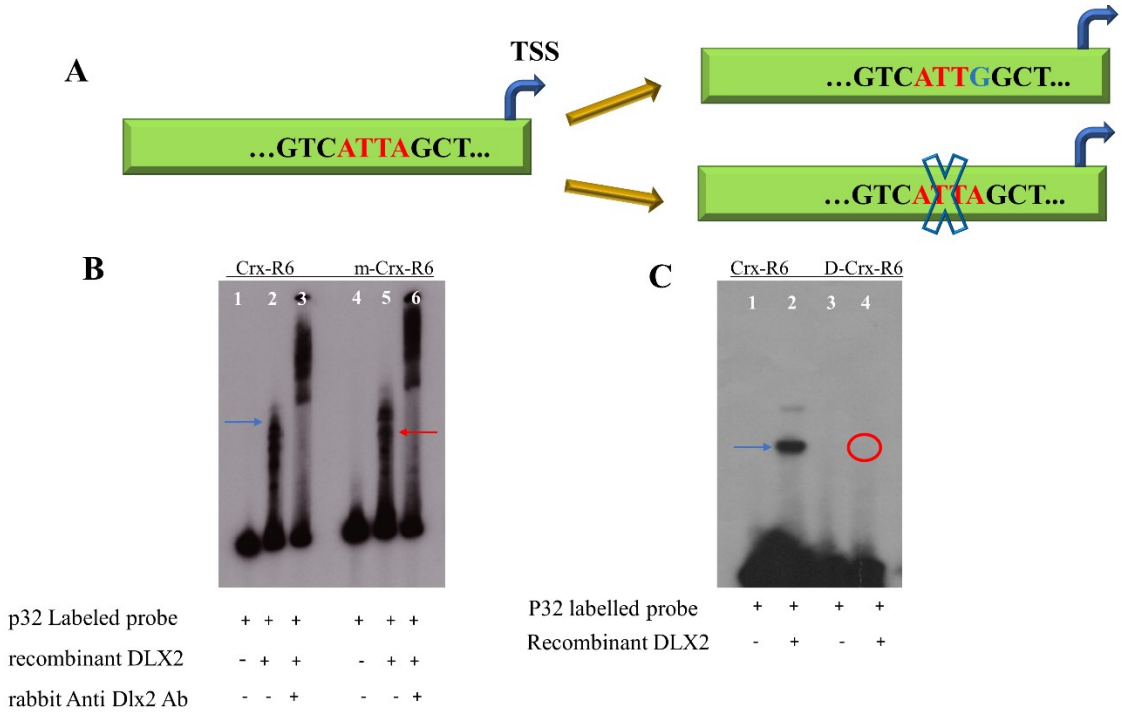

Figure 3.3. DLX2 directly and specifically binds to a *Crx* regulatory element *in-vitro*

(A) Schematic image of DLX2 binding sites alterations. The ATTA binding site was introduced to point mutation of A to G, and the entire binding site deletion (B). Using recombinant DLX2 protein and radioactively labelled *Crx-R6* probes, *Crx*-R6 was shown to bind directly to DLX2 as protein-DNA complexes "shift" (blue arrow) in a non-denaturing polyacrylamide gel relative to a free probe. Free *Crx-R6* probe (lane 1), *Crx-R6*/rDLX2 probe gel shift (lane2), *Crx-R6*/rDLX2/αDlx2 supershift (lane 3). Mutated labelled probe (*m-Crx-R6*) and WT labelled *(Crx-R6)* probe were incubated with recombinant DLX2 (rDLX2) protein. rDLX2/probe complexes were then resolved on a non-denaturing acrylamide gel; binding was found between *m-Crx-R6* and rDLX2 (red arrow) (B) Free m-*Crx-R6* probe (lane 4), m-*Crx-R6*/rDLX2 probe gel shift (lane 5), m-*Crx-R6*/rDLX2/αDlx2 supershift (lane 6) (C) Deletion of ATTA motifs was performed to show the critical role of each binding site to DLX2 transcription factor binding. Deleted labelled probe (*D-Crx-R6*) and WT labelled *(Crx-R6)* probe were run on an acrylamide

gel, and no binding was found between *D-Crx-R6* and rDLX2 (encircled). Free *Crx-R6* probe (lane 1), *Crx-R6*/rDLX2 probe gel shift (lane 2), Free *D-Crx-R6* probe (lane 3), *D-Crx-R6*/rDLX2 probe gel shift. Transcriptional start site; TSS, Dlx2 antibody; Dlx2 Ab

3.3.3 DLX2 negatively regulates *Crx* expression *in-vitro*

Although protein-DNA binding is an important first step for TF regulatory action, it does not necessarily have functional consequences. The luciferase reporter assay is a commonly used tool to study gene expression at the transcriptional level *in-vitro.* To investigate the functional consequences of DLX2 on the identified *Crx* regulatory element *in-vitro*, the luciferase reporter assay was carried out. Since *Crx*-R6 was positive for both ChIP and EMSA, I co-transfected HEK293 cells with a plasmid encoding DLX2 protein and *Crx*-R6 promoter cloned upstream of the luciferase gene. HEK 293 cells were transfected with empty pGL3 plasmids and empty pcDNA3 plasmids as controls. In the presence of DLX2, the *Crx*-R6 promoter had repressive effects on luciferase expression relative to empty pGL3 in the presence of DLX2 protein (Figure 3.4A). This data suggests that DLX2 has a repressive functional effect on *Crx* gene expression *in-vitro*. As the deletion of the most proximal binding motif led to no DLX2 binding on the *Crx* promoter, we decided to further confirm it by performing the reporter gene assay using D-*Crx*-R6 subcloned into the pGL3 vector. Based on luciferase expression results, the functional effect of DLX2 was altered in the presence of D-*Crx*-R6, and luciferase expression was no longer decreased (Figure 3.4B). Therefore, the DLX2 protein not only binds to the *Crx* promoter but also functionally decreases *Crx* expression *in vitro*.

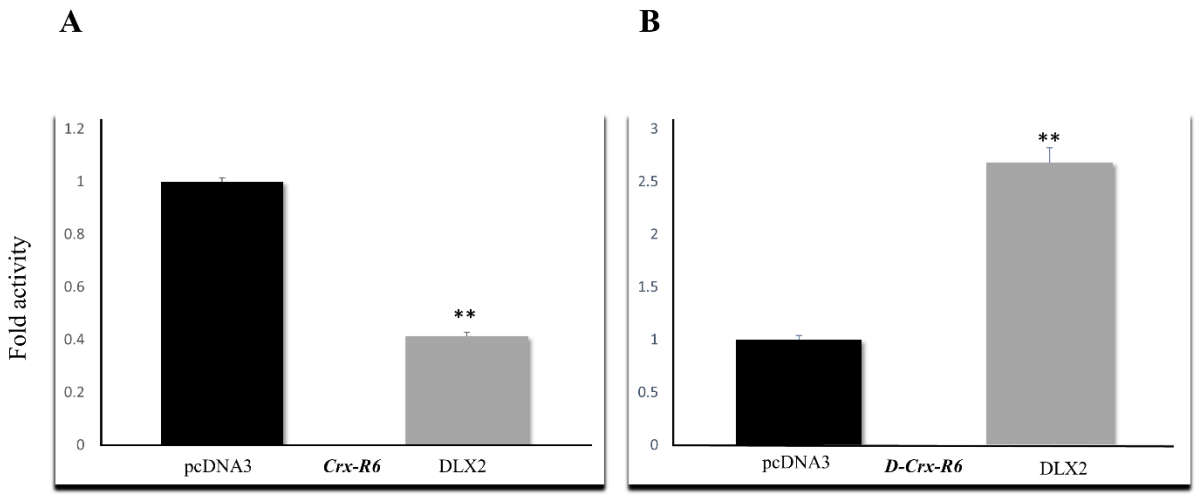

Figure 3.4. DLX2 represses *Crx* expression *in-vitro* by specifically binding to *Crx* promoter region 6

The functional consequence of DLX2 binding to *Crx* regulatory elements *in-vitro* was examined using luciferase reporter gene assays (A). In the presence of DLX2 expression vector and *Crx* Region 6, reporter vector luciferase expression is reduced compared to empty vector (pcDNA3) controls (B) The deletion of the *Crx*-R6 binding site changed the DLX2 regulatory effect on luciferase expression, where in the presence of DLX2 expression vector and *D-Crx-R6* reporter vector luciferase expression did not reduce compared to empty vector. n=3, **=P ≤ 0.01, *Crx* region 6; *Crx-R6,* Deletion *Crx* region 6; *D-Crx-R6*

3.3.4 DLX2 represses *Crx* gene expression during late retinal ganglion cell differentiation

Based on our *in-vitro* findings DLX2 binds to the *Crx* promoter via TAAT/ATTA motifs and represses its expression. TFs are one of the major cell fate determining factors for RPC during development. They often interact with several other factors, intrinsic or extrinsic, in networks to guide the specification of RPCs (Zuber et al., 2003). As a result, DLX2 may play a role in regulating RPC fate decision during retinal development. Based on the *in-vitro* data we hypothesized that *Dlx2* and *Crx* could interact with each other in a network to specify RGC versus PR cell fate during late retinal development. To investigate DLX2 negative regulation on *Crx* expression *in-vivo, Dlx1/Dlx2* DKO/WT pregnant mice at time point E18 were used since CRX is involved in late PR differentiation and maintenance. WT and DKO eye tissues were fixed in 4% PFA, and the frozen sections were immunostained with a CRX antibody. At E18, CRX expression was increased in the *Dlx1/Dlx2* DKO mouse retina (Figure 3.5C, D) compared to WT controls (Figure 3.5A, B).

Reporter mouse models are a great tool to monitor specific gene expression, therefore the LacZ reporter gene was placed under the control of a *Crx-R6* promoter *in vivo* (A. Furukawa et al., 2002). To further verify that DLX1/DLX2 repress *Crx* gene expression *in-vivo*, these *CrxLacZ* reporter mice were crossed with our *Dlx1/Dlx2* heterozygous mouse. We analyzed the β-galactosidase expression by performing X-gal staining on the E18 retina and compared DKO/WT retina tissues for CRX expression. In the absence of *Dlx1/Dlx2* function, increased levels of LacZ were reported compared to *Dlx1/Dlx2* controls (Figure 3.6A-F). To quantify *Crx* transcript expression between *Dlx1/Dlx2* DKO and WT, quantitative RT-PCR on the E18 retina tissues was performed. As expected, *Crx* expression was significantly increased in the absence of *Dlx1/Dlx2* function in the compound *CrxLacZ* reporter mice (Figure 3.6G). Altogether these

results support that DLX2 may negatively regulate the expression of *Crx* so as to block PR differentiation, as in the absence of both DLX1 and DLX2, a higher number of *Crx*-expressing cells was observed.

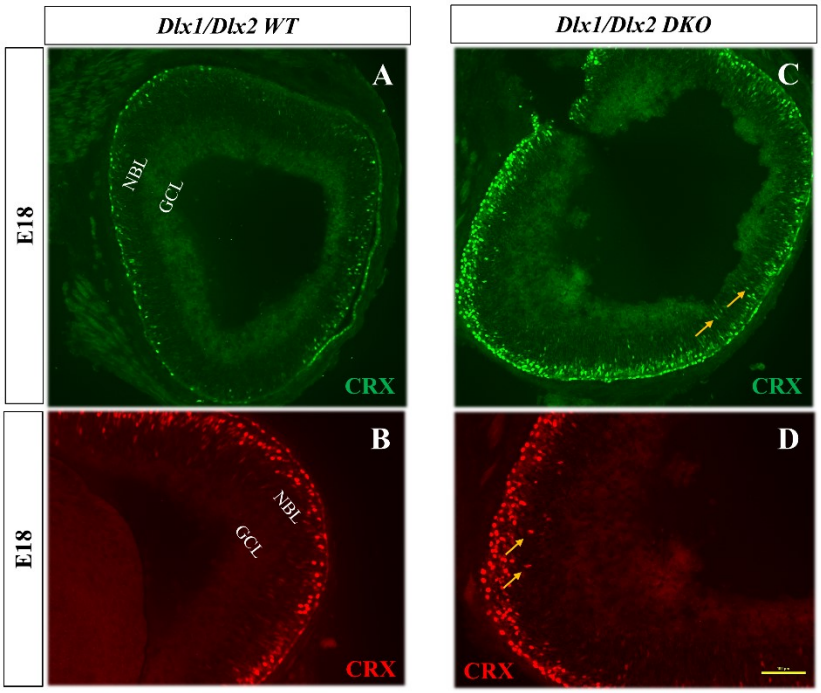

Figure 3.5. CRX expression is increased in the absence of *Dlx1*/*Dlx2* at E18 in mouse retina

Immunofluorescence with CRX antibody on *Dlx1/Dlx2* DKO and *Dlx1/Dlx2* WT E18 retina was carried out. (A, B) *Crx* is expressed in the outer neuroblastic layer in wild type mice retina tissues at E18. (C, D) *Crx* expression is increased in the outer neuroblastic layer with ectopic expression (yellow arrow) in the inner neuroblastic layer in *Dlx1/Dlx2* DKO E18 retina compared to control mice. GCL; ganglion cell layer, NBL; neuroblastic layer, Scale = 100 µm

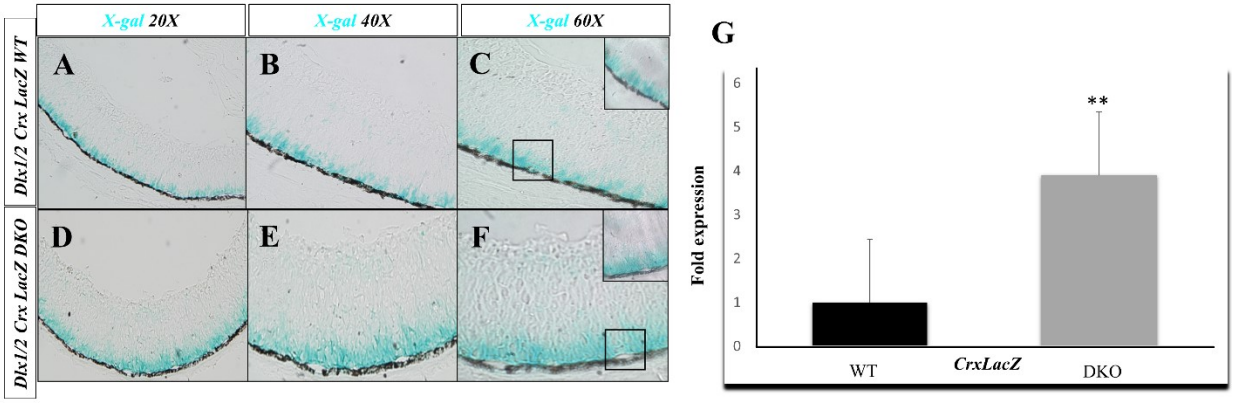

Figure 3.6. *Crx* expression is increased in *Dlx1/Dlx2* X *CrxLacZ DKO* compared to *Dlx1/Dlx2* X *CrxLacZ* WT in E18 retina tissues

X-gal staining of *Dlx1/Dlx2 X CrxLacZ* DKO versus *Dlx1/Dlx2 X CrxLacZ* WT E18 was carried out. (D, E, F) *LacZ* expression was higher in *Dlx1/Dlx2* DKO reporter mouse compared to (A, B, C) *Dlx1/Dlx2* WT reporter mouse. (G) The transcript level of *LacZ* expression was quantified by qRT-PCR, and *LacZ* expression was increased in the absence of *Dlx1/Dlx2.* The Xgal staining experiment was performed by Mehdi Eshraghi; n=3, **=P ≤ 0.01

3.3.5 DLX2 occupies the *Otx2* promoter at E18 *in-vivo*

Our studies showed that DLX2 is involved in the negative regulation of *Crx* expression during late retina development. We consider this as part of a GRN which decides between RGC and PR cell fate during retinal development. The GRN often contains several nodes that interact with one another; hence, it is possible that the *Dlx2* regulatory network has several nodes. It has been shown that OTX2 is critical for PR differentiation, as it is located upstream of *Crx* to turn on its expression in the developing retina (Glubrecht, Kim, Russell, Bamforth, & Godbout, 2009). We proposed that DLX2 repression of *Otx2* expression can be an additional mechanism by which *Crx* expression is repressed, supporting the fact that DLX2 is required for RPC cell fate decisions.

I performed ChIP assays on E18 mice retina tissues in order to identify whether DLX2 interacts with the *Otx2* promoter. There are 27 putative homeodomain binding sites in the 3 kb of the *Otx2* promoter sequence. To simplify future sub-cloning, the *Otx2* promoter was divided into 10 regions with the candidate homeodomain TAAT/ATTA DNA-binding motifs (Figure 3.7A). Out of ten *Otx2* promoter regions, DLX2 occupied: region 2 (R2), region 4 (R4), region 8 (R8), region (9), and region (R10) (Figure 3.7B-F). The hindbrain was used as a negative control as DLX2 is not expressed in the hindbrain. This data suggests that the DLX2 occupies multiple regions of the *Otx2* promoter during late RGC development and I proceeded to study whether DLX2 block its transcription to promote RGC fate at this stage.

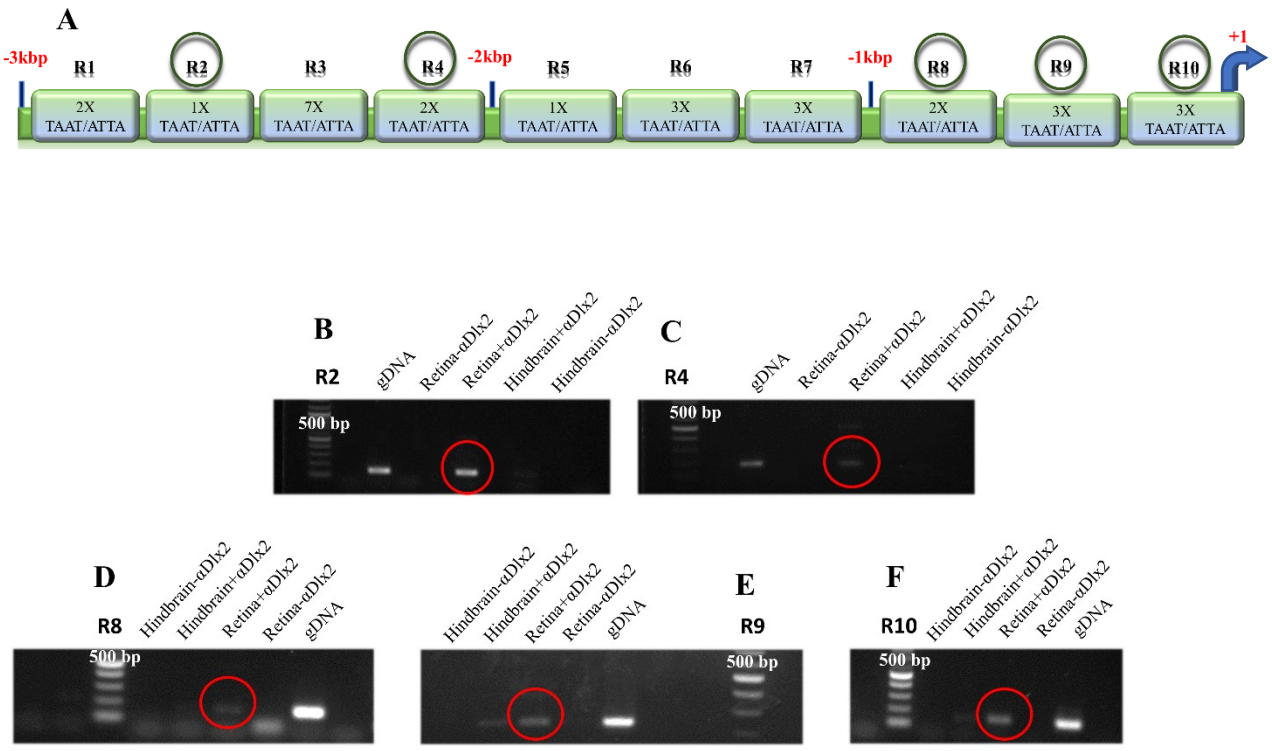

Figure 3.7. DLX2 binds to the *Otx2* promoter *in-vivo*

(A) Schematic diagram of the *Otx2* promoter with potential homeodomain binding sites. *Otx2* promoter map with 27 potential DLX binding sites. The promoter was divided into 10 regions (R1-R10), each region at least has one potential binding site (1X). (B-F) Using an antibody (Ab) specific for DLX2, occupation by DLX2 was observed at *Otx2* promoter regions at E18 retina as indicated by the encircled bands (encircled) (B) Encircled region 2 (R2), (C) region 4 (R4), (D) region 8 (R8), (E) region 9 (R9), and (F) region 10 (R10) were positive for DLX2 occupancy. DLX2 is not expressed in the hindbrain which was used as a negative tissue control. gDNA (genomic DNA) was used as a PCR positive control. Hindbrain (HB), Retina (R), Genomic DNA (gDNA), base pair (bp), Dlx2 antibody (αDlx2)

3.3.6 DLX2 directly binds to *Otx2* promoter *in-vitro*

Based on our ChIP experiments, several *Otx2* promoter regions were occupied by the DLX2 protein *in vivo*. Radioactive EMSA was used to confirm the direct binding of DLX2 to *Otx2* regulatory sequences using DLX2 recombinant protein. ChIP-positive regions were labeled by α-32P and incubated with DLX2 protein. A shifted band in the polyacrylamide gel was observed for R2, R4, and R8 as DLX2 directly binds to the probes, due to the delayed migration of larger molecular weight complexes compared to the migration of radiolabelled probe alone (Figure 3.8A-C). The DLX2-DNA complex was incubated with DLX2 specific antibody (supershift) as a specificity control. Site-directed mutagenesis of putative homeodomain DNA binding motifs located in the *Otx2* promoter was performed to identify the critical binding sites. Region 2 and region 4 TAAT/ATTA binding motifs were deleted (D-*Otx2*-R2 and D-*Otx2*-R4), and EMSA was repeated using mutant *Otx2* promoter probes along with WT (*Otx2*-R2 and *Otx2*-R4) probes to determine whether these sites are critical for DLX2 binding *in-vitro* (Figure 3.9A, C). Following the R2 TAAT binding motif deletion, no band was observed in the presence of rDLX2 (Figure 3.9B). The region 4 mutant was created by deleting one of the ATTA motifs (from 5′to 3′). While *Otx2*-R4 wild-type promoter showed a strong band for shift and supershift, the D-*Otx2*-R4 mutant promoter presented a faint shifted band on the gel (Figure 3.9D). Our findings suggest that DLX2 directly binds to *Otx2* regulatory elements at multiple regions, and that the R2 binding sites are critical for DLX2 promoter occupation *in vitro*.

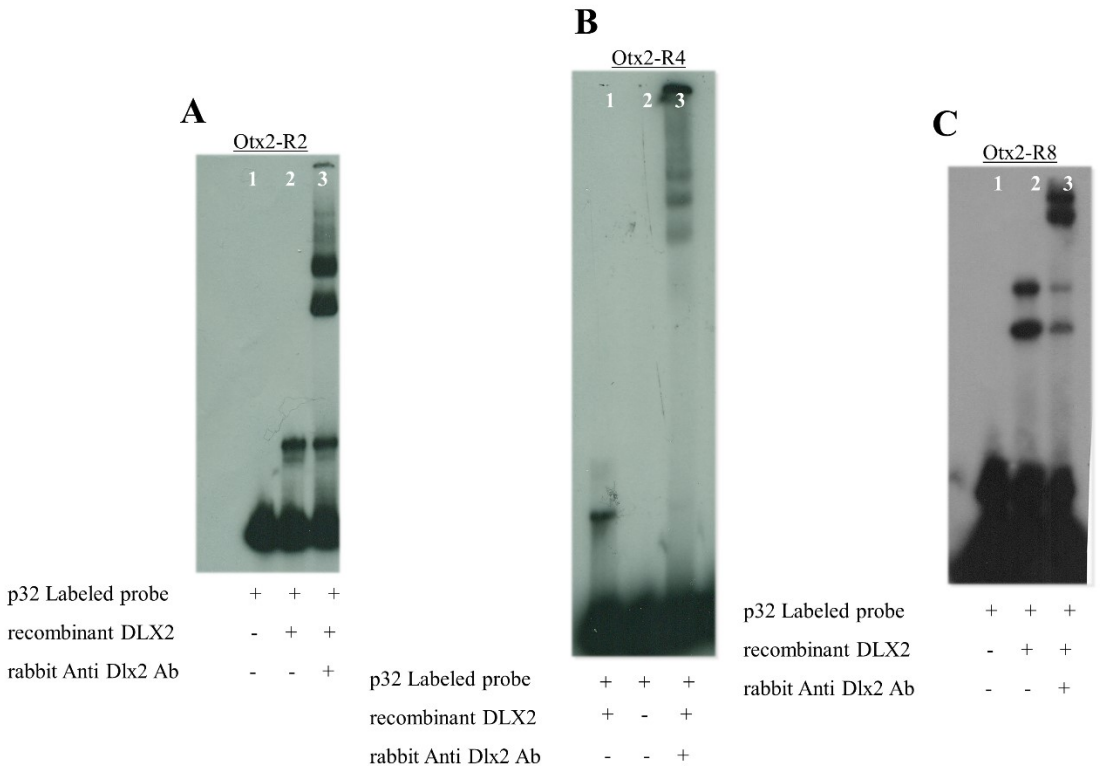

Figure 3.8. DLX2 direct binds to the *Otx2* promoter *in vitro*

Three *Otx2* ChIP positive regions were selected and labelled with α-32P for EMSA experiments. (A) Using recombinant DLX2 protein and radioactively labelled *Otx2-R2* probe, DLX2 binds to *Otx2-R2* as shift and supershift with DLX2 antibody were observed relative to free probe. Free probe (lane 1), *Otx2-R2*/rDLX2 shift (lane 2), and *Otx2-R2*/rDLX2/αDLX2 supershift (lane 3) (B) Using recombinant DLX2 protein and radioactively labelled *Otx2-R4* probe, DLX2 binds to *Otx2-R4* as shift and supershift with DLX2 antibody were observed relative to free probe. *Otx2-R4/*rDLX2 shift (lane 1), free probe (lane 2), *Otx2-R4/*rDLX2/αDLX2 supershift (lane 3) (C) Using recombinant DLX2 protein and radioactively labelled *Otx2-R8* probe, DLX2 binds to *Otx2-R8* as shift and supershift with DLX2 antibody were observed relative to free probe. Free probe (lane 1), *Otx2-R8/*rDLX2 shift (lane 2), and *Otx2-R8/*rDLX2/αDLX2 supershift (lane 3). Dlx2 antibody (Dlx2 Ab)

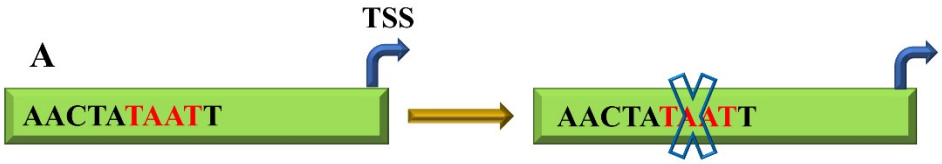

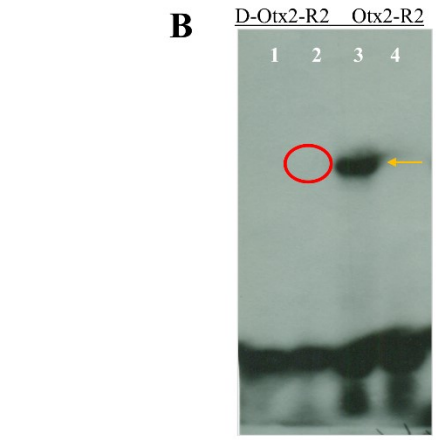

p32 Labeled probe	+	+	+	+
recombinant DLX2	-	+	-	+

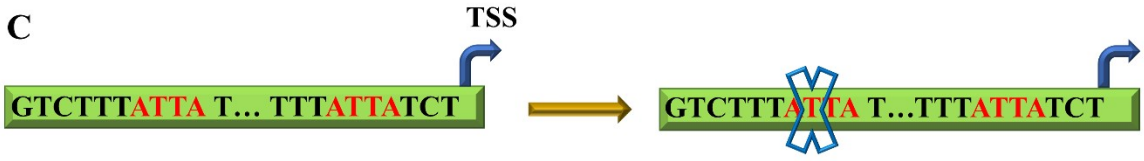

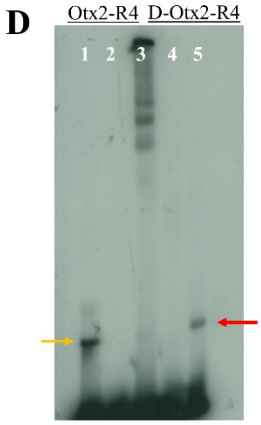

p32 Labeled probe	+	+	+	+	+
recombinant DLX2	+	-	+	-	+
rabbit Anti Dlx2 Ab	-	-	+	-	-

Figure 3.9. R2 and R4 binding sites are critical for DLX2 interaction with the *Otx2* promoter

ATTA/TAAT motif deletions were performed to show the critical role of binding sites to DLX2 transcription factor (A) Schematic image of region 2 binding site deletion. (B) Using recombinant DLX2 protein and radioactively labelled *D-Otx2-R42* probes, it was shown that DLX2 could not bind to labelled probe as protein-DNA complexes had no shift (encircled) in a non-denaturing polyacrylamide gel relative to WT probe. Free *D-Otx2-R2* probe (lane1), *D-Otx2-R2*/rDLX2 probe no gel shift (lane 2), *Otx2-R2*/rDLX2 gel shift (lane 3), and *Otx2-R2* free probe (lane 4). (C) Schematic diagram of region 4 first binding site deletion (5′ to 3′). (D) Mutated labelled probe (*D-Otx2-R4*) and WT labelled *(Otx2-R4)* probe were incubated with recombinant DLX2 (rDLX2) protein. rDLX2/probe complexes were then resolved on a non-denaturing acrylamide gel, while the WT labelled *(Otx2-R4)* were shifted (yellow arrow), a faint band was found between *D-Otx2-R4* and rDLX2 (red arrow). *Otx2-R4*/rDLX2 probe gel shift (lane 1), free *Otx2-R4* probe (lane 2), *Otx2-R4*/rDLX2/αDlx2 supershift (lane 3), D-*Otx2-R4* free probe (lane 4). Transcriptional start site; TSS

3.3.7 Functional effect of DLX2 binding on *Otx2* gene regulation *in-vitro*

The DLX2-*Otx2* protein-DNA interaction experiments indicate that DLX2 can occupy the *Otx2* promoter; however functional *in-vitro* and *in-vivo* assays are necessary to further investigate our hypothesis. Luciferase reporter gene assays were performed to confirm the functional effect of DLX2 binding on *Otx2* transcription *in-vitro.* The positively confirmed sequences from ChIP experiments were cloned into the pGL3 basic vector and co-transfected with a DLX2 expression vector into HEK293 cells. The luciferase reporter gene expression is under control of *Otx2* promoter regions and was measured using a luminometer. The pcDNA3 expression vector was used as the vector for the *Dlx2* cDNA expression plasmid. An empty pcDNA3 plasmid was used as a control. The R2, R4, R8 and R9 which were positive for both ChIP and EMSA experiments were assayed. All positive regulatory regions from ChIP had reduced luciferase expression in the presence of DLX2 protein relative to empty pCDNA3 vector (Figure 3.10). The lower expression of luciferase in the presence of DLX2 supports its negative regulatory effect on *Otx2* expression *in-vitro.*

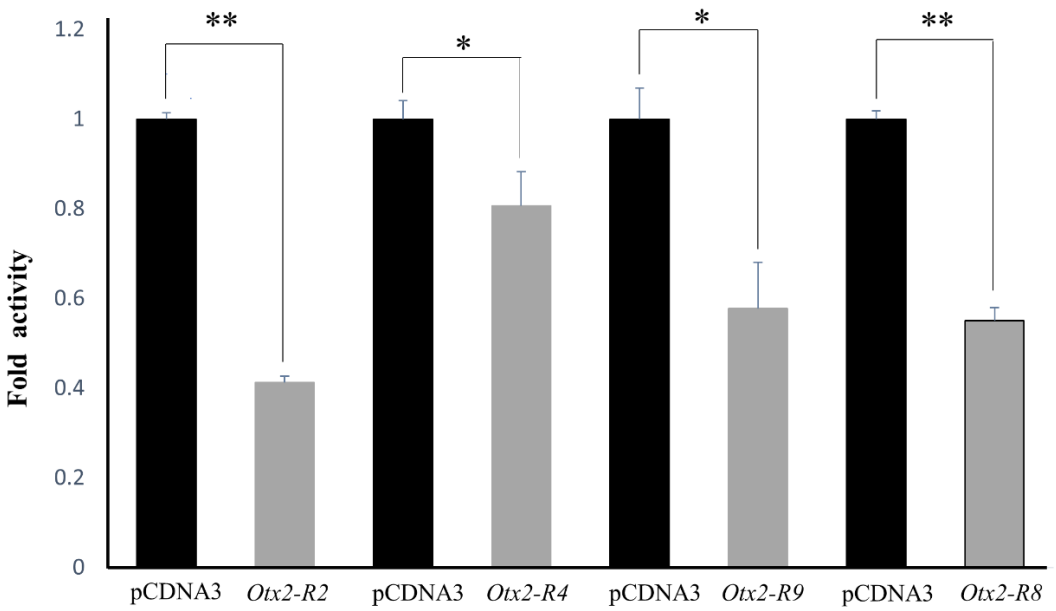

Figure 3.10. DLX2 represses *Otx2* expression *in-vitro*

Luciferase reporter assay experiment were carried out using the ChIP positive regions (*Otx2*-R2, *Otx2*-R4, *Otx2*-R9 and *Otx2*-R8) which were subcloned into the PGL3 vector. The HEK293 cell lines were transfected with *Dlx2*-pcDNA3 and empty pcDNA3 expression vectors. In the presence of DLX2, the *Otx2* promoter regions (R2, R4, R9 and R8) were all repressed at varying degrees. n=3, **=P ≤ 0.01, *=P ≤ 0.05

3.3.8 OTX2 protein and mRNA expression is comparable in *Dlx1/Dlx2* DKO and *Dlx1/Dlx2* WT mice at E18

Dlx2 is expressed in the GCL and *Otx2* is present in the outer neuroblastic layer of the retina at E18; thus, their expression is exclusive from each other at this time (V. Pinto and D. Eisenstat, unpublished data). While *Otx2* activates *Crx* and other PR cell-specific genes, *Dlx2* suppresses *Crx* expression (Rath et al., 2007 and my data). Our lab also demonstrated that DLX2 and PR-specific marker expression are mutually exclusive (de Melo et al., 2003). Altogether, these data support the possible repression of *Otx2* by DLX2 during late retinogenesis. To confirm this *in-vivo*, OTX2 expression was assessed comparing the *Dlx1/Dlx2* wild type and *Dlx1/Dlx2* DKO retina tissues at the E18 time point. The eye tissues of E18 embryos from *Dlx1/Dlx2* DKO and WT mice were dissected, and the frozen sections were immunolabelled using OTX2 antibody in several litters. Contrary to what was expected based upon our *in vitro* results, the *in-vivo* expression of OTX2 was unaffected by the absence of *Dlx1/Dlx2* function at this specific time point (E18) (Figure 3.11A-B). To further investigate and quantify the amount of *Otx2* mRNA expression, quantitative real-time PCR (qRT-PCR) was performed on E18 *Dlx1/Dlx2* WT and DKO retina tissues. Consistent with the immunofluorescence results, *Otx2* expression remains unchanged between *Dlx1/Dlx2* DKO and WT tissues (Figure 3.11C). The *in-vivo* data suggests that DLX1/DLX2 may not regulate *Otx2* expression level at this stage (E18).

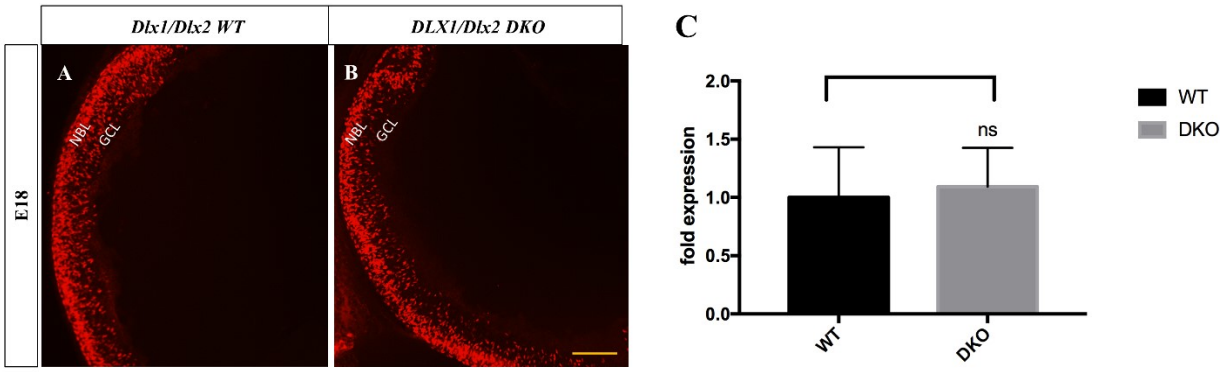

Figure 3.11. OTX2 expression was unaltered in *Dlx1/Dlx2* DKO compared to the *Dlx1/Dlx2* WT E18 retina *in-vivo*

OTX2/*Otx2* expression levels were investigated by immunofluorescence and qRT-PCR in *Dlx1/Dlx2* DKO/WT E18 retina tissues. (B) The OTX2 expression in *Dlx1/Dlx2* DKO shows a similar pattern relative to (A) *Dlx1/Dlx2* WT retina sections at E18. (C) The *Otx2* transcript level remained unchanged in *Dlx1/Dlx2* DKO compared to *Dlx1/Dlx2* WT retina tissues at E18. GCL; ganglion cell layer, NBL; neuroblastic layer, ns; not significant, Scale = 100 μm, n=3

3.3.9 DLX2 occupies the *Otx2* promoter region at E13 retina tissues

In addition to the luciferase reporter assay that supported *Otx2* repression in the presence of DLX2 protein *in vitro*, our ChIP and EMSA also both supported DLX2 binding to the *Otx2* promoter at multiple regions. However, the *in-vivo* functional assays did not support these data, since the *Otx2* expression level remained unchanged in the absence of *Dlx1/Dlx2* at E18. The dynamic reprogramming of genetic networks enables cells to adapt to the changing environment, and the gene expression pattern is temporally dynamic due to inputs from external signals and regulatory interactions between TFs and their targets (Swift & Coruzzi, 2017). *Dlx2* and *Otx2* are both expressed as early as E11.5 in the neuroblastic layer of the retina; they are both involved in RPC differentiation to GCL (*Dlx2*) and PR (*Otx2*) precursors (Zhang et al., 2017; Omori et al., 2011) Thus, we hypothesized that the DLX2 transcription factor may repress *Otx2* gene expression during early retinal progenitor cell fate decision, leading to a ganglion cell fate over a photoreceptor fate at E13. Our lab previously showed that DLX2 expression overlaps with several RPC neuronal markers (de Melo et al., 2003). However, the regulatory role of DLX2 has not been investigated during early retinal development. Initially, we performed additional ChIP-qPCR experiments to find out whether DLX2 occupies the *Otx2* promoter at E13. Since we had already tested DLX2 binding at the later time point (E18), we used three regions (R2, R4, R8) from the *Otx2* regulatory regions which were positive for DLX2 binding at E18. The E13 eyes were collected from the E13 mice embryos, cross-linked, and the chromatin was fragmented to isolate the DNA-protein bounded regions and analyzed by qPCR. We also included IgG and the chromatin without DLX2 antibody as our negative controls. H3K27me1 antibody was applied as a positive control. Among the three *Otx2* promoter regions (R2, R4, and R8) studied, region 2 (R2) was occupied by the DLX2 protein at E13 (Figure 3.12). To further investigate the

functional role of DLX2 on *Otx2* expression *in-vivo*, eye tissues from *Dlx1/Dlx2* DKO and WT mice were immunostained with OTX2 antibody at the E13 time point (Figure 3.13A-D). These results showed that OTX2 expression levels were not altered in *Dlx1/Dlx2* DKO retina tissues (Figure 3.13B, D) compared to WT (Figure 3.13A, C). However, the OTX2 expression pattern appeared to be shifted toward the outer neuroblastic layer in *Dlx1/Dlx2* DKO compared to WT mice where OTX2 expression was distributed from the center to the outer neuroblastic layer suggesting a partial spatial redistribution in the DKO (Figure 3.13E, G, F, H). *Otx2* transcript levels were measured by qRT-PCR in DKO/WT mice retina tissues, and we did not observe significant changes of *Otx2* transcript levels between *Dlx1/Dlx2* DKO/WT (Figure 3.13I). These data indicate that DLX2 interacts with *Otx2* promoter; however, the number of cells which express *Otx2* was not increased in the absence of *Dlx1/Dlx2*. Although the number of cells did not increase, the *Otx2* positive cells demonstrated a possible difference in the spatial distribution pattern between the *Dlx1/Dlx2* DKO mice retina compared to the control littermates at this developmental stage.

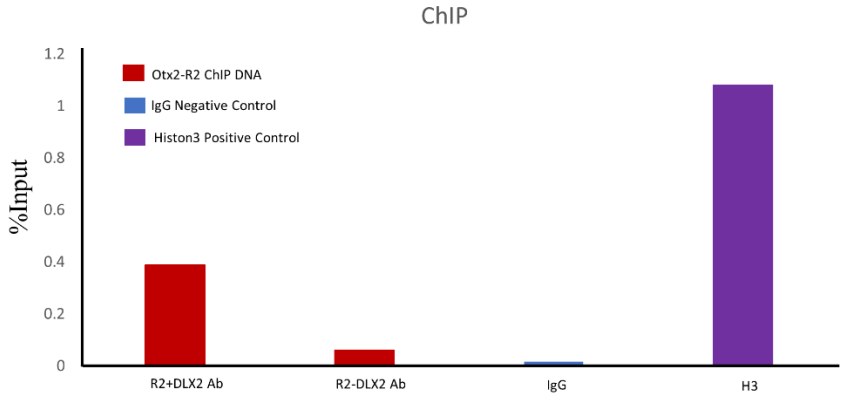

Figure 3.12. DLX2 occupies the *Otx2* promoter at E13 in mouse retina

E13 mouse retina tissues were qChIPed out by DLX2 antibody and analyzed by qPCR using *Otx2* primers. (A) *Otx2* promoter region 2 (R2) was pulled down from the ChIPed chromatin. Retina plus DLX2 antibody (R2+DLX2 Ab) input was higher compared to retina minus DLX2 antibody (R2-DLX2 Ab) input. IgG was used as a ChIP negative control, H3K27me1 Ab was used as a ChIP positive control. n=2

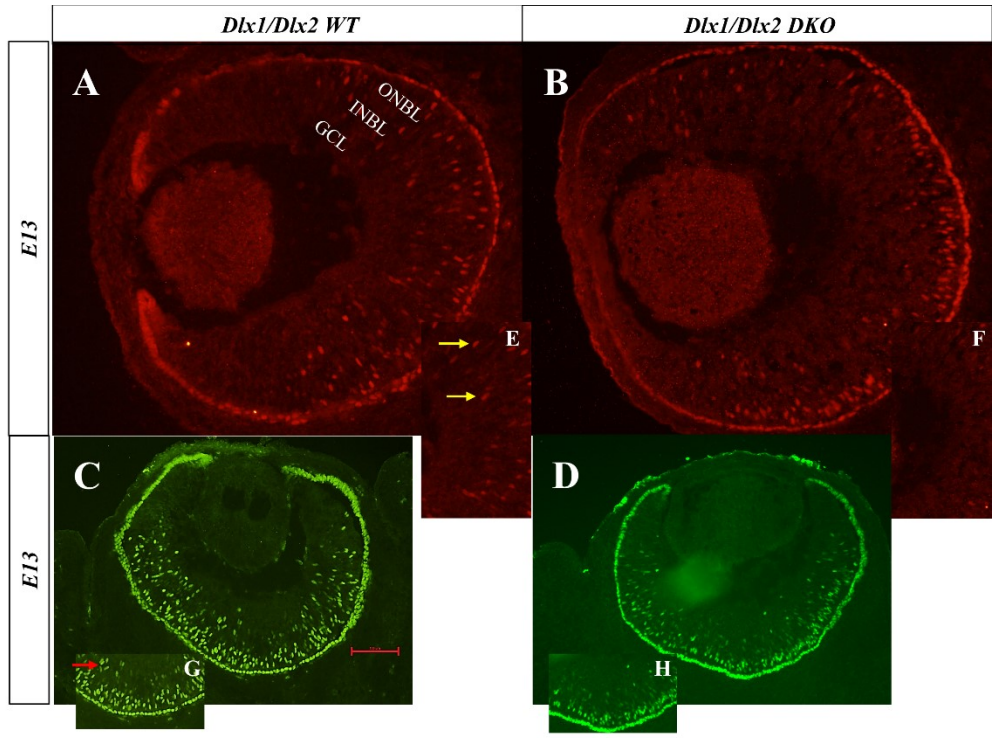

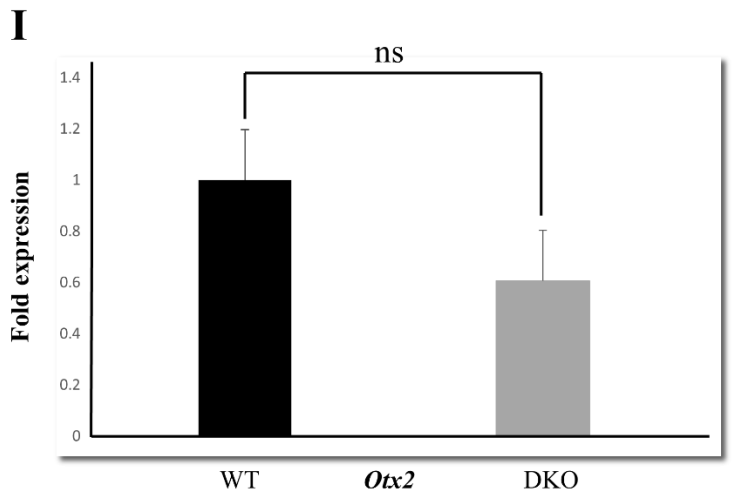

Figure 3.13. The OTX2 expression pattern was spatially altered in the *Dlx1/Dlx2* DKO compared to *Dlx1/Dlx2* WT in retina at E13

E13 eyes were labelled by OTX2 antibody using immunofluorescence (B, D, F, H). The OTX2 expression pattern seems to be shifted toward the outer neuroblastic layer in the *Dlx1/Dlx2* DKO compared to (A, C, E, G) *Dlx1/Dlx2* WT retina tissues at E13 where OTX2 expression is more distributed from INBL to ONBL (yellow and red arrows) n≥3. (I) *Otx2* mRNA expression level

was not significantly changed in the *Dlx1/Dlx2* DKO relative to the *Dlx1/Dlx2* WT at E13. GCL; ganglion cell layer, INBL; inner neuroblastic layer, ONBL; outer neuroblastic layer, Scale = 100 μm, n=3, ns; not significant

3.3.10 OTX2 occupies the *Dlx2* promoter at E13 in retina tissues

OTX2 is involved in multiple GRNs including photoreceptor cell differentiation from RPC in the retina. It is required to induce RPCs toward photoreceptor cell fates at early stages (E13) by regulating PR cell specific genes (Brzezinski et al., 2015). *Otx2* expression has been observed in RPCs as early as E12.5, at approximately the same time as *Dlx2* expression initiation in the neural retina. Thus, OTX2 may regulate *Dlx2* expression in a retina progenitor pool which gives rise to PR cells or possibly other type of cells. Based on this, I proposed the presence of a GRN between *Otx2/Dlx2*, more specifically for early neuronal cells differentiation. Initially, *Dlx1/Dlx2* gene regulatory elements including their intergenic enhancer elements were explored for the presence of OTX2 binding sites (TAATCC) (Figure 3.14A). We found several OTX2 binding motifs in *Dlx1/Dlx2* promoter regions, as well as in intergenic enhancer regions (Figure 3.14A). To investigate whether OTX2 interacts with *Dlx1/Dlx2* regulatory regions, ChIP-qPCR analysis, whichnot only shows binding but also clarifies binding site enrichment, was performed on the five potential promoter regions. Region 1 (R1) and region 2 (R2) demonstrated positively for *Otx2* antibody occupation relative to chromatin samples without OTX2 antibody (Figure 3.14B-C). Interestingly, R1 showed a higher percentage input than the H3 positive control, which could mean OTX2 binds with higher affinity (Figure 3.14C). Our result indicates that OTX2 may interact with the *Dlx2* promoter region in retina tissues at E13 embryonic development. However, further functional studies are required to find out if OTX2 regulates *Dlx2* transcriptional expression during early RPCs differentiation.

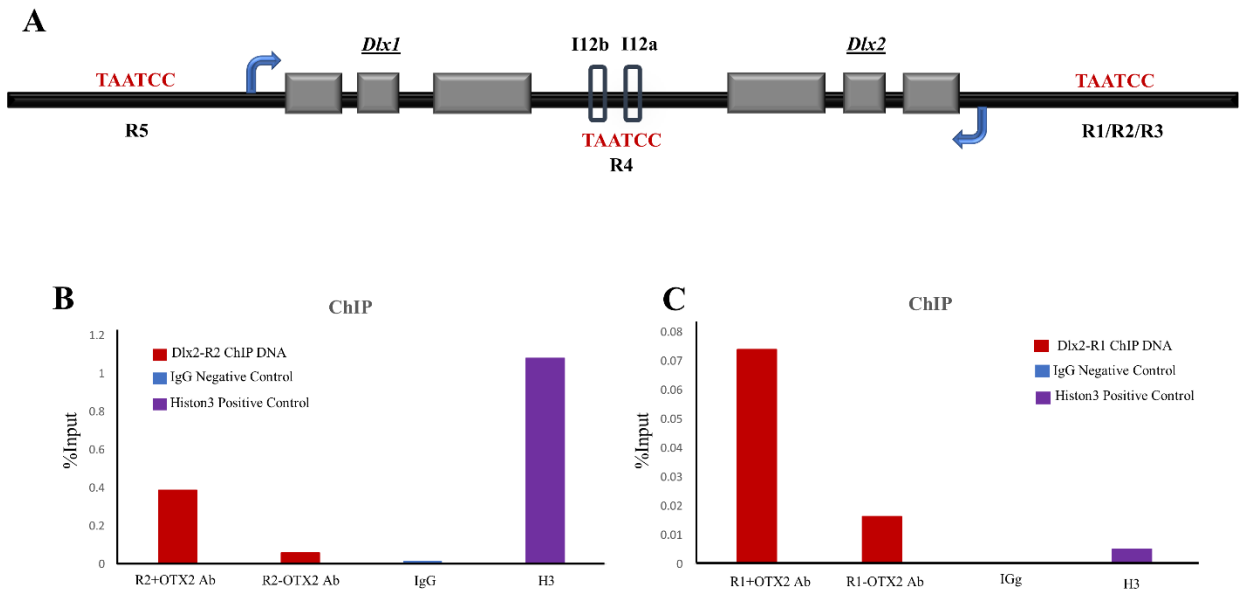

Figure 3.14. OTX2 occupies the *Dlx2* promoter region at E13 mouse retina

(A) A schematic picture of the *Dlx1* and *Dlx2* bigenic cluster including their promoters and intergenic regions. The *Otx2* binding sites were identified in both *Dlx1* and *Dlx2* promoter regions 1, 2, 3 and 5 (R1, R2, R3 and R5), as well as their intergenic region 4 (R4). (B) *Dlx2* region 2 binding was enriched by OTX2 in the presence of OTX2 antibody (R2+Otx2 Ab) relative to the *Dlx2* region 2 (R2-Otx2 Ab) in the absence of OTX2 antibody. (C) *Dlx2* region 1 binding was highly enriched by OTX2 in the presence of OTX2 antibody (R1+Otx2 Ab) relative to *Dlx2* region 1 in the absence of OTX2 antibody (R1-Otx2 Ab). IgG were used as a ChIP negative control, H3K27me1 antibody was used as a ChIP positive control, n=1, Ab; Antibody

3.3.11 *Dlx2* and miR-124 may interact in a double-negative feedback loop

MicroRNAs bind to target sites at 3'UTR of mRNAs and negatively regulate gene expression post-transcriptionally. MiRNAs and their TF targets usually interact in a double-negative feedback loop (Carthew & Sontheimer, 2009). During neurogenesis, miR-124 is highly expressed in differentiating and mature neurons (Deo, Yu, Chung, Tippens, & Turner, 2006). Based on *in-situ hybridization* results, we demonstrated that *Dlx2* and miR124 are co-expressed in the same retinal cell population from E13 to P14 (Q. Zhang and D. Eisenstat, data unpublished). TargetScan analysis was performed to analyze the *Dlx2* 3'-UTR region for putative miRNA binding seeds *in-silico*, and a highly conserved miR-124 binding motif was found in the *Dlx2* 3'UTR (Figure 3.15A, B). Additionally, to determine if the miR-124 promoter has potential DLX2 binding motifs, its proximal promoter sequence was analyzed, and eleven TAAT/ATTA motifs were identified (data not shown). To investigate the DLX2 functional effect on *miR-124* retinal expression, retina tissues were collected from *Dlx1/Dlx2* DKO and *Dlx1/Dlx2* WT mice, and mi*R-124* mRNA expression was analyzed by qRT-PCR. MiR-124 expression was increased in the absence of *Dlx1/Dlx2* during late retinal development (E18) (Figure 3.16). *In-silico* data indicated that *Dlx2*/miR-124 could potentially bind to each other's regulatory elements. In addition, the quantitative result shows that miR-124 mature mRNA expression is higher in the absence of *Dlx1/Dlx2* compared to the WT at E18 retina. Altogether, it is probable that *Dlx2* and miR-124 reciprocally regulate the expression of one another during late retinogenesis in a double negative feedback loop; however, additional functional experiments for both *Dlx2* and miR-124 are required to clarify this possible regulatory interaction.

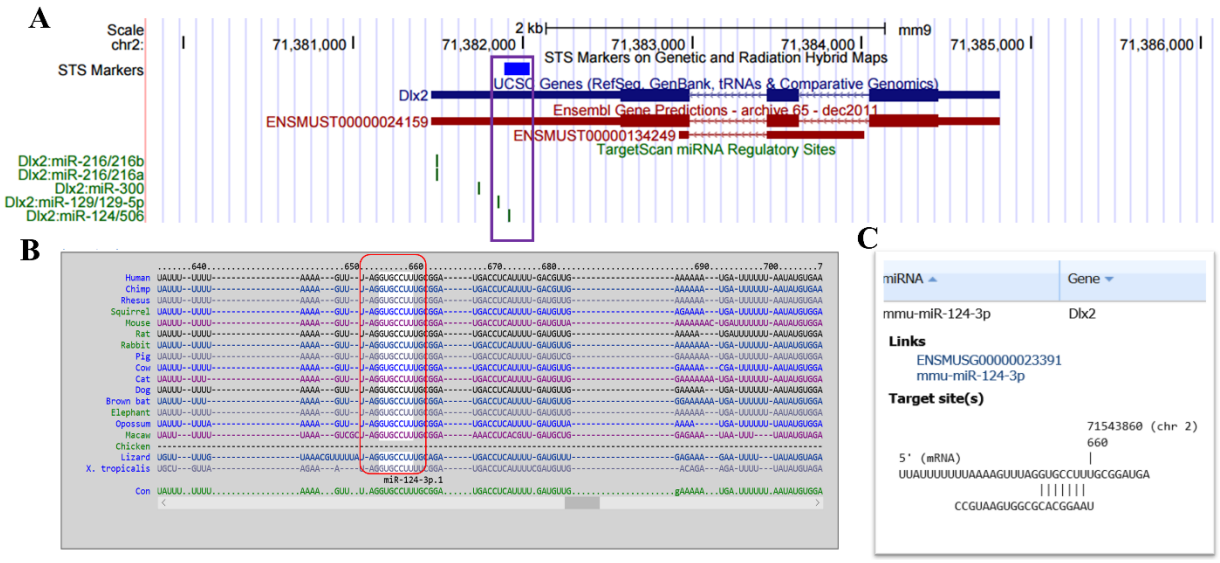

Figure 3.15. miR124 binding site prediction of the *Dlx2* 3´UTR *in-silico*

The *Dlx2*-3´UTR was scanned for miR-124 binding seeds *in-silico.* (A) Multiple miRNAs binding seeds were detected in *Dlx2*-3´UTR sequence by the Ensemble Gene Prediction tool. (B, C) One highly conserved (between vertebrate) miR-124 binding sequence was detected in the *Dlx2*-3´UTR region (encircled)

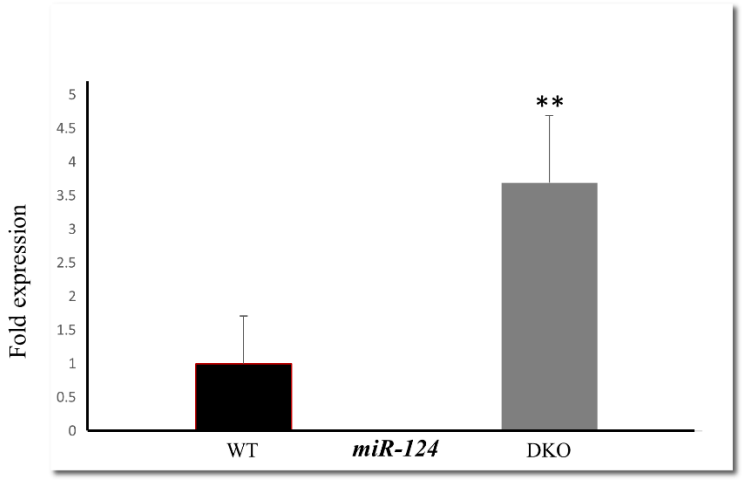

Figure 3.16. The transcript levels of miR-124 were increased in the absence of *Dlx1/Dlx2* in E18 retina tissues

miR-124 transcript expression was measured by qRT-PCR in *Dlx1/Dlx2* DKO and *Dlx1/Dlx2* WT retina tissues at E18. miR-124 expression was significantly increased in the absence of *Dlx1/Dlx2.* n=3, **=P ≤ 0.01

3.3.12 Investigating *Dlx2* expression and function in the postnatal mouse

The phenotype of the *Dlx2* single KO (SKO) retina (dies ~P0) is less severe than *Dlx1/Dlx2* DKO (J. Zagozewski, A. Globa and D. Eisenstat, unpublished data). The SKO and DKO die at birth preventing the functional assessment of the postnatal retina. Thus, our lab decided to study *Dlx2* expression and function post-natally by generating a *Dlx2* retina conditional knockout using the *Dkk3-Cre* mouse line. *Dkk3* is a member of the Dickkopf gene family and encodes a secreted protein that modulates Wnt signaling activity. The BAC-*Dkk3-Cre* transgenic mouse has become the *Cre*-model of choice for several retina-specific conditional knockout (CKO) mice (Sato et al., 2007). *Dkk3* is expressed throughout the retina in the retinal progenitor cells, and embryonic lethality is usually circumvented in CKOs using this *Cre* line. The onset of retinal *Dkk3-Cre* activity is at E10.5, preceding DLX2 expression by one day. DLX2 expression was found in the adult GCL and INL of postnatal mouse retina; hence, we expected that DLX2 may have a function in the postnatal and adult retina as well.

The *floxed Dlx2* mouse is viable and fertile and grows to adulthood with a seemingly normal phenotype. However, when crossed with the *Dkk3-Cre* mouse we noticed cloudy lenses in $Dlx2^{fl/+}$ compared to $Dlx2^{+/+}$ in a one-month old mouse (Figure 3.17A-B). To further investigate the eye phenotype, histology staining was carried out on P30 retina tissues from $Dlx2^{fl/+}$ and $Dlx2^{+/+}$ mice crossed with the *Dkk3-Cre* mouse. Eye morphology appeared to be disrupted in the heterozygous mouse as compared to the control. The retinal IPL and ONL layers were expanded in $Dlx2^{fl/+}$ retina compared to $Dlx2^{+/+}$ mouse crossed with the *Dkk3-Cre* mouse (Figure 3.17C-F). Following the generation of the *Dlx2* CKO homozygous mouse, we used the $Dlx2^{fl/fl}$ mouse crossed with the *Dkk3-Cre* mouse to perform OCT imaging tests in order to take a cross-sectional image of the retina structure. The overall thickness of retina was increased in

the *Dlx2*-CKO mouse compared to WT retina structure (Figure 3.18A, B). Also, light microscopic imaging of the retinas of these mice revealed some disruption in the GCL, and expanded IPL and PR layers (Figure 3.19A-D). All together, the *Dlx2* CKO may have an abnormal retina phenotype; however, more homozygous *Dlx2* CKO mice have to be studied to confirm these phenotypes, and further investigations must be done on the molecular mechanisms.

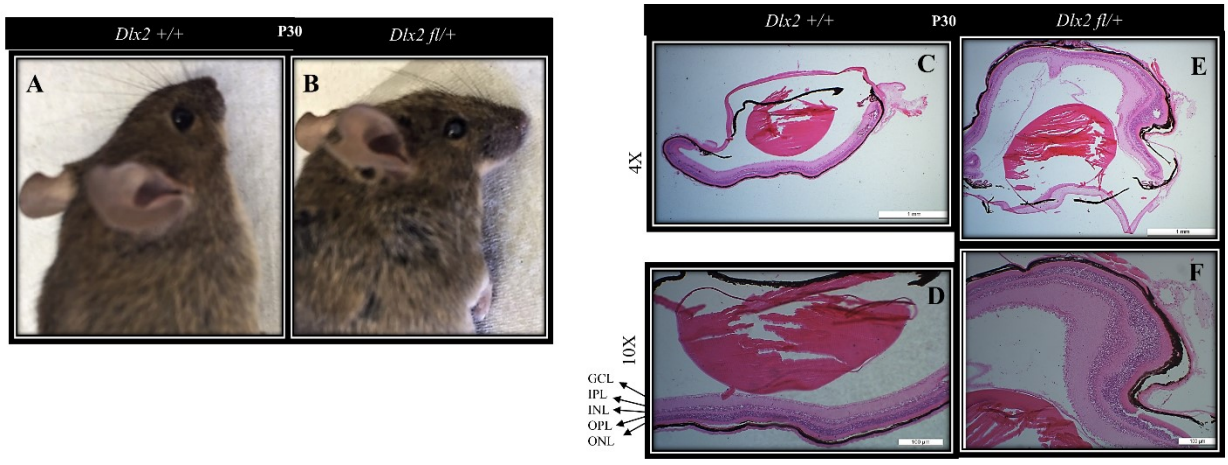

Figure 3.17. The *Dlx2* heterozygous CKO mouse showed an abnormal phenotype in the eye

(A, B) The *Dlx2* $^{fl/+}$ mouse crossed with the *Dkk3-Cre* mouse had a cloudy lens at P30. (C-F) H&E staining was performed on P30 retina paraffin sections of *Dlx2* $^{fl/+}$/*Dlx2*$^{+/+}$ (E, F) Retina structure was disrupted, with an expanded IPL and ONL in *Dlx2* $^{fl/+}$ compare to (C, D) *Dlx2*$^{+/+}$ mouse. GCL; ganglion cell layer, IPL; inner plexiform layer, INL; inner neuroblastic layer, OPL; outer neuroblastic layer, ONL; outer neuroblastic layer, Postnatal day30; P30, n=1

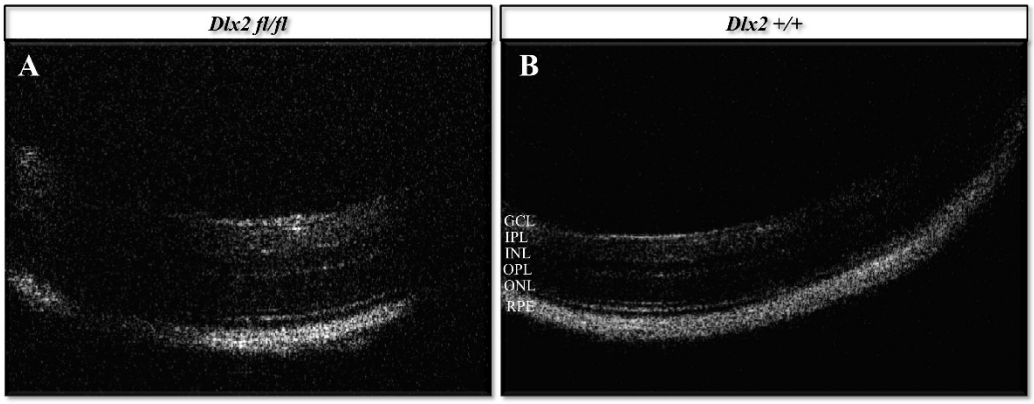

Figure 3.18. The IPL and ONL of the retina may have been expanded in *Dlx2* $^{fl/fl}$ relative to *Dlx2* $^{+/+}$ adult mice

Optical Coherence Tomography analysis was performed on the *Dlx2* CKO and *Dlx2* WT retina. (A) The *Dlx2* $^{fl/fl}$ crossed with the *Dkk3-Cre* mouse retina's overall thickness appears to be expanded compared to (B) *Dlx2* $^{+/+}$ retina layers. GCL; ganglion cell layer, IPL; inner plexiform

layer, INL; inner neuroblastic layer, OPL; outer neuroblastic layer, ONL; outer neuroblastic layer, RPE; retina pigmented layer, n=1

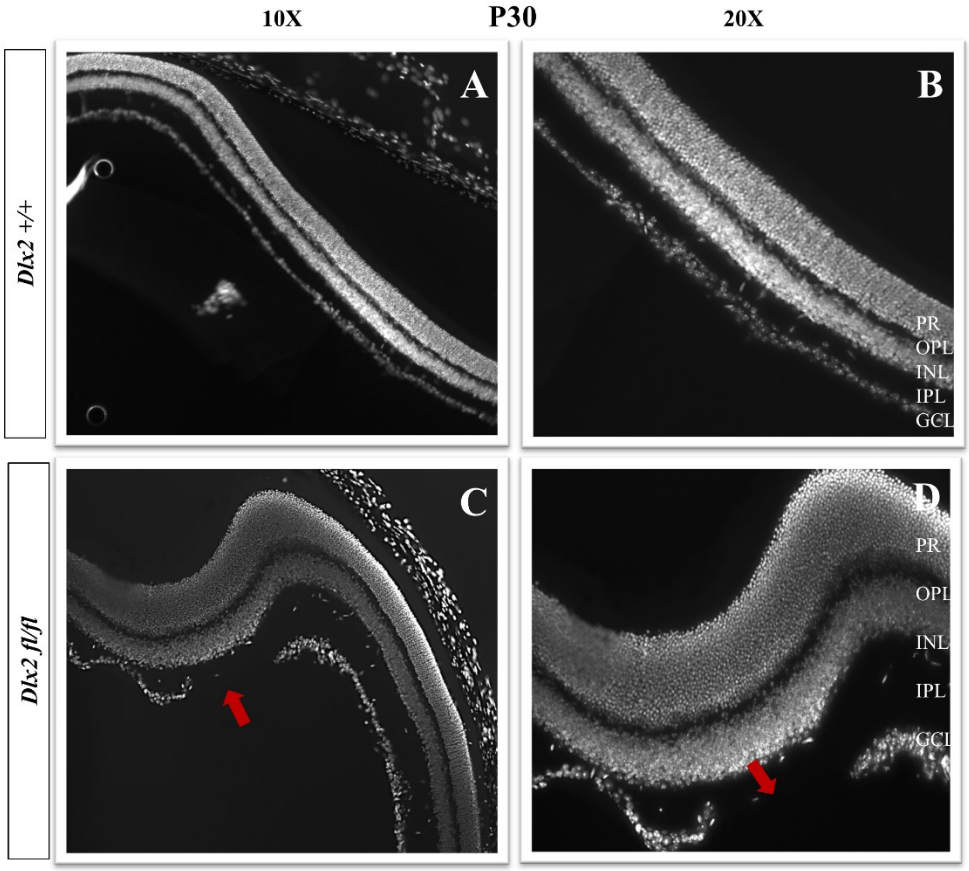

Figure 3.19. The retina structure was abnormal in *Dlx2 fl/fl* mouse at postnatal day 30

Light microscopic imaging was carried out to investigate retina structure. (A, B) Normal retina morphology in *Dlx2*$^{+/+}$ (C, D) Retinal folding was disrupted along with disrupted GCL (red arrow), and expanded PR layer and IPL in *Dlx2 fl/fl* crossed with the *Dkk3-Cre* mouse at P30. GCL; ganglion cell layer, IPL; inner plexiform layer, INL; inner neuroblastic layer, OPL; outer neuroblastic layer, PR; photoreceptor, n=1

3.4 Discussion

In this chapter, I investigated the regulatory function of DLX2 during retinal neuronal cell development and identified possible GRNs which could be involved in retinal neuronal cell fate specification during retinogenesis. DNA, RNA, and proteins build millions of networks inside the progenitor cells, which trigger pathways and signals intrinsically and extrinsically to give rise to various cell types, tissues and eventually organs. Therefore, to better understand the process of development, it's crucial to identify and understand these networks, their components and functions. Retina progenitor cells make heterogenous pools of various cell fate-determining identity; these cells go through many rounds of cell division with each successive progeny becoming less competent, until terminal cell division is reached, and the fate of the post-mitotic cell is determined (Swaroop et al., 2010). This process is tightly regulated in a temporal order in the mouse retina, and RPCs differentiate starting around E10 until the second week of after birth (C. Cepko, 2014). The intrinsic model of RPC fate determination is partly controlled by transcription factors, and their networks, as well as other determining factors such as signaling pathways and non-coding RNAs (Cepko et al., 2014). This makes gene regulatory networks complex in terms of communicating with one another, and we are still far from fully understanding the biological function of these networks. I have been trying to shed light on DLX2 GRN in retina. The presence or absence of a specific transcription factor such as DLX2, and its collaboration with other factors and sometimes with itself can be determining factors to induce a specific type of neuronal cell (Livesey et al., 2001). This research found that *Crx* is a direct transcriptional target of the DLX2 homeobox transcription factor at E18 during retinal development. DLX2 binds to the *Crx* promoter and restricts its expression in the developing retina, which could mean a potential mechanism through which DLX2 regulates *Crx* expression

in the post-mitotic progenitor cells to repress photoreceptor specification in the mammalian retina. *Crx* is an upstream activator of several photoreceptor-specific genes such as *Nr2e3, Nrl* and RORβ, and its repression can lead to less photoreceptor cell differentiation (Swaroop et al., 2010). The TFs are more likely to interact with the proximal promoter close to the transcription start site (TSS); thus we chose to investigate 3kbp upstream of the TSS. It has been shown that distal regulatory elements and intergenic regulatory regions are also TF targets in many genes (Yu, Lin, & Li, 2016).

We were able to isolate *Crx* promoter region 6, containing four homeodomain binding motifs for DLX2 binding. The direct or indirect binding of TFs to DNA is necessary to initiate target gene transcription regulation; however, TF binding to the gene promoter does not always result in the functional regulation of the gene (Wang et al., 2012). Homeobox genes encode a protein with a homeodomain binding region, and because of this region's unique feature (three helices), they recognize specific DNA-sequences (AT-rich sequence) (Bobola & Merabet, 2017). Based on our ChIP-PCR results, not all the consensus motifs present on the targeted promoter is bound by the respective TF (*Crx*-R6 is bound by DLX2). This could be explained by the chromatin landscape and sequence context (flanking sequence) as DNA-TF interaction is vastly shaped by them (Inukai, Kock, & Bulyk, 2017). There are TFs called pioneer TFs, which can open condensed chromatin and thus, the presence of these TFs may contribute to the homeodomain TF's preferred binding sites (Zaret & Mango, 2016). It is also probable that some of the DLX2 putative binding motifs are occupied by other TFs at the specific time, therefore the respective TF cannot bind to all binding sequences on the promoter (Dror, Golan, Levy, Rohs, & Mandel-Gutfreund, 2015). However, *Crx* promoter-R6 occupation by DLX2 could be sufficient to trigger further actions in order to recruit or block the transcriptional machinery. DLX2 direct

binding and binding specificity was confirmed by EMSA, where the deletion of the R6 binding site blocked DLX2 interaction with this promoter region. The presence of radiolabelled DNA (*Crx* promoter) and only rDLX2 protein in the complex demonstrated the direct binding of DLX2 to the *Crx* promoter, and the loss of binding in the absence of the specific binding motif could indicate the critical binding site for DLX2 binding. Some TFs have the ability to recognize multiple binding sites, and the TAAT/ATTA deletion eliminates the possibility that DLX2 may bind to another motif. Only one binding site deletion from four present in R6 was able to disrupt the TF affinity to this region. It is possible that this binding site is crucial for DLX2 binding or the presence of all TAAT/ATTA binding sites is required for DLX2 interaction with this specific region. To confirm this notion, however, additional experiments are required where other R6 binding sites are deleted, and DLX2 binding is investigated by EMSA. We can also speculate that since only R6 was cloned and not the whole promoter, the affinity of DLX2 to the R6 significantly dropped by deleting even one binding motif.

Although DNA binding is required for transcriptional regulation initiation, it does not necessarily lead to the functional regulation of the targeted gene expression by the TF. Since there is a significant presence of homeodomain binding sites throughout the genome, a large number of TFs display widespread non-functional binding to the DNA promoters (Todeschini, Georges, & Veitia, 2014). Hence, *in-vitro* and *in-vivo* functional assays are necessary to determine DLX2 regulatory function on *Crx* expression. Consistent with our ChIP and EMSA results, the luciferase reporter assay revealed that DLX2 negatively regulates *Crx* expression. However, in the absence of the DLX2 binding site (*D-Crx-R6)*, more luciferase expression was found in the presence of DLX2 compared to the empty vector. Although DLX2 loses its regulatory function in the absence of its homeodomain binding site, there are other TFs present

in the HEK293 cells which may bind to *D-Crx-R6* and induce luciferase expression. Our *Dlx1/Dlx2* DKO mice functional research demonstrated that DLX2 regulates *Crx* expression by suppressing its expression at E18 which is consistent with the luciferase reporter assay. *Crx* has been characterized to be expressed in the mouse photoreceptor cells pre- and post-natally and its activation by *Otx2* in photoreceptor precursors induces several photoreceptor differentiating networks which eventually determine cone or rod cell fate decisions. Thus, *Crx* overexpression in the absence of *Dlx1/Dlx2* could lead to more photoreceptor cell differentiation. Since fewer ganglion cells have been found in the absence of *Dlx1/Dlx2* in the developing retina (de Melo et al., 2005), a partial cell fate switch from ganglion cells to PR cells is one possible explanation. The application of the *CrxLacZ* reporter mice which were crossbred with *Dlx1/Dlx2* heterozygous mouse and their progeny further crossbred provided additional evidence that DLX2 may have a functional role on *Crx* transcriptional expression *in vivo*. The nucleotide sequences around the transcription start site of the mouse *Crx* gene (consistent with our ChIP result R6 of *Crx* promoter) fused with β-galactosidase, were used to generate the *CrxLacZ* mice used in this study (Furukawa et al., 2002). The X-gal staining of the cross-bred mouse retina strongly supports that DLX2 binds to this specific region of *Crx* promoter and represses its expression *in vivo*, which is presented by higher β-galactosidase expression in the absence of *Dlx1/Dlx2.*

Otx2 is a key photoreceptor fate regulator in post-mitotic RPCs; it is located genetically upstream of *Crx*, and their regulation is interconnected (Nishida et al., 2003). Thus, we proposed a possible gene network with three nodes (*Dlx2-Otx2-Crx),* where DLX2 may repress *Crx* and *Otx2* expression simultaneously to promote RGC fate over PR fate at E18. We showed that *Otx2* occupies the *Crx* promoter (M. Hejazi, Z. Li and D. Eisenstat, unpublished data) and activates its expression (Omori et al., 2011). In $Crx^{-/-}$ mouse models *Otx2* expression increased by a greater

than two-fold in the retina (Furukawa et al.,1997); therefore, the simultaneous repression of both *Crx* and *Otx2* could secure RGC fate over PR fate. The ChIP experiment showed that DLX2 occupies multiple *Otx2* promoter regions in the retina tissues at E18. Out of ten putative regions, DLX2 occupies five regions, which are located distally (R2 and R4) and proximally (R8, R9, and R10) relative to the TSS, which supports DLX2 interaction with multiple *Otx2* proximal promoter regions *in vivo*.

The schematic DLX2 binding map to the *Otx2* promoter shows a gap in the middle of (-1kbp to -2kbp) the proposed promoter. This could be explained by specific DNA features (rotational parameters) or epigenetic features (DNA methylation) of this region which may inhibit TF binding (Inukai et al., 2017). DNA shape features and epigenetic information of the promoters are determining factors for TF binding (Inukai et al., 2017). Despite this gap, the *Otx2* promoter is highly enriched with DLX2 proteins at E18, which could be an indication of possible *Otx2* transcription regulation by DLX2. DLX2 direct and specific binding was confirmed with EMSA for *Otx2* ChIP positive promoter regions. DLX2 revealed a functional effect on *Otx2* expression *in-vitro* since all the *Otx2* positive regions repressed the luciferase reporter gene expression in the presence of DLX2. Contrary to all of our *in-vitro* results, *Otx2* mRNA and protein expression were unaltered in *Dlx1/Dlx2* DKO compared to control embryos *in-vivo* at E18. Given that DLX2 recognizes short motifs (4bp), they appear on DNA sequences with high frequency simply by chance; thus, DLX2 may bind to these sequences at open chromatin regions without any function. The *Otx2* promoter chromatin landscape could be in an open state in various regions since *Otx2* is involved in many genetic pathways (Samuel, Housset, Fant, & Lamonerie, 2014).

The ChIP-PCR experiment identifies the promoter region occupied by specific proteins, but it does not determine the direct or indirect binding of that specific protein to the promoter. For instance, Mbp1 and Swi6 are yeast TFs which form a complex to regulate downstream cell cycle genes. Swi6 binds to Mbp1, while Mbp1 directly contacts DNA at targeted binding motifs (Taylor et al., 2000). In addition, sometimes TFs facilitate the binding of other TFs to DNA, and they do not have any functional role on a specific gene. Therefore, it is possible that DLX2 acts as a co-factor for another TF or works in a complex with one or multiple proteins to regulate *Otx2* expression, and in the absence of DLX2, there are other co-factors or redundant proteins (*Dlx5* or *Dlx6*) to replace its function. The luciferase and EMSA assays contained the sequence amplified from the ChIP positive regions, and the absence of flanking sequences may be required for proper DLX2 binding and activity. Also, development is not considered a linear relationship between two genes, but more of a multi-dimensional relationship where space and time play a critical role, which are not accounted for in luciferase and EMSA assays. Another example of spatial importance is the promoter's capability to form secondary loops. These loops allow for protein binding at one site but due to physical dynamics, loops can regulate sites located in other regions of the promoter (Ogata, Sato, & Tahirov, 2003). Therefore, transcriptional regulation is not an isolated process but is rather part of a highly complex and interconnected GRN containing other factors. This could explain the absence of a direct functional relation between DLX2-*Otx2* at this specific time point. The *Otx2* reporter mouse would be an additional tool to perform functional investigation on transcriptional regulation of *Otx2* by DLX2 protein during development (Fossat et al., 2007). These reporter mice could be bred into the *Dlx1/Dlx2* DKO background.

Neuronal temporal birth order during development is a conserved feature not only in the retina but within other areas of the CNS. It has been shown that a TF which has a specific function during one developmental time point, acts differently (depending on the presence of other factors) at another time point to give rise to various cell types. For instance; Ikaros is a vertebrate homologue of Hunchback in *D. melanogaster* which is required for ventral nerve cord early specification (Isshiki, Pearson, Holbrook, & Doe, 2001). Gain and loss of function of Ikaros in the mouse retina revealed regulatory effects on several genes during early retinogenesis but not during late retinogenesis (Elliott & Evans, 2008). Extrinsic cues might be involved in the regulation of the temporal progression of retinal cell fates. Bipolar cell genesis in the retina is regulated by both OTX2 and VSX1 expression in *X. laevis* during late retinal development. *Otx2* and *Vsx1* mRNA is present during early retinogenesis, but they are not translated to the functional proteins until the later in retinal development. The treatment of early retina with Cyclopamine, which blocks Shh signaling, promoted early *Otx2* and *Vsx1* translation, which lead to early bipolar specification (Pannese et al., 1995). Temporal regulation may alter DLX2 function differentially in early versus late retina development. *Otx2* has a major role in initiating photoreceptor fate from progenitor cells at earlier time points; thus, its expression drops significantly at E18. However, *Otx2* expression is significantly higher at E13 with expression in a population of post-mitotic progenitor cells which have the potential to become photoreceptor cells (Nishida et al., 2003). DLX2 expression is also present in an RPC population, which may later adopt RGCs fate (de Melo et al., 2003). It has been shown that *Brn3b* induces early ganglion fate by transient repression of *Dlx1/Dlx2*, which could mean that *Dlx1/Dlx2* may be involved in ganglion differentiation as well as in other neuronal cell-type differentiation at E13. We repeated the ChIP and functional *in-vivo* experiments at an earlier time point (E13). In

contrast to DLX2 interaction with the *Otx2* promoter at multiple sites at E18, we only found *Otx2*-R2 occupation out of five tested regions (R2, R4, R8, R9 and R10). The homeodomain protein binding to the genome is in a context-dependent manner; therefore, various cellular environments at different time points could explain this dissimilarity (Yesudhas, Batool, Anwar, Panneerselvam, & Choi, 2017). Despite the DLX2 interaction with the *Otx2* promoter (*Otx2*-R2), the *Otx2* protein or transcript expression did not change in the absence of *Dlx1/Dlx2* at E13 in mice retina tissues, which means that DLX2 may not suppress *Otx2* expression at E13 consistent with our E18 data.

Although the *Otx2*-expressing cell quantities are comparable between *Dlx1/Dlx2* DKO and WT animals, it appears that there are some OTX2 positive cells located at the inner NBL of wild type animals, which is absent in the *Dlx1/Dlx2* DKO. We also observed some overlap between OTX2 and DLX2 expression in the inner NBL at E13 (data not shown). It is possible that *Otx2* and *Dlx2* are both expressed in a small population of RPCs located in the inner NBL at E13. Based on our ChIP-qPCR data, the *Dlx2* promoter region is highly enriched by OTX2 binding in the retina tissues at E13. This data intensifies the possible presence of *Otx2* and *Dlx2* in the same network at E13. It has been suggested that *Otx2*-expressing RPCs harbour the potential to differentiate to bipolar or horizontal cells depending on the intrinsic profile of the progenitor cell. For instance; in the presence of *Vsx2, Otx2*-expressing progenitor cells may become bipolar cells (Brzezinski et al., 2015). *Otx2* retina CKO mice showed fewer horizontal cells compared to *Otx2* WT mice (Koike et al., 2007). Horizontal cell differentiation starts as early as E12 during retina development. Small numbers of horizontal *Dlx2*-expressing cells are present in the NBL at P0 in the mouse, as DLX2 expression overlaps with calbindin and NF165 (horizontal cell marker) in the NBL at this time (de Melo., et al., 2003). *Dlx2* is highly expressed

in the inner NBL of retina at E13 and its expression overlaps with *Vsx2* (an early RPC marker) at this time. This population of RPCs could be regulated by the temporal and spatial expression of extrinsic cues.

Notch signaling maintains RPC proliferation during early retinal development by using receptor-ligand signaling to regulate several transcription factors such as *Hes1/Hes5* (Artavanis-Tsakonas, Rand, & Lake, 1999). *Notch1* (Notch receptor) and *Delta* (Notch ligand) are strongly expressed in the inner NBL at E13 (Lindsell, Boulter, diSibio, Gossler, & Weinmaster, 1996). During CNS early development, *Dlx2* negatively regulates Notch signaling by repressing *Hes5* and *Notch1* expression. Our lab previously found a significant increase of *Notch1* and *Hes1*expression in *Dlx1/Dlx2* DKO mice forebrain at E13 (J. Zagozewski and D. Eisenstat, unpublished data). Muranishi *et al.* discovered an evolutionarily conserved *Otx2* enhancer which they called the embryonic enhancer locus for photoreceptor *Otx2* transcription (EELPOT). The enhancer is active in a subset of early embryonic retinal cells (E13), but not in the postnatal mouse retina. The sequences analysis of the enhancer revealed that they have multiple binding sites for E-boxes of bHLH genes of *Hes* families, which are the direct downstream target of Notch signaling. HES1 directly binds to the EELPOT enhancer to suppress *Otx2* expression and maintain proliferating RPCs at E13.5 (Muranishi et al., 2011). It is probable that there is an alternative genetic network in which *Otx2* and *Dlx2* work cooperatively in postmitotic RPCs to produce a subtype of horizontal cells. Notch signaling, which is a key regulator of the RPC pool during this time, induces *Hes1* expression to suppress *Otx2* expression by binding to the EELPOT regulatory region. In the absence of *Otx2,* neuronal differentiation is blocked, and progenitor cells maintain their progenitor pool. In the *Dlx2*-expressing progenitor cells, *Notch1* expression is blocked by DLX2 thus the *Hes1* activation signal is blocked in these RPCs. In the

absence of *Hes1, Otx2* maintains its expression, and the possible *Otx2/Dlx2* network amplifies signals to regulate downstream major horizontal differentiation genes. Altogether, this model may be an alternative network present to the early ganglion cell versus photoreceptor network (Figure 3.20). Importantly, several *in-vitro* and *in-vivo* functional assays have to be carried out to obtain evidence supporting this model. Specifically; we can start with investigating *Hes1/Notch1* expression levels in *Dlx1/Dlx2* DKO in mouse retina at E13.

We also started to investigate *Dlx2* upstream regulation during retinal development. *Dlx2* is a target of miR-124 in the adult subventricular zone (SVZ) during neurogenesis and is repressed by miR-124 in Hela cells *in-vitro* (X. S. Liu et al., 2011). Our previous *in-situ* data showed overlap of *Dlx2* and miR-124 mRNA expression mostly at GCL and the inner NBL at E13 and E18. miR-124 expression is significant in GCL and INBL at E18, which is consistent with global microarray profiling of retinal miRNAs expression at a variety of retina development time points. The retina miRNA expression profile demonstrated that the highest retina enrichment for miRNAs is from E18 to adulthood in mice (Hackler, Wan, Swaroop, Qian, & Zack, 2010). MiR-124 is most abundantly expressed in the retina and has been speculated to regulate many genes. It has been suggested that miR-124a is one of the main miRNAs functioning in photoreceptor cell maturation (Sanuki et al., 2011). We found one highly conserved miR-124 binding motif at the *Dlx2* 3´UTR region. This region is broadly conserved between all the vertebrates which could be indicative of its critical function during retina development. MiRNAs and their transcription factor targets often interact in a double-negative feedback loop (Tsang, Zhu, & van Oudenaarden, 2007). There are several DLX2 binding sites on miR-124 promoter 1kbp upstream of TSS, and miR-124 transcript expression was significantly

higher in the absence of *Dlx1/Dlx2*. Hence, DLX2 could prevent photoreceptor specification by repressing miR-124 and *Crx* expression at E18 (Figure 3.20).

Studies show that the interplay of miRNAs and TFs regulate key developmental events and cell fate decisions. Specifically, during skeletal muscle development, *Ezh2* and miR-124 form a double negative feedback loop wherein the high *Ezh2* expression in undifferentiated myoblasts suppresses miR-124. Upon differentiation, MyoD expression is activated and forces transcription of miR-124, which negatively regulates *Ezh2* expression to maintain skeletal muscle cell differentiation (Juan, Kumar, Marx, Young, & Sartorelli, 2009). However, to study the miR-124 function in this network, *Dlx2* expression must be investigated in miR-124 loss or gain of function experiments.

The *Dlx1/Dlx2* DKO retina mice tissues were used in our *in-vivo* functional studies. Thus, we must take into consideration that the *Dlx1* may also play a role in these networks. Multiple Dlx family functional studies in mice revealed that they are often redundant, specifically the ones that cluster together (*Dlx1* and *Dlx2*, *Dlx5* and *Dlx6*) (Debiais-Thibaud et al., 2013). *Dlx1* and *Dlx2* single knockout mice have subtle defects compared to *Dlx1/Dlx2* DKO mice, which suggest functional redundancy (Eisenstat et al., 1999). Furthermore, *Dlx1/Dlx2* global DKO mice die at birth for reasons unknown, which may interfere with the retina development process as well. To overcome this problem and investigate *Dlx2* function postnatally, we generated *Dlx2* eye-specific conditional knockout mice. We used the *Dkk3-Cre* line, as *Dkk3* is expressed in retinal progenitor cells from E10; thus, breeding this mouse with the *Dlx2*-floxed mouse deletes *Dlx2* in the retinal progenitor cells (Sato et al., 2007). Although this mouse has been used before to generate CKO in the retina for other genes, it has some disadvantages. The first progeny from *Dkk3-Cre* female breeder mouse showed complete

deletion in all tissues (Sakai & Miyazaki, 1997). As well, a small population of *Dkk3* expressing cells were found in the adult hippocampus and cerebral cortex. The *Dlx2* CKO retina morphology and structure was severely disrupted in both heterozygous and homozygous mouse compared to the control mouse. It seems that there are gaps in the GCL of the retina and the PR layer is expanded in *Dlx2* CKO retina, which could be consistent with *Dlx2* function in promoting RGC fate and repressing PR fate at E18. This also could explain the potential role of the DLX2 in RGC maintenance during adulthood. Photoreceptor differentiation (mostly rods) continues postnatally; it may be possible that the absence of *Dlx2* forces some ganglion precursors to switch and become rods. However, they have to be labeled with specific gene markers to determine the neuronal cell types, and to quantify their transcription levels. There has not been any research in the role of Dlx genes post-natally in retina and thus, there is no evidence on its possible effects after birth on the postnatal retina. Here, we found that the eyes of *Dlx2* CKO heterozygous mice are affected by probable cataracts, which could be caused by lens or ocular anomalies such as retinal degeneration and retinal folding. *Dlx2* has not been identified as one of the genes associated with cataracts, although it could be involved in the regulation of cataract genes (Nr2e3) (Messina-Baas & Cuevas-Covarrubias, 2017). *Dkk3* is part of the Wnt/β-catenin signaling pathway, and it is expressed in the ventricular and subventricular zone at E12.5 and continues to be expressed in the thalamus and cerebral cortex from E18 to adult mice. *Dlx2* is also expressed in the ventricular and subventricular zone at E12.5 (Petryniak et al., 2007). The overlap of *Dkk3* and *Dlx2* expression could potentially cause a problem in generating CKO mice, either by interfering in *Dlx2* function in the eye or by causing embryonic lethality by co-expression in a vital brain region such as the hypothalamus. There are several other Cre line mice

(*Rax*-*Cre* and BAC-*Chx10*-*Cre*), which have been used to generate specific gene conditional knockouts in the eye; these lines could be used as alternatives to *Dkk3*-Cre.

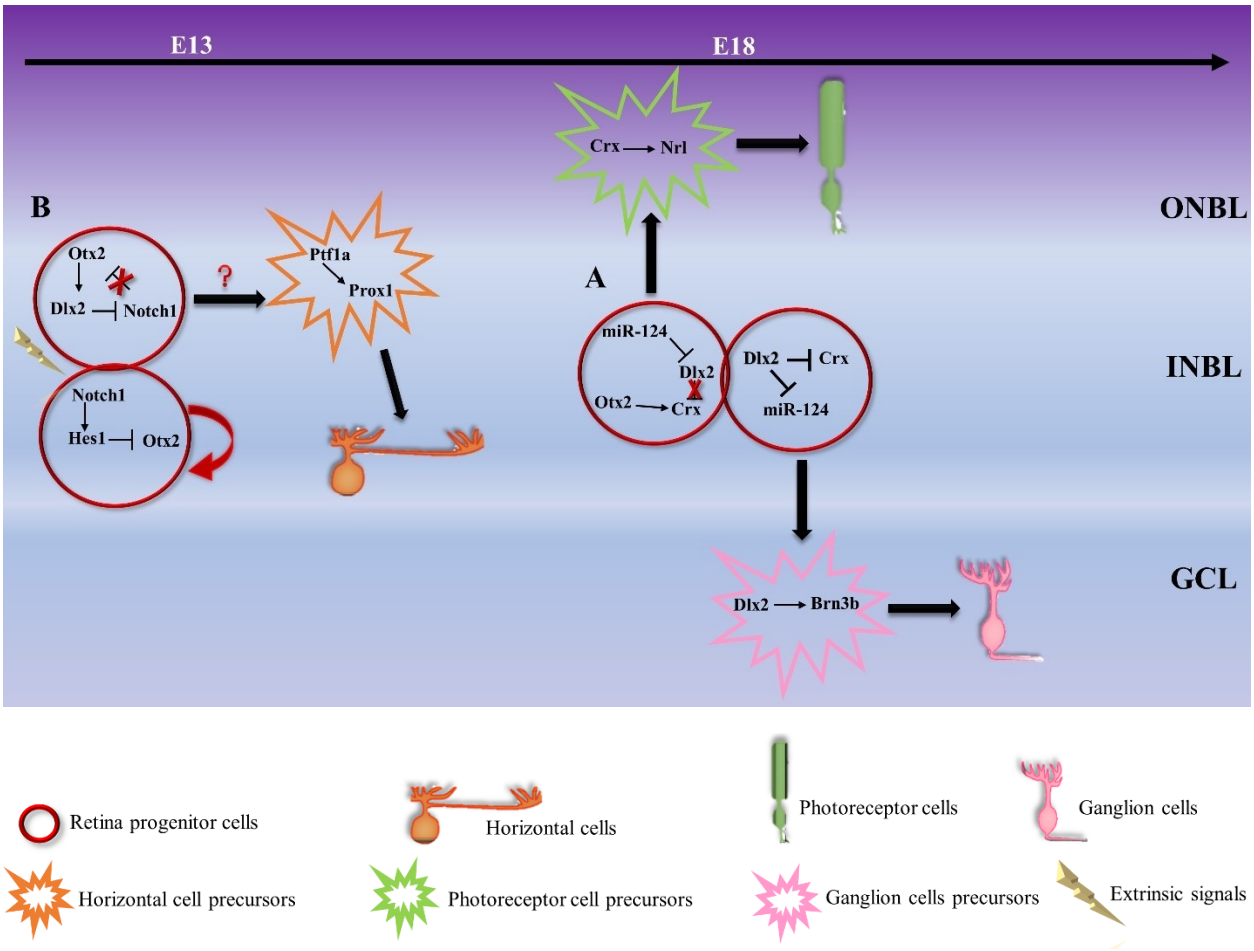

Figure 3.20. A schematic proposed model of the *Dlx2* genetic regulatory network during early/late retinogenesis

A schematic model of *Dlx2* involvement in the RPC determination network at E13/E18 mouse retina development. (A) At E18, the RPC population with *Dlx2* expression induces RGC precursors by repressing both *Crx* and miR-124. Other RPC populations wherein *Dlx2* expression is blocked. *Crx* maintains its expression and promotes PR precursor fate. (B) At E13, *Dlx2* plays a different role due to different environmental cues. Notch signaling is highly present in the INBL to maintain the progenitor pool at E13. Notch performs its function by sending signals through the RPCs and blocking the differentiation signals (*Otx2).* In the presence of Dlx2, Notch1 expression become suppressed and *Otx2-Dlx2* build a network to induce horizontal cell fate. The precursor cells have higher potency to go through terminal division and become fully differentiated to RGC, Horizontal or PR cells. To become fully differentiated other cell specific gene networks have to act to induce a specific fate. Embryonic day 13-18 (E13-E18), Outer neuroblastic layer (ONBL), Inner neuroblastic layer (INBL), Ganglion cell layer (GCL)

4 Chapter 4. *Dlx2* genes and evolution

4.1 Chapter abstract

There are eight *dlx* genes expressed in zebrafish. Five of the zebrafish *dlx* genes, *dlx1a/dlx2a*, *dlx5a/dlx6a* as well as *dlx2b* are expressed during zebrafish forebrain development. Additionally, *dlx* genes have been observed in the branchial arches, and in the median fin fold (Quint, Zerucha, & Ekker, 2000). Unlike the mouse, there have not been any studies on the expression and function of *dlx* genes in the zebrafish eye during development or adulthood. Based on our lab's preliminary data (J. Zagozewski, A. Waskiewicz and D. Eisenstat, unpublished data), we did not detect *dlx* gene expression in the zebrafish eye at 28hpf or 48hpf using wholemount *in situ* hybridization, limiting further study of their role in zebrafish eye development. During evolution of the zebrafish, expression of *dlx* genes appears to be lost in the zebrafish retina, but their expression and function is conserved in the developing forebrain and pharyngeal arches. However, the absence or the possibly low-level expression of *dlx* genes might assist us in studying its function by expression of the mouse *Dlx* gene in the zebrafish eye during embryogenesis.

Thus, I investigated the role of *Dlx* genes in the eye during development by expressing the mouse *Dlx2* in the zebrafish eye under control of the rx3 promoter (*Tg[rx3:Dlx2])*. I hypothesized that the mouse *Dlx2* would drives RGC differentiation by repressing PR-specific gene expression (consistent with that found in mice) in the zebrafish retina. I generated a mouse *Dlx2* transgenic stable zebrafish line (*Tg[rx3:Dlx2])* to further investigate *Dlx2* involvement in retina development.

4.2 Introduction

4.2.1 Eye Evolution

"To suppose that the eye, with all its inimitable contrivance, could have been formed by natural selection, seems, I freely confess, absurd in the highest possible degree… Yet reason tells me, that if numerous gradations from a perfect and complex eye to one very imperfect and simple, each grade being useful to its possessor, can be shown to exist… and if any variation or modification in the organ be ever useful to an animal under changing conditions of life, then the difficulty of believing that a perfect and complex eye could be formed by natural selection, though insuperable by our imagination, can hardly be considered real" (Darwin & Carroll, 2003) Charles Darwin (1809–1882).

Around 600 million years ago (Mya), some early organism evolved photoreceptors that were capable of signaling light, although it wasn't until 540 Mya that the image-forming eye emerged (Conway Morris, 2006). The emergence of bilaterally symmetrical animals gave rise to both invertebrates and vertebrates, followed by extensive genome duplication (Suga et al., 1999). In addition, a whole genome duplication happened early in vertebrate evolution (Pasquier et al., 2017), which had a critical role in the development of early vertebrate. All these genetic changes led to the emergence of new features. The lamprey is an early vertebrate in which the eyes are very similar to those of jawed vertebrates, with lens, iris and extra-ocular muscles, and a retina similar to other vertebrates with three nuclear layers comprising of photoreceptors (with opsin expression), bipolar cells, horizontal cells and ganglion cells. This implies that the camera-like eye must have been evolved when lampreys and gnathostomes diverged (Lauder, 1997). Looking at earlier Chordates such as hagfish, the eyes are small without lens or cornea, and the retina contains two layers with photoreceptor cells that directly connect to the output neurons (ganglion

cells) (Fernholm & Holmberg, 1975). The hagfish eye is the earliest model to exhibit structural similarities to the vertebrate. However, functionally their eyes resemble the pineal organ of a non-mammalian vertebrate. Therefore the hagfish eye seems not to contribute to vision; instead, it appears more likely to function as a circadian organ, similar to the gnathostome pineal complex (Newth & Ross, 1955). Thus, it was concluded that bilateral eye evolution started as early as chordates, and eventually evolved to the camera-like eye.

Animal photoreceptors are classified into two types: rhabdomeric or ciliary. One of the main differences between these types relates to the topology of the large area of membrane in which the photopigment (opsin) is incorporated: rhabdomeric photoreceptors incorporate this membrane into apical microvilli, whereas ciliary photoreceptors extend membranes from a modified cilium. The phylogenetic analysis of eye-specifying transcription factors revealed that the bilateral common ancestor of protostomes and deuterostomes contained both rhabdomeric and ciliary photoreceptors (Arendt, 2003). In addition, it has been suggested that ganglion cells are sister cells to rhabdomeric photoreceptors on the basis of close homology of their transcription factors. Therefore, it is possible to view our own retinal ganglion cells as rhabdomeric photoreceptors that have lost their rhabdomeric membrane structure, but retaining their axons (Arendt, Tessmar, de Campos-Baptista, Dorresteijn, & Wittbrodt, 2002).

Ciliary photoreceptor morphology went through several stages of evolution from tunicates to mammals. From the hagfish eye to the jawed vertebrate retina, the photo-pigment containing membrane extends from the cilium. In hagfish the membrane radiates more laterally, whereas the outer segment has a more stacked organization in lamprey. Finally, in vertebrates, the membrane is highly ordered and stacked. Ribbon synapses evolved in the synaptic terminal along with the membrane (P. W. Holland, Garcia-Fernandez, Williams, & Sidow, 1994). Cone-

bipolar cells possibly evolved from cone photoreceptors, increasing the computing power of retina, by developing new contacts from photoreceptors to ganglion cells. This led to the development of a three-layered neuronal structure with intervening plexiform layers in the retina (Reichenbach & Robinson, 1995). Rhodopsin evolved from cone opsin, and rod-bipolar cells evolved from rod photoreceptors. During this process, genome duplication created multiple copies of phototransduction genes, which eventually elaborated the vertebrate phototransduction process that converts light signals to chemical signals for the brain.

4.2.2 The evolution of *Dlx* genes

Dlx genes are widespread through Metazoa, and it is likely that they evolved early during metazoan evolution (McDougall, Korchagina, Tobin, & Ferrier, 2011). *Dll*-like genes in *C.elegans* are proposed to be representative of the *Dll* gene ancestor (Plavicki, Squirrell, Eliceiri, & Boekhoff-Falk, 2016). A tandem gene duplication led to the formation of convergently transcribed *Dlx* genes in early chordates (*Ciona intestinalis* contains two *Dlx* genes). Subsequently, a series of gene duplications produced at least three pairs in vertebrates. Since *Dlx* genes are linked to *Hox* genes, multiple *Dlx* genes may have arisen from *Hox* genes duplication (Stock et al., 1996). For instance, the *hox* cluster duplication in zebrafish resulted in the emergence of *dlx2b* and *dlx4a* (Amores et al., 1998). There are several commonalities between *Dll* and *Dlx* expression which are suggestive of the ancestral function of *Dll*/Dlx. *Dll* genes are closely related to *Dlx1* which has been speculated to be the founding member of the *Dlx* vertebrate family (N. D. Holland, Panganiban, Henyey, & Holland, 1996). *Dll*/*Dlx* expression in the vertebrate and invertebrate nervous systems led to the hypothesis that the original function of *Dll*/*Dlx* genes was in the nervous system and that other functions evolved later during evolution (Panganiban et al., 1997). The DLX proteins are also highly conserved, not only in the

homeodomain region and its adjacent sequences, but also, close to N-terminal of the protein, and the hydrophobic domain close to C-terminal of the protein (Stock et al., 1996).

Dlx expression is found in Planarian eyes, which are simpler than the vertebrate camera eye. These *Dlx* genes are a homologue of the *Distal-less* family and are involved in Planaria eye regeneration (Lapan & Reddien, 2011). *Dlx* expression also has been described in chicks, frogs, rodents and human during eye development. Although *dlx* genes are present in zebrafish forebrain during development, it has not been reported to be detected in the eyes.

Table 6. Dlx genes expression in the eye

Animal model	Embryo	Adult	Cell type	Reference
Human	Yes	Yes	GCL, RPC	Merlo et al., 2000
Mouse	Yes	Yes	GCL, RPC	de Melo et al., 2005
Chicken	Yes	Yes	GCL	Q. Jiang and D. Eisenstat, unpublished data
Zebrafish	?	?	?	M. Hejazi, J. Zagozewski, A. Waskiewicz, W.T. Allison and D. Eisenstat, unpublished data
Catshark	Yes	-	Optic cup	Debiais-Thibaud et al., 2013
Planarian	Yes	Yes	Optic cup	Lapan & Reddien, 2011

4.2.3 *dlx* gene family expression in the zebrafish

The zebrafish genome has eight *dlx* genes of which six show similar bigenic arrangements to the mouse: *dlx1a/dlx2a*; *dlx3b/4b*; and *dlx5a/6a* clusters are orthologous to *Dlx1/Dlx2*; *Dlx3/Dlx4*; *Dlx5/Dlx6*, respectively (Quint et al., 2000). The first *dlx* genes expressed in zebrafish are *dlx3b* and *dlx4b* during gastrulation, and later they become confined to the olfactory and otic placodes (Ellies et al., 1997). *dlx1a/dlx2a, dlx2b*, and *dlx5a/6a* are expressed in zebrafish forebrain with a similar pattern found in mice in the telencephalon and diencephalon. Lineage tracing experiments revealed that *dlx1a/dlx2a* are expressed in zebrafish telencephalon and prethalamus during forebrain development (Solek, Feng, Perin, Weinschutz Mendes, & Ekker, 2017). *dlx1a/dlx5a* co-express with *gad1* within the telencephalon to regulate GABAergic interneuron differentiation. *dlx1a/dlx2a* and *dlx5a/dlx6a* are in part involved in GABAergic interneuron differentiation. *dlx1a/dlx2a* or *dlx5a/dlx6a* knockdown using morpholinos in zebrafish, result in disruptions in *gad1b* expression in the developing embryo (MacDonald et al., 2013). All *dlx* genes except *dlx2b* are expressed in the branchial arches and teeth, and all 8 *dlx* genes are expressed in median fin fold development. The only report suggesting *dlx* expression in the zebrafish eye is in the I12a and I12b intergenic regions, which have been implicated to be active in retina where expression of *dlx1a* or *dlx2a* has not been previously reported; however, their function remains unknown (MacDonald, Debiais-Thibaud, Talbot, & Ekker, 2010).

4.3 Results

4.3.1 *dlx* genes are not expressed in the retina during zebrafish development or adulthood

dlx genes are consistently expressed in forebrain development in parallel with their expression in the retina in most vertebrates studied (Stock et al., 1996). Our lab has been exploring *Dlx* gene family expression and function during retinal development in multiple species including mice and chickens, which provide us with various animal models to study *Dlx* GRN during retinal development. Initially, our lab was interested in investigating the role of *dlx* in zebrafish retinal development, as the expression pattern of *Dlx* genes is highly conserved in mouse and zebrafish CNS development (MacDonald et al., 2010). Six of eight zebrafish *dlx* genes are involved in forebrain neurogenesis; hence, we predicted that their homologous *dlx* genes are expressed in the zebrafish eye. *dlx* RNA probes were generated for *in-situ hybridization* and *dlx* expression was examined at 28hpf and 48hpf (peak time for retinal development in zebrafish eye) larvae development (J. Zagozewski, A. Waskiewicz, D. Eisenstat, unpublished data). Unlike their strong regional expression in the telencephalon, *dlx* expression was not found in the eye at either time point. To quantify *dlx* orthologue transcript expression, the eye tissues were collected from 5dpf larvae and qRT-PCR was performed with primers designed for *dlx* genes. The whole larvae were also collected at the same age (5dpf) to provide the relative expression of *dlx* genes in other tissues. While *dlx1a, dlx2a*, *dlx2b* and *dlx3b* transcripts were detected in whole larvae ($Ct \leq 28$) (Figure 4.1A), their mRNA expression was relatively low ($Ct \geq 31$, except *dlx3b* Ct=29) in the eye (Figure 4.1B). The adult eye and the adult retina tissues were separately dissected from zebrafish, and qRT-PCR were repeated with the same *dlx* primers. *dlx* mRNA expression of four *dlx* genes in the adult eye and the retina presented similar Ct values to each other ($Ct \geq 31$, except *dlx3b* Ct=29), consistent with *dlx*

transcript expression in the eye at 5dpf larvae development (Figure 4.2A-B). β-actin was used as reference housekeeping gene in both larval and adult tissues (Ct=18). Our results indicate that, unlike in the forebrain, endogenous *dlx* gene expression is extremely low in the eye and retina tissues during late larval development and in adult fish.

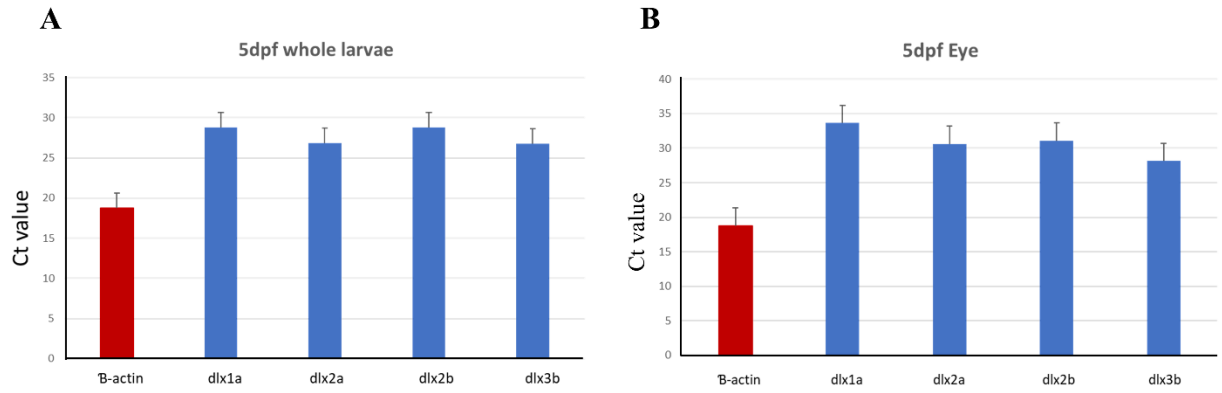

4.1. Zebrafish *dlx* gene mRNA expression is low in 5 dpf zebrafish eye

dlx1a, dlx2a, dlx2b and *dlx3b* transcript expression was measured in the whole larvae and the eye of 5 dpf larvae (A) The Ct value of the four (*dlx1a, dlx2a, dlx2b,* and *dlx3b) dlx* genes was Ct ≤ 28 in the whole larvae (B) The Ct value of three (*dlx1a, dlx2a,* and *dlx2b) dlx* genes was Ct ≥ 31. β-actin were used as our house keeping gene. Ct values did not change between the whole larvae and the eye, Ct=18.

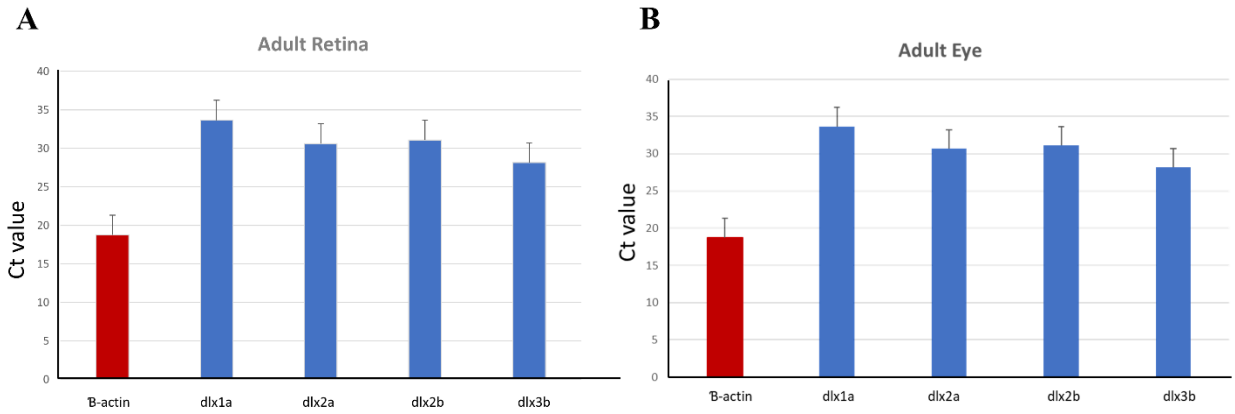

Figure 4.2. Zebrafish *dlx* gene mRNA expression is low in adult eye and retina

dlx1a, dlx2a, dlx2b and *dlx3b* transcript expression was measured in the tissues collected from adult zebrafish eye, as well as retina (A). The Ct values of the three *dlx* genes (*dlx1a, dlx2a,* and *dlx2b)* was Ct ≥31 in the adult retina tissues (B) The Ct values of the three *dlx* genes (*dlx1a, dlx2a,* and *dlx2b)* was Ct ≥31 in the adult eye tissues. β-actin was used as our housekeeping gene; its Ct value did not change between the adult retina and the eye, Ct=18.

4.3.2 Creating mouse *Dlx2* transgenic zebrafish *Tg[rx3:Dlx2]*

To investigate the absence of *dlx* expression in the zebrafish retina and its expression in the mouse, and to investigate a potential GRN of *Dlx2* switching photoreceptor fate to retinal ganglion cell fate, we designed a construct with the mouse *Dlx2* coding region, under the *rx3* promoter (expressed in retinal progenitor cells). We aimed to drive mouse *Dlx2* expression in zebrafish retina by creating *Tg[rx3:Dlx2]* zebrafish. The *rx3* promoter previously has been used to create retina specific transgenic fish, as it is required for early optic vesicle development (13hpf) (Yin et al., 2014). A 3XFLAG-tag was added to the construct to detect *Dlx2* expression in the retina. The cloned construct was microinjected into zebrafish single cell embryos. To confirm *Dlx2* expression in the stable transgenic lines, the presence of *Dlx2* protein and mRNA was detected by immunostaining, Western blotting, and qRT-PCR. Transgenic and wild embryos were selected at 5dpf, and wholemount immunostaining was performed with FLAG and *Dlx2* antibodies. The FLAG-tag expression was detected in *Tg[rx3:Dlx2]* larvae and was not detected in WT controls (Figure 4.3A-B). DLX2 expression was also evident in the *Dlx2* transgenic zebrafish compared to WT controls; however, some signal from the DLX2 antibody was detected in wild type zebrafish (Figure 4.3C-D). To further investigate the presence of *Dlx2* expression in the zebrafish eye, *Dlx2* transcript levels were measured in the 5dpf eye tissues dissected from zebrafish larvae. In addition, to find out whether *Dlx2* expression is maintained during adulthood, *Dlx2* mRNA was also measured in adult transgenic and wild type eyes. The *Dlx2* transcript level was significantly higher in both *Tg[rx3:Dlx2]* larvae and adult fish compared to the WT controls (Figure 4.4A-B). To confirm DLX2 protein expression during zebrafish adulthood, eye tissues were collected from *Dlx2* transgenic and WT adult zebrafish and Western blotting was performed using mouse DLX2 and FLAG antibodies. Inconsistent with our previous

results, we could not detect DLX2 or FLAG protein expression by Western blotting in adult zebrafish. Altogether, there is a high probability that our transgenesis was successful, and mouse *Dlx2* is expressed in the zebrafish retina, although further optimization is required for confirmation.

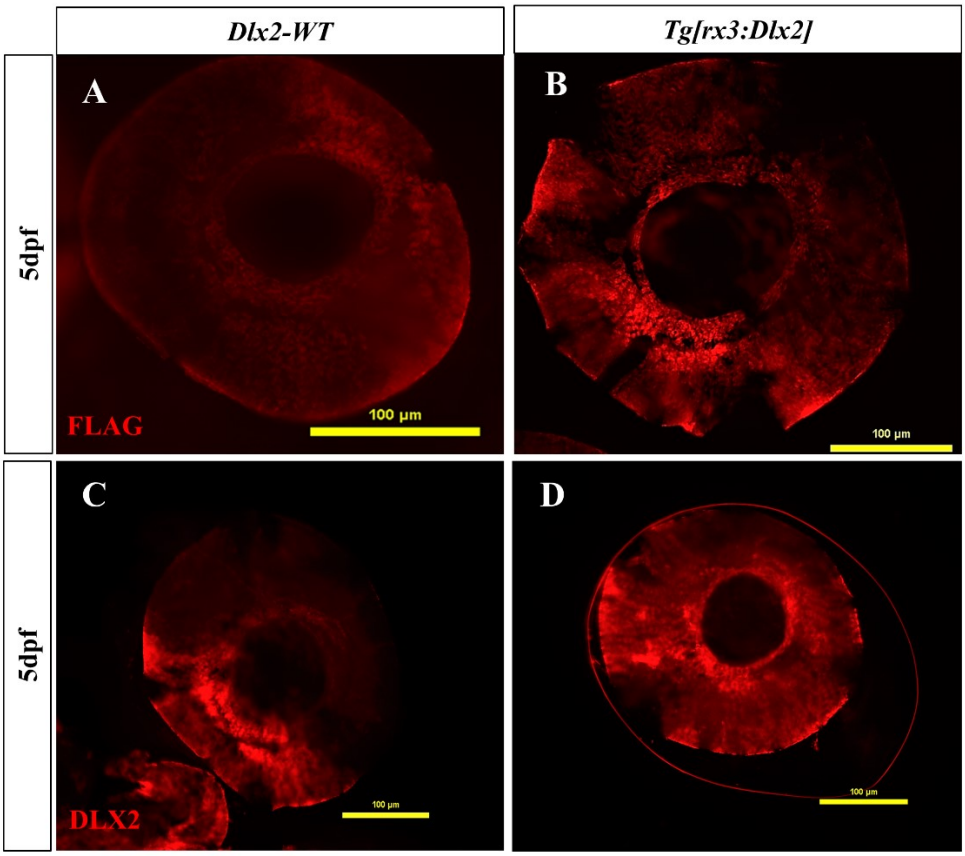

Figure 4.3. Mouse DLX2 expression was found in the *Tg[rx3:Dlx2]* zebrafish eye at 5dpf

Whole mount staining of 5dpf zebrafish larvae using mouse DLX2 and FLAG antibodies (Messina-Baas & Cuevas-Covarrubias). There is no FLAG expression in the *Dlx2*-WT eye, however, FLAG expression was present in the transgenic eye. (C-D) DLX2 is highly expressed in the transgenic fish eye compare to its partial signal in WT animal. 5dpf; 5 days post fertilization, Scale = 100 µm

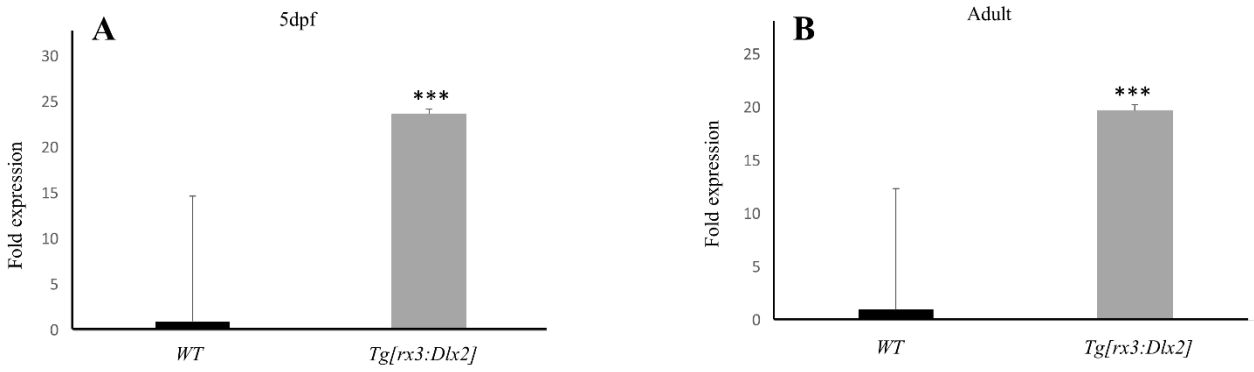

Figure 4.4. Mouse *Dlx2* mRNA levels of *Tg[rx3:Dlx2]* were significantly higher than *Dlx2*-WT in 5dpf larvae and adult zebrafish

Dlx2 transcript expression was measured by qRT-PCR in the eye tissues. (A) Mouse *Dlx2* mRNA expression is significantly increased in 5dpf *Dlx2*-Tg eye tissues (B) Similarly, *Dlx2* is highly expressed in the adult *Dlx2*-Tg eye tissues. 5dpf; 5days post fertilization; n≥3; ***=P ≤ 0.001

4.3.3 The transcript levels of retinal ganglion cell specific genes are altered in *Tg[rx3:Dlx2]* zebrafish compared to WT fish

DLX2 is involved in mouse neuronal cell specification during retinal development. In the absence of *Dlx1/Dlx2,* RGC numbers are reduced in the developing retina (de Melo at al., 2005). PR cell numbers were increased in *Dlx1/Dlx2* DKO mouse compared to WT controls at E18. Thus, we investigated the expression of these neuronal cells in the *Tg[rx3:Dlx2]* adult zebrafish compared to non-transgenic WT fish. Initially, several zebrafish RGC gene specification markers were selected (*brn3a, brn3b* and *isl1*) and their expression was measured in the *Tg[rx3:Dlx2]* and WT adult eye tissues by qRT-PCR. The transcript expression level of all three RGC markers was reduced in *Tg[rx3:Dlx2]* eyes relative to WT eyes during adulthood (Figure 4.5). This result suggests that RGC differentiation may be decreased in *Tg[rx3:Dlx2]* adult zebrafish eyes based upon reduced expression of RGC markers. Further experiments are ongoing, including assessment of PR-specific markers.

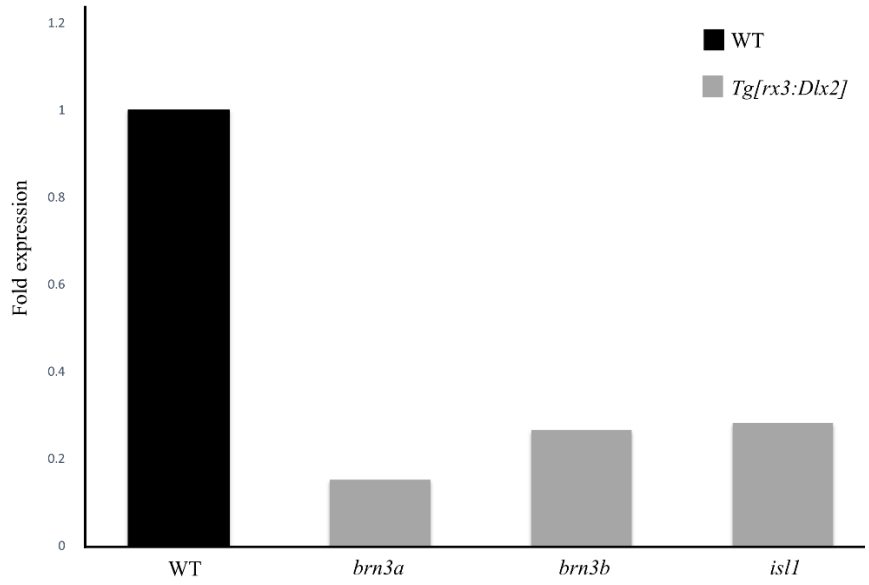

Figure 4.5. The RGC number is reduced in the *Tg[rx3:Dlx2]* relative to *Dlx2*-WT adult zebrafish

Transcript expression levels of *brn3a, brn3b* and *isl1* were quantified in *Dlx2*-Tg and WT eye tissues by qRT-PCR. *Brn3a, brn3b* and *isl1* expression were decreased in the transgenic eyes compared to the controls. n=2

4.4 Discussion

The transcription of many TFs, including the *Dlx* family, is highly conserved between vertebrates and invertebrates (Neidert et al., 2001). This is an indication of the critical function of *dlx* genes during evolution in animal development. The *dlx* genes function in the development of pharyngeal arches, otic vesicles, fins, forebrain and a few other tissues in zebrafish (Talbot, Johnson, & Kimmel, 2010). However, their expression and function have not been studied in the zebrafish eye. Zebrafish *dlx* genes have extensive similarities in their combinatorial expression with orthologs of other vertebrates such as the mouse. For instance; mouse *Dlx2* is orthologous with zebrafish *dlx2a* and *dlx2b* (Ekker et al., 1998). Thus, the study of *Dlx* genes in zebrafish would provide us with additional knowledge on their gene regulatory network during retinogenesis. Initially, the *in-situ hybridization* for endogenous *dlx* expression in zebrafish larvae with *dlx* probes did not produce any signal in the eye, which maybe due to the lack of *dlx* expression in the eye during larvae development. mRNAs with low copy number might not be detected by *in-situ hybridization*; therefore qRT-PCR was a sensible alternative technique to quantify *dlx* genes expression in the eye (Levsky & Singer, 2003). The overlapping expression pattern of *dlx1a/dlx2a* and *dlx3b/dlx4b* is evident in most zebrafish *dlx*-expressing tissues; thus, we started by testing these genes (*dlx4b* was replaced with *dlx2b* due to technical problems). *dlx1a, dlx2a* and *dlx2b* presented with low transcript expression in 5dpf and adult zebrafish eyes. However, *dlx3b* expression was relatively higher compared to other *dlx* genes. Other than *dlx3b,* this result is consistent with *dlx* gene detection by *in situ hybridization* in which *dlx* gene expression was not detected in the eye. It is possible that *dlx3b* primers amplified an unspecified gene in addition to *dlx3b* which is also expressed in fish retina tissues. Designing new primers could clarify whether *dlx3b* is expressed in the retina. It is important to note that the samples for

qRT-PCR were collected from 5dpf larvae; eye samples from 24hpf or 48hpf might be more informative since eye development has not been completed at these time points (unfortunately, I could not obtain sufficient samples for qRT-PCR at these embryonic time points). Also, further protein detection experiments are required to investigate the presence of *dlx* proteins in the fish retina. However, it is probable that *Dlx* genes expression is lost in zebrafish retina and gained back in mice, or *Dlx* genes was expressed only during optic cup development in earlier species (Lapan & Reddien, 2011) and gained retina expression from the optic cup in mammals during evolution to adapt with the changing environment (Kim et al., 2016). Investigating multiple fish species as well as earlier Chordates may provide us with more insight on *Dlx* expression patterns in the retina during evolution.

As described previously, *Dlx2* is highly expressed in the mice retina, with a possible role in cell fate decision (de Melo et al., 2005). Nucleotide blasting of *Dlx2* CDS shows up to 79% sequence identity with *dlx1a*, *dlx2b* and *dlx5a*, and 76% sequence identity with *dlx3b* and *dlx4b*. In addition, Dlx2 homeodomain protein sequence is highly conserved between mouse (DLX2) and zebrafish (*dlx2a* and *dlx2b*) (Figure 4.6). Therefore, we decided to generate a transgenic zebrafish with mouse *Dlx2* under *rx3* (expressed in RPC) regulation, which could help us to gain a better understanding of *Dlx* gene evolutionary function. We assumed that mouse *Dlx2* works with the zebrafish transcriptional machinery and presents its normal protein function in the zebrafish retina. This method has been previously used to study evolutionary traits. For example, mice with the human version of *FOXP2* speech genes revealed some differences in their neuronal electrical stimulation and ultrasonic calls compare to normal mice, which started a path to explore human speech evolution (Enard et al., 2009). In an attempt to detect the expression of *Dlx2* in the transgenic zebrafish, we detected the mouse *Dlx2* by immunofluorescence and qRT-

PCR, but not by Western blotting. For Western Blots, eye tissues were initially collected from adult zebrafish, but we did not detect either DLX2 or FLAG protein, which suggests that adult transgenics may not have sustained DLX2 protein expression in the retina. However, *Dlx2* mRNA transcript was detected by real-time PCR in adult zebrafish, so it is still probable that *Dlx2* transcript expression is maintained, but the mRNA degrades before translation in the adult fish. Alternatively, significantly increased quantities of proteins should have been loaded onto the gels prior to immunoblotting. The adult zebrafish eye is constantly growing and therefore new retina cells are added the retinal margins at a slow rate, so it is possible that DLX2 protein is being produced at low and/or transient levels. In contrast, FLAG tag and DLX2 expression were detected by whole mount immunofluorescence during larval development. Zebrafish embryo whole mounts are a straightforward technique to detect gene expression, although it has its own limitations. Therefore, embedded eye sectioning is required to confirm DLX2 expression in the retina using immunohistochemistry or immunofluorescence.

Dlx2 could be involved in RGC fate decision during mouse retinal development and based on our model it may promote ganglionic cell fate over PR fate. We chose to investigate ganglion cell-specific gene expression in the *Tg[rx3:Dlx2]* zebrafish in accordance with the *Dlx2* function in mice retina, where *Dlx2* has a direct relation to RGC gene expression. Our quantifications revealed an inverse relation of ganglion cell marker expression with the presence of *Dlx2*, as zebrafish ganglion cell marker expression was reduced in *Tg[rx3:Dlx2]* adult eyes compared to wild type eyes. I used Tol2-mediated transgenesis to insert the *rx3*-driven *Dlx2* coding region into the zebrafish genome, for which integration into the genomic DNA occurs in a randomized way. The randomness of integration may cause endogenous gene disruption, which may potentially interfere with normal retina development. *Brn3a* (Q. Zhang and D. Eisenstat,

unpublished results) and *Brn3b* are direct DLX2 transcriptional targets during mouse retinal development. They build an alternative pathway to *Atoh7-Brn3b*/*Isl1* for RGC development (Zhang et al., 2017). *Dlx2* expression in the retina may initially lead to RGC generation, which could interfere with the endogenous *brn3a/brn3b/isl1* network that induces RGC fate in the zebrafish, and thus the overall number of RGC may decrease in *Tg[rx3:Dlx2]* fish. As mentioned before, active *dlx1a* and *dlx2a* intergenic regions were detected in the zebrafish retina (Poitras et al., 2007); thus, these regions could have an unknown function in regulating ganglion cells. For instance; it has been shown that *ascl1* binds to the l12b enhancer and activate *dlx1a/dlx2a* expression in zebrafish forebrain. Since *ascl1* is also expressed in zebrafish retina, in the presence of mouse *Dlx2* it may interact with intergenic enhancers, and repress ganglionic cell differentiation (MacDonald et al., 2013). The *dlx1a* and *dlx2a* intergenic enhancers are conserved in mice and located in the *Dlx1/Dlx2* cluster; hence, it is possible that mouse *Dlx2* could bind to these enhancers in zebrafish and trigger several downstream genes related to intergenic enhancer function. However, several other retinal neuronal cells including PR markers *Otx2* and *Crx* remain to be quantified in *Tg[rx3:Dlx2]* and compared to wild type zebrafish to reach a more definitive conclusion. Similar to mice, both *crx* and *otx* genes are expressed during zebrafish photoreceptor development. However, unlike mammalian retina which *Crx* is mostly involved in cone-rod maturation and survival, in zebrafish *crx* expression has been found during early retina differentiation in retinal progenitor cells (Shen et al., 2004. *otx1a, otx1b* and *otx2* are mammalian *Otx1* and *Otx2* orthologue in zebrafish, and they are expressed during zebrafish RPE and retinal development (Brandon M.Lane and Lames A.Lister, 2012). Thus, further experiments, investigating *crx* and *otx* expression in the presence of mouse DLX2 may help us to better understand the possible differences between mice and zebrafish retinal development.

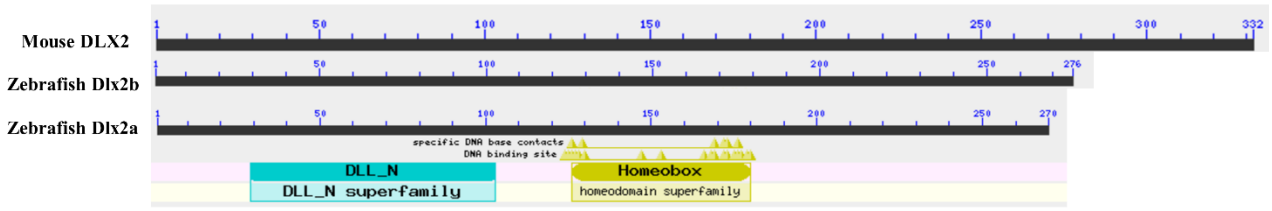

Figure 4.6. Putative conserved domains of mouse DLX2, and zebrafish Dlx2b/Dlx2a proteins

Mouse DLX2 and zebrafish Dlx2b/Dlx2a proteins have approximately 50% protein sequence identity; however their homeobox domain and Homeobox protein distal-less-like N terminal (DLL_N) are highly identical

5 Chapter 5. The role of *Nrp2* in retina development

5.1 Chapter abstract

Neuropilins are critical for vascular, cardiovascular, and neuronal development (Kawasaki et al., 1999). While there have been a few reports regarding the role of *Nrp1* during the development of the retinal vasculature, little is known about the role of *Nrp2* during eye development. Following our previous graduate student's initial research (J. Zagozewski), regarding the eye phenotypic abnormalities of *Nrp2* KO mice, our objective (in collaboration with Dr. D. Graf and Dr. Y. Sauvé) was to study the eye physiology and retinal structure of the *Nrp2* KO mouse post-natally, as well as assess the biological function of *Nrp2* during eye development. We hypothesized that consistent with our previous findings in the embryonic *Nrp2* KO eye, retina structure and folding maintain its abnormal phenotype after birth. Additionally, we speculated that eye physiology would be abnormal in the adult *Nrp2* KO mice. We characterized altered retinal neuronal cell differentiation as well as aberrant ERG and OCT findings in *Nrp2* KO mice post-natally. We also found retina layer misfolding and expansion post-natally.

5.2 Introduction

5.2.1 Retina vasculature development

Retinal development starts at E8.5 to E9 and finalizes post-natally, especially in rodents. The retinal neuronal cells are born in an overlapping temporal order, and within the first few weeks after birth, neuronal lamination as well as synaptogenesis and dendritogenesis is completed (Fan et al., 2016). Retinal vasculature development starts post-natally at P1 and continues to post-natal week four (P28). Initially, neuronal development is supported by a transient hyaloid vasculature network embryonically. The hyaloid vasculature is a network of

temporary blood vessels in the vitreous, which later become replaced by the mature retina vasculature network (Albaroudi, Tijani, Lezrek, Daoudi, & Laghmari, 2017). In mice, embryonic stage astrocytes invade the retina and form a mesh-like network to provide a template for later vascular development (Fruttiger, 2002). The invading astrocytes arise from the optic nerve head and proliferate through the inner surface of the retina (Ling & Stone, 1988). Angiogenesis begins the first week after birth, where retinal vessels that originated at the optic nerve enter the retina, to subsequently reach the retinal periphery. From P0 to P7, the superficial vascular primary plexus guided by the astrocyte network expands radially through the GCL by sprouting, and reaches the peripheral retina by P7 (Selvam, Kumar, & Fruttiger, 2018). At P7, a deep capillary plexus starts to grow from primary veins and vertically sprouts into the plexiform layers to form an interconnected vessel network, and by the third postnatal week the intermediate/deep plexus development is complete (Fruttiger, 2007).

The extension of vessel sprouts is critical for the formation of the vascular network during its development. This process requires different behaviours of endothelial cells, based on their location. The endothelial cells located at the tip of the sprout are migratory compared to the cells located at the stalk (Gerhardt et al., 2003). “Endothelial tip cells” extend numerous filopodia, which grow the sprouts by responding to attractant and repellent guidance cues. These cues, including VEGF and other angiogenic factors, play a crucial role in guiding the endothelial cells in a proper direction (Adams & Eichmann, 2010). These tip cells guide the direction of vessel growth by sensing VEGF gradients; on the contrary, the cells located in the stalk proliferate, maintaining sprout extension. The Notch signaling ligand, Delta like 4 (DLL4) regulates the tip/stalk state of endothelial cells. DLL4 is highly expressed in the tip state, and activates Notch1 in the neighboring cells where it suppresses DLL4 transcription and inhibits

them to enter the tip state (Benedito et al., 2012). The artificial inhibition of the DLL4/NOTCH1 pathway allows more endothelial cells to enter the tip state, and leads to increased branching of primary plexus vessels (Hellstrom et al., 2007). The Notch network is tightly connected to VEGF signaling, as the VEGF receptor-2 (VEGFR2) promotes *Dll4* transcription which promotes the tip state in the cell, and the tip cells move toward higher VEGF concentrations. VEGF is regulated by oxygen tension and its expression becomes upregulated in the non-vascularized peripheral retina which is hypoxic. The cells at the tip state are more sensitive to VEGF signaling, which favours the tip state at the leading edge of the growing plexus to grow toward higher VEGF concentrations. Altogether, the interaction of NOTCH and VEGF produces VEGF gradients which guide the sprouting of the endothelial cells into the retina (Blanco & Gerhardt, 2013). In addition, retinal neuronal cells also modulate the tip/stalk state of endothelial cells. For instance, RGC suppress DLL4 expression by releasing a Semaphorin 3A (Sema3A) signal to negatively regulate the tip state and prevent misdirection of developing vasculature (Fukushima et al., 2011). Additionally, RGC are able to sense hypoxia in developing retina by its G protein-coupled receptor-91 (GPR91), and coordinately regulate the production of angiogenic growth factor (Sapieha et al., 2008). In fact, RGC have a critical role in retinal blood vessel development, since the primary vascular plexus fails to develop post-natally in *Math5 (Atoh7)* deficient mice (Edwards et al., 2012).

Deeper plexus vasculature development is initiated from veins in the superficial plexus. Although the deeper plexus development is less well studied, many signaling pathways acting on primary plexus spreading act on deeper plexus development as well. Deleting many previously mentioned genes (VEGF and NRP1) not only impaired the primary vascular plexus but negatively affected the development of deeper vascular plexus (Hirota et al., 2015). VEGF

signaling plays a key role in inducing and guiding deeper vascular plexus development. Around P7 during mouse retinal development, the neuronal expression of VEGFR2 (VEGF endothelial receptor) is reduced, resulting in a higher concentration of VEGF and triggering deeper vascular plexus sprouting (Okabe et al., 2014). Upon retinal vasculature maturation, by P28 the hyaloid vasculature is fully regressed, and the retinal vasculature network is complete.

5.2.2 Neurovascular development

Neurovascular development is the parallel appearance and patterning of vascular and nervous systems throughout CNS early development. This cross-talk between neurons and vessels is essential for CNS development, and it initiates early embryogenesis and continues during later stages. There is a direct link between angiogenesis and neurogenesis, as endothelial cells release cues for neurogenesis and vice versa (Huxlin, Sefton, & Furby, 1992). Once vessels invade the developing CNS, the cues provided by neuronal cells guide them in a specific direction; on the other hand, the vessel sprouts migrate through progenitor cells and regulate their proliferation. Endothelial cells and the pericytes form a communicative interaction with the neurons and astrocytes at the cellular level. This associative grouping is called the neurovascular unit (Lok et al., 2007). Neurovascular communication is facilitated by molecular cues between neurons and endothelial cells such as VEGF receptors, semaphorins/plexin receptors, and the neuropilins which are co-receptors of both VEGF and plexins. VEGF endothelial cell conditional knockout mouse demonstrate disruption of neuronal progenitor cell (NPC) proliferation, differentiation and lamination during CNS development. On the other hand, it has been shown that neuronal progenitor cells are another source of VEGF (Ogunshola et al., 2000), and consequently, *Vegf* deletion in NPC resulted in disrupted angiogenesis and neuronal defects in mice early CNS development (Raab et al., 2004). Another study which used the *Tie2-cre* mouse

to delete *Vegf* in endothelial cells, showed reduced vessel density in the telencephalon, but also the morphology of the telencephalon was impaired by E17. The cortical brain layer cytoarchitecture was abnormal, and the cortical laminar organization was disrupted. Several types of cortical neuronal cell (including GABAergic interneurons) proliferation and migration were affected by E15 in the dorsal telencephalon. They concluded that endothelial VEGF regulates neuronal proliferation and migration by enforcing the "stop" signal during telencephalon development; thus, in the absence of the signal, overproduction of neuronal cells combined with disrupted migration leads to abnormal lamination of the cortical zone (Li, Haigh, Haigh, & Vasudevan, 2013).

The retina is an excellent model to study neurovascular communication during development, since as described above, neuronal and vasculature development proceed in a distinct temporal and spatial pattern. Investigating the interactions between the inner nuclear layer and intermediate/deep vasculature reveals a tight interaction between horizontal cells and deep plexus capillaries, as well as amacrine cells and the intermediate vascular plexus. Amacrine and horizontal neurons which express VEGF form a neurovascular unit in the intermediate and deep vascular plexus in the IPL and OPL and act as a metabolic and oxygen sensor which regulate angiogenesis. Consequently, the *Vegfa* amacrine/horizontal conditional knockout mouse demonstrates a significant reduction of intermediate vascular plexus (Usui et al., 2015). RGC are also involved in vasculature development; for instance; RGC-driven Sema3E signaling controls retinal vessel branching. Endothelial cell PlexinD1 expression is regulated by VEGF at the sprouting tip of vessels and Sema3E/PlexinD1 signaling controls VEGF activity in a negative feedback loop. Sema3E or PlexinD1 loss of function disrupts normal Notch activity thorough Dll4, leading to uneven growth and a less branched vascular network (Kim, Oh, Gaiano,

Yoshida, & Gu, 2011). RGC are sensitive to chemoattractants via VEGF-A signals transduced by the *Nrp1* receptor to promote contralateral axon projection across the optic chiasm (Erskine et al., 2011). It has been speculated that NRP1 regulates neurovascular RGC patterning in the optic pathway, as it is expressed in both RGC and endothelial cells. Mice with RGC deletion of *Nrp1* have defective axon crossing at the optic chiasm, and mice with endothelial-cell *Nrp1* ablation reveal disrupted optic tract morphology (Erskine et al., 2017). Another study showed that NRP1 is a positive regulator of endothelial cell tip state during primary vascular plexus sprouting; thus, *Nrp1* inhibition in endothelial cells leads to thickened sprouts and slower vessel expansion (Aspalter et al., 2015). However, *Nrp2's* role remains unknown during retinal neurovascular development. Despite all the available knowledge in neuronal and vasculature development, we are just beginning to understand the neurovascular cross talk and the underlying mechanisms of their communication.

Neurodegenerative diseases such as Alzheimer's disease (AD) and Amyotrophic lateral sclerosis are considered to be a neuronal disorders; however, vascular defects are also involved in their pathogenesis. Alzheimer's patients and animal models present severe changes in the cerebrovascular structure including the deposition of amyloid beta in the mural wall of blood cells (Perlmutter & Chui, 1990). Blood vessel abnormalities and retinal neuronal cell reduction (eg. RGC) are evident in patients with AD (Hart, Koronyo, Black, & Koronyo-Hamaoui, 2016).

Neovascularization (NV) is a process where new vessels sprout from pre-existing vessels, which are involved in wound repair in many tissues. However, in the retina neovascularization is not productive but instead may cause problems. A common complication of many ocular diseases such as age-related macular degeneration (AMD), diabetic retinopathy (DR), and retinal vein occlusion (RVO) is abnormal growth of neovascular blood vessels, which can be driven by

defects in vascular VEGF or SEMA3. AMD is directly related to choroidal neovascularization and affects a large population over 65 years old. However, finding appropriate treatment remains challenging due to its complicated underlying mechanism. Furthermore, since cerebral and retinal vasculature development have close similarities, investigating the retina is a valuable tool for the development of new treatments.

5.2.3 Neuropilins

Neuropilins are single-pass transmembrane co-receptors for both vascular endothelial growth factor (VEGF) and class-3 semaphorins (sema3), with a wide range of roles including development, axonal guidance, angiogenesis, immunity, as well as involvement in pathological conditions such as cancer (Klagsbrun, Takashima, & Mamluk, 2002). Neuropilins have two family members, neuropilin-1 (*Nrp1)* and neuropilin-2 (*Nrp2),* encoded by distinct genes on a different chromosome, each composed of 17 exons. They both have an extracellular N-terminal, a transmembrane region and a short cytosolic tail with NRP2 exhibiting a 44% sequence homology with NRP1 (Roy et al., 2017) (Figure 5.1). The extracellular part of the protein has two domains (a1 and a2) plus two coagulation factor domains (b1 and b2), and a MAM (c) domain, followed by a transmembrane domain (TM), and a cytoplasmic domain (cyto) (Raimondi, Brash, Fantin, & Ruhrberg, 2016). As mentioned before, two well-known ligands bind to neuropilin receptors; semaphorins (bind to a1 and a2 domains) which are a class of signalling proteins associated with several functions such as axonal guidance, angiogenesis and immune responses. There are around 30 semaphorin proteins (8 classes) among different phyla that bind to various receptors such as plexins, integrins and neuropilins.

NRP1 and NRP2 are best known for binding to class 3 semaphorins, which require NRPs as a co-receptor to interact with distinct plexins to transduce the signal inside the cell. The

signals can activate various gene networks to regulate several aspects of development such as neuronal migration, axonal, and vasculature guidance. They also bind to the VEGF family of angiogenic signaling cytokines, which play a major role in vasculogenesis (endothelial cell progenitor differentiation to primary capillary plexus) and angiogenesis (sprouting of new capillaries from pre-existing vessels) during vascular and cardiovascular development. The VEGF-A121, VEGF-A145, VEGF-A165 and VEGF-A189 isoforms bind to NRP receptors and convey VEGF signals. VEGF signaling initiates at a high level in the yolk sac to induce vessel formation and maintain its expression for organ development during the later stages of development. VEGF is essential for retinal vasculature development, and multiple eye diseases such as Proliferative Diabetic Retinopathy (PDR), neovascular Age Related Macular Degeneration (AMD), and Branch Retinal Vein Occlusion (BRVO) are caused by VEGF-driven angiogenesis (Haigh et al., 2003). VEGF-A165 signaling has been found via *Nrp1* in RGC axons to enable axonal guidance (Mackenzie & Ruhrberg, 2012). In addition, VEGF-dependent arterial differentiation has been found through NRP1 in the heart (Fantin et al., 2014).

Nrp1 and *Nrp2* are expressed in neuronal cells and blood vessels during CNS development (Herzog, Kalcheim, Kahane, Reshef, & Neufeld, 2001). There have been several studies on neuropilin deficient animal models. *Nrp1* KO mice are embryonically lethal between E10-E13 and show neuronal, vascular, and cardiovascular defects (Kawasaki et al., 1999). Transgenic *Nrp1* overexpression mice also die embryonically due to excessive capillary formation, extensive hemorrhage, a malformed heart, and defects in the nervous system (Kitsukawa, Shimono, Kawakami, Kondoh, & Fujisawa, 1995). In contrast, *Nrp2* knockout mice are viable and survive to adulthood where they show a reduction in smaller lymphatic vessels and impaired development of cranial nerves, spinal sensory axons and defects in the arrangement

of fiber tracts in the adult brain (Giger et al., 2000). Compound *Nrp1/Nrp2* mutant mice are also embryonically lethal with severe defects in the vasculature and their yolk sacs fail to develop branching arteries and connections between blood vessel sprouts (Takashima et al., 2002). *Nrp1* knockdown zebrafish shows defects in the nervous system, including aberrant migration and branching of motor neurons. The *Nrp1* role in heart development has been demonstrated by endothelial-specific *Nrp1* null mice, which die during mid-late embryonic development due to multiple defects in major arteries (Gu et al., 2003). The endothelial-specific *Nrp1* null mice resulted in early NSCs cell exit in the hindbrain, with premature neuronal cell differentiation during embryogenesis (Tata et al., 2016). Neuropilins have been characterized with altered expression in multiple cancer tissues, and as they have the ability to modulate vascular responses in tumour growth, there is considerable interest for Neuropilins as a new therapeutic target.

Neuropilins are expressed during ocular development in vertebrates. For instance, in *Xenopus, Nrp1* expression is found in RGC along with *sema3a* and *sema3f* to regulate proper neuronal polarization. In *Nrp1* endothelial specific knockout mice, choroidal blood vessel neovascularization is affected during the development of the eye (Fernandez-Robredo, Selvam, Powner, Sim, & Fruttiger, 2017). SEMA3A signaling regulates vascular permeability through NRPs in the eye, as *Sema3a* is upregulated in the retinas of type I diabetes mouse models. Blocking VEGF binding to NRP1 of mouse retina leads to impaired retinal angiogenesis which supports *Nrp1's* role in vessel growth. *Nrp1* involvement in endothelial cells sprouting during early post-natal angiogenesis has been demonstrated. The *Nrp1* endothelial cell mutant reduces sprouting activity of primary plexus leading to reduced branching (Aspalter et al., 2015). Unlike *Nrp1, Nrp2's* role during nervous system development is less well characterized. There have been a few studies on *Nrp2* knockout mouse brain. *Nrp2* knockout mice present with abnormal

cranial nerve trajectories and hippocampus morphology (Chen et al., 2000). The *Nrp2* deficient mice reveal defects in limbic tracts, including the complete absence of both limbs of the anterior commissure (Giger et al., 2000). Additionally, most of our knowledge of neuropilin's role in retinal development is from investigation of *Nrp1's* role in axon projection and vasculature development; very little is known about *Nrp2's* role. Here, we investigated *Nrp2* involvement during retinal development using *Nrp2* KO mice. Our lab's previous studies on the embryonic *Nrp2* KO mouse retina showed abnormal hyaloid vasculature development compared to WT littermates. We also observed an expanded inner retina (J.Zagozewski, PhD thesis, U. Alberta). We investigated retina structure and function in *Nrp2* KO mice post-natally. We found abnormal retina folding as well as disrupted retina function using ERG in *Nrp2* KO mouse after birth. We also investigated neuronal retinal cell marker expression post-natally. Aberrant expression of retinal neuronal cell markers in *Nrp2* KO was observed compared to controls post-natally.

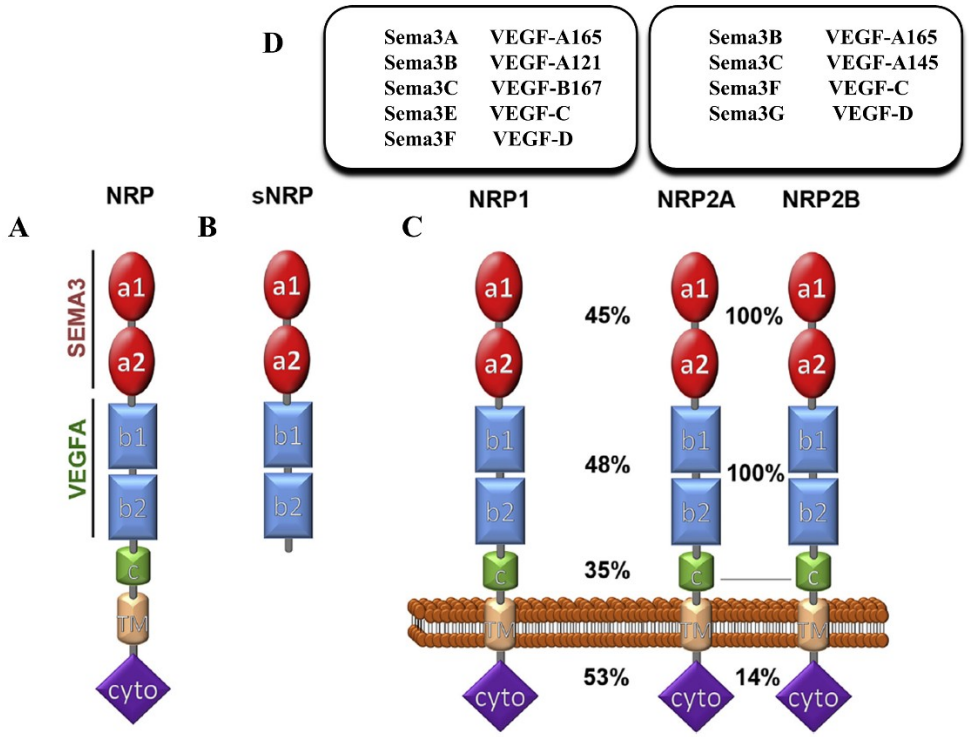

Figure 5.1. NRP1 and NRP2 protein structure

(A) The transmembrane NRPs contain seven domains: two complement (CUB) domains (a1 and a2), two coagulation factor (FV/FVIII) domains (b1 and b2), a MAM domain (c), a transmembrane region (TM) and a cytoplasmic (cyto) domain that interacts with intracellular proteins containing a PDZ domain. Soluble NRPs have the a and b domains but lack the transmembrane and cytoplasmic domains. The numbers show amino acid identity between transmembrane NRPs domains. (B) Schematic representation of the soluble sNRPs structure. (C) Schematic representation of transmembrane NRP1, and the NRP2 splice variants NRP2a and NRP2b. (D) Sema3 and VEGF ligands that bind to NRP1 and (E) NRP2. Adapted from: Raimondi, Brash, Fantin, & Ruhrberg, 2016.

5.3 Results

5.3.1 *Nrp2* is expressed in the retina during eye development

As discussed previously, there has been limited research on *Nrp2's* role in CNS neurovascular development. *Nrp2* is expressed in mouse hippocampus along with *Sema3f* to direct cortical and hippocampal circuit synaptic organization (Won et al., 2002). Its expression also has been characterized in olfactory sensory neuron axons to form an olfactory circuit, and induce a social response to odours (Inokuchi et al., 2017). Additionally, NRP2 involvement has been implicated in tumour growth and invasion of lung cancer (Drabkin, Starkova, & Gemmill, 2017). Following, the discovery of an abnormal eye phenotype in *Nrp2* knockout mice in our lab, we were determined to further explore the *Nrp2* role in ocular development. Based on our previous data, *Nrp2* expression was found in the neural retina at E13; its expression also was present in hyaloid vasculature and choroidal vasculature surrounding the optic cup. At E18, the expression of *Nrp2* was observed in the GCL, as well as hyaloid vasculature in the vitreous (J. Zagozewski and D. Eisenstat, unpublished data). In collaboration with Pranidhi Baddam (Dr. Daniel Graf's laboratory), we investigated *Nrp2* expression at P7 and P28 in the wild type mouse retina. Both neuronal and vascular development is at their peak at P7 in the retina; thus, the *Nrp2* expression pattern is important for investigating its role during development. At P7, *Nrp2* showed robust expression in the GCL and less expression in the INL. *Nrp2* expression was reduced at P28 compared to P7; however, its expression is still present in the GCL and INL (Figure 5.2A-B). Altogether, our findings showed that *Nrp2* is expressed during early eye development, as well as post-natally including adulthood in the retina. Its expression pattern shows consistent presence in GCL and INL, with robust expression at P7.

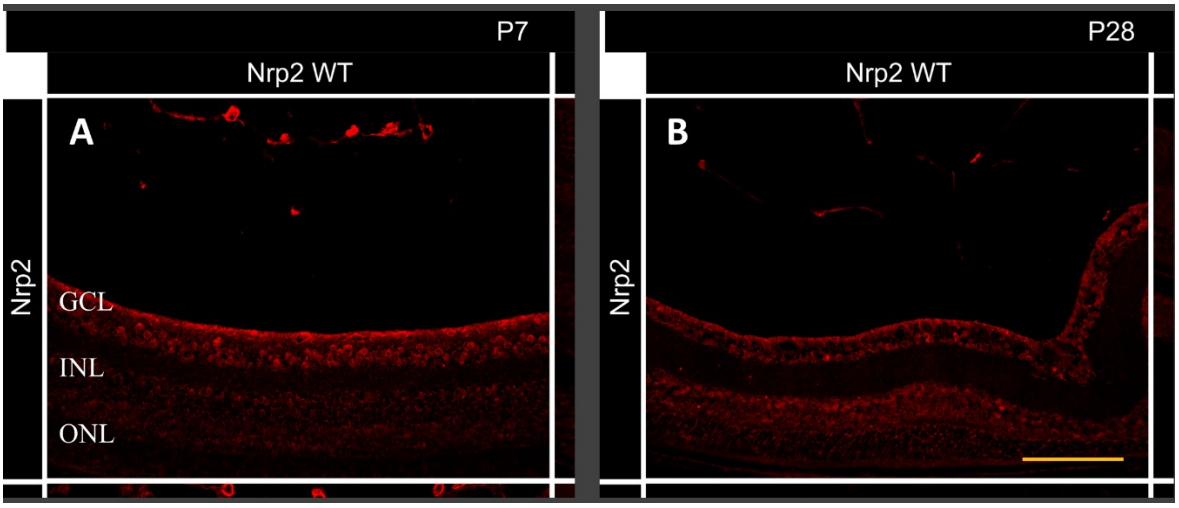

Figure 5.2. NRP2 expression at P7 and P28 mouse retina

NRP2 expression at P7 and P28 in mouse retina. (A) At P7, NRP2 expression is evident in the GCL (B) Expression is still present in the GCL and INL at P28. Ganglion cell layer, GCL; inner neuroblastic layer, INL; Outer neuroblastic layer, ONL. Scale = 50 μm, In collaboration with Pranidhi Baddam.

5.3.2 *Nrp2* knockout mice present with an abnormal eye phenotype and morphology

Funduscopic imaging and fluorescent angiography between *Nrp2* KO and WT mice showed leukocoria in the *Nrp2* KO (J. Zagozewski, D. Eisenstat unpublished data) eye during adulthood. To identify the eye and retina morphology during (P7) and after (P28) vascular development, paraffin sections of *Nrp2* WT and *Nrp2* KO mice were stained with Hematoxylin and Eosin. At P7, the retina in the *Nrp2* KO was expanded with disrupted laminar structure in comparison to the control (Figure 5.3A-I). The expansion of retinal layers and misfolding continued with less severity at P28 in *Nrp2* KO mice (Figure 5.3A′-I′). The *Nrp2* KO mouse retina presented with phenotypic variation where mild KO retina structure was less disrupted at P7 (Figure 5.3D, E, F) and P28 (Figure 5.3D′,E′,F′) compared to severe KO phenotypes at P7 (Figure 5.3G, H, I) and P28 (Figure 5.3G, H, I′). Hence, postnatal and adult retina structure is severely disrupted in *Nrp2* KO mice compared to wild type controls.

P7

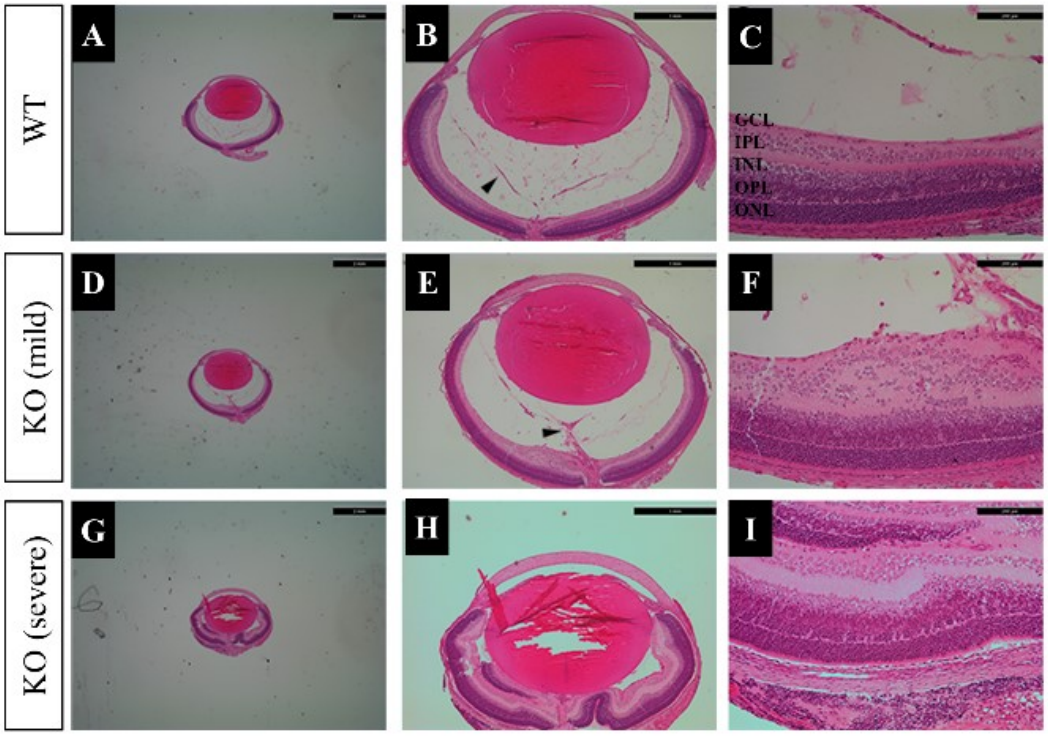
WT
KO (mild)
KO (severe)
A
B
C
D
E
F
G
H
I
GCL
IPL
INL
OPL
ONL

P28

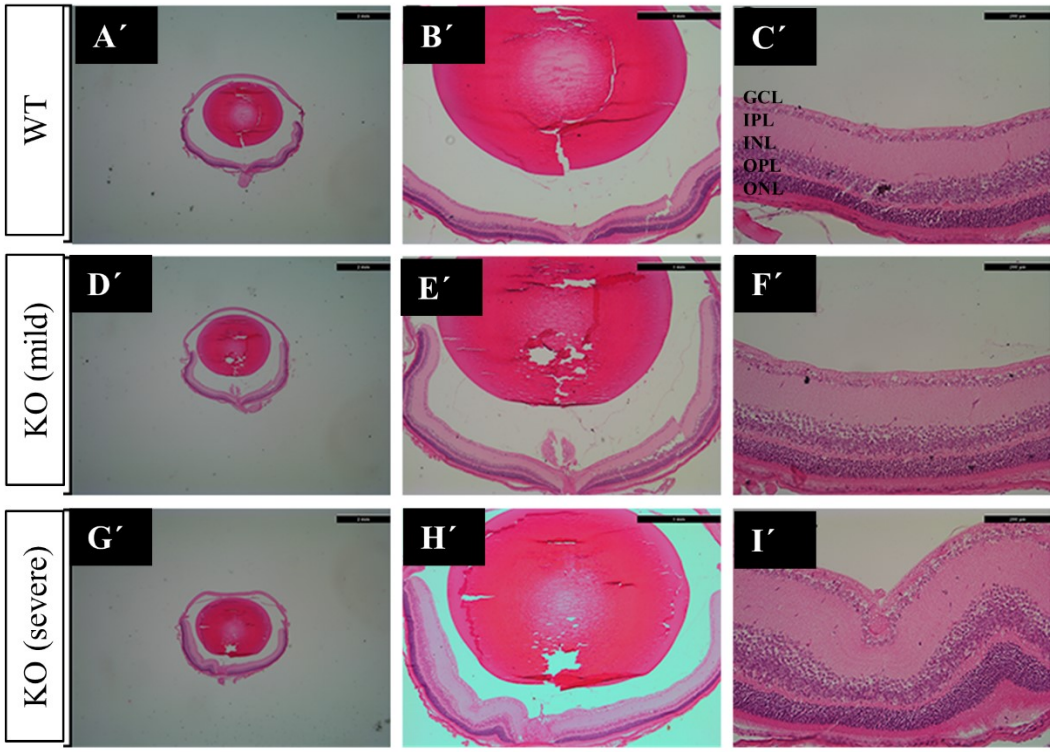
WT
KO (mild)
KO (severe)
A′
B′
C′
D′
E′
F′
G′
H′
I′
GCL
IPL
INL
OPL
ONL

Figure 5.3. H&E staining of *Nrp2* KO/WT mouse eye at P7/P28

(A, B, C) *Nrp2* WT eye at P7. The eye size, lens and retina structure are evident in histology staining. (D, E, F) *Nrp2* KO with mild eye phenotype at P7. (D) The eye appears to be microphthalmic. (E) The hyaloid vasculature is disrupted in the vitreous area compared to WT vessel sprouting (black arrow). (F) The IPL retina layer is expanded. (G, H, I) *Nrp2* KO with a severe eye phenotype at P7. (G) The eye is microphthalmic. (H) The lens morphology is severely disrupted, and the retina is misfolded and expanded. (I) Retina cytoarchitecture is altered along with laminar expansion.

(A′, B′, C′) *Nrp2* WT eye at P28. The eye size, lens and retina structure are evident in histology staining. (D′, E′, F′) *Nrp2* KO with mild eye phenotype at P28. (D′) The eye size appears to be normal. (E′) The eye morphology is comparable with *Nrp2* WT. (F′) The retina structure is not disrupted. (G′, H′, I′) *Nrp2* KO with severe eye phenotype at P28. (G′) The eye is microphthalmic. (H) The lens morphology is severely disrupted, and retina is misfolded and expanded. (I) Retina cytoarchitecture is altered along with IPL expansion. GCL: ganglion cell layer; IPL: inner plexiform layer; INL: inner neuroblastic layer; OPL: outer neuroblastic layer; ONL: outer neuroblastic layer; H&E staining was performed by: Pranidhi Baddam and Jamie Zagozewski.

5.3.3 Altered neuronal gene expression in *Nrp2* knockout mice

Nrp2 KO eye histology demonstrated significant disruption in retina structure along with neuronal layer expansion. We proposed that the layer expansion could be the result of neuronal cell proliferation. To understand the gene profile underlying the histological changes, gene expression analysis of P7 and P28 retina was conducted by qRT-PCR. Several markers representing each retina layer were chosen, and specific primers were designed. GCL (Brn3a and Brn3b), Inner Plexiform Layer/IPL (Syntaxin), Amacrine and Horizontal cell (Calbindin and Prox1), Bipolar cell (Chx10/Vsx2), Outer Nuclear Plexiform (Recoverin), Cones (M/S opsin), and Rods (Rhodopsin) were quantified. Ribosomal phosphoprotein (36b4) was used as a reference gene. At P7, all the retina makers showed increased expression in the *Nrp2* KO mice, however, only Calbindin, Recoverin and S-opsin were significantly increased (Figure 5.4A). At P28, the expression of retinal genes normalized with no significant changes observed (Figure 5.4B). These results suggest that in addition to altered vasculature, the neuronal markers are also altered in the *Nrp2* KO mice in comparison to the *Nrp2* WT at P7 retina tissues, but this normalizes with subsequent maturation.

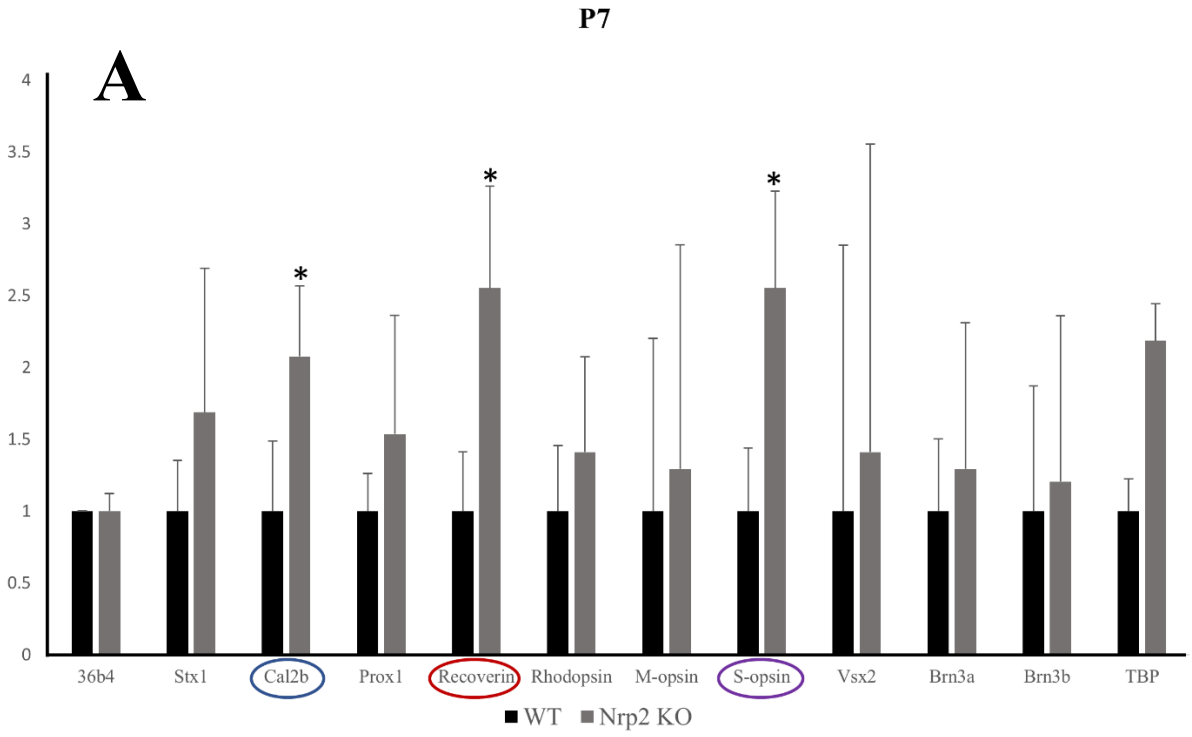
P7
A
4
3.5
3
2.5
2
1.5
1
0.5
0
*
*
*
36b4
Stx1
Cal2b
Prox1
Recoverin
Rhodopsin
M-opsin
S-opsin
Vsx2
Brn3a
Brn3b
TBP
WT
Nrp2 KO

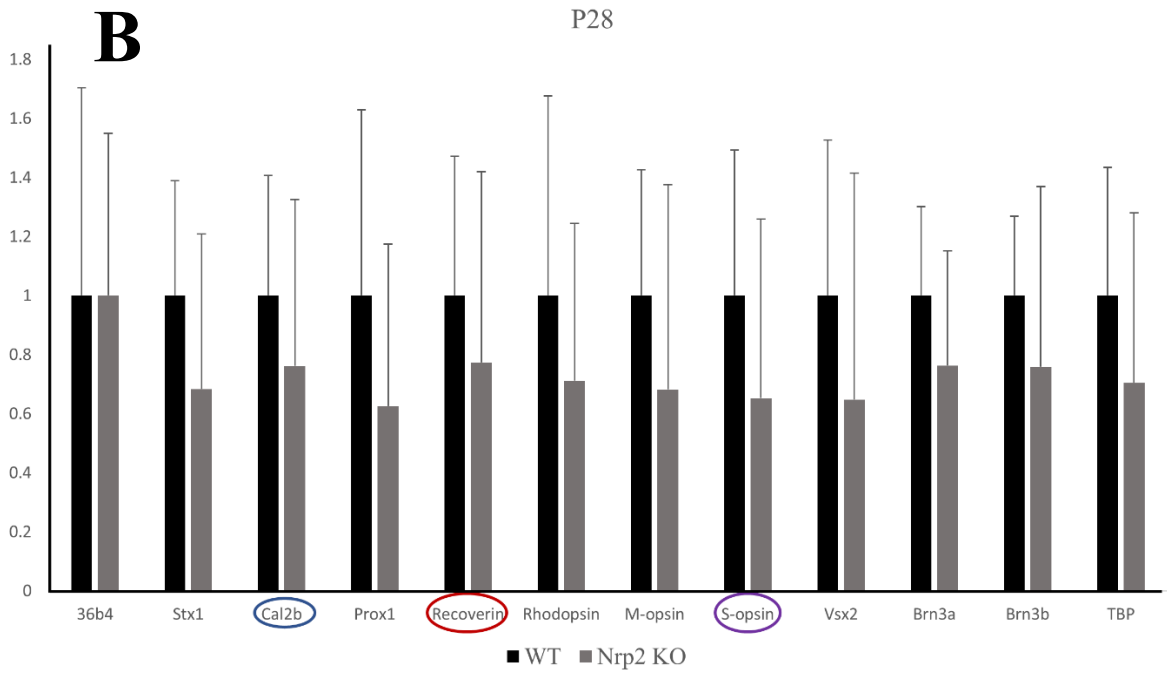
B
P28
1.8
1.6
1.4
1.2
1
0.8
0.6
0.4
0.2
0
36b4
Stx1
Cal2b
Prox1
Recoverin
Rhodopsin
M-opsin
S-opsin
Vsx2
Brn3a
Brn3b
TBP
WT
Nrp2 KO

Figure 5.4. Retinal neuronal marker's quantification at P7 and P28 *Nrp2* KO/WT mice.

(A) Neuronal cell marker specific mRNA levels of *Nrp2* KO/WT dissected retina from P7 mice were quantified by qRT-PCR. The expression level of Calbindin (horizontal cells), recoverin (OPL) and S-opsin (cone cells) is raised (circled) in *Nrp2* KO mice. (B) The neuronal cell marker specific mRNA levels of *Nrp2* KO/WT dissected retina from P28 mice were quantified by qRT-PCR. Neuronal cell marker specific gene expression appears to be comparable (circled) with control mice in *Nrp2* KO at this postnatal age. n=5, P value *≤ 0.05, GCL (Brn3a and Brn3b), Inner Plexiform Layer IPL (Stx1), Amacrine and Horizontal cell (Prox1, and Cal2b), Bipolar cell (Vsx), Outer Nuclear Plexiform (Recoverin), Cones (M/S opsin), Rods (Rho), Reference Gene (36b4). In collaboration with Pranidhi Baddam.

5.3.4 Immunofluorescence using retinal neuronal markers demonstrate results consistent with transcript quantification

While qPCR suggested a significant increase of Calbindin, S-Opsin and Recoverin gene expression in *Nrp2* KO retina at P7, immunofluorescence was performed to identify whether these changes translated in the context of protein expression. Immunofluorescence of paraffin embedded eye sections using antibodies against Calbindin, S-Opsin and Recoverin supported an increase in the expression of Calbindin (Figure 5.5A, B), S-Opsin (Figure 5.5C, D), and Recoverin (Figure 5.5E, F) in the *Nrp2* KO in comparison to the WT at P7 retina. However, when the same antibodies were used to stain the P28 retina, analysis of the *Nrp2* KO mice suggested that expression of Calbindin (Figure 5.5G, H), and S-Opsin (Figure 5.5I, J) was only slightly increased in comparison to the control. In the case of Recoverin (Figure 5.5K, L) expression in P28 retina, the WT and the *Nrp2* KO appeared quite similar with no obvious differences observed. Consistent with our histology staining, retina misfolding, specifically in GCL and INL is obvious in both P7 and P28. Altogether, neuronal cells are severely disrupted at P7, along with misfolded retina at both P7 and P28 time points, but retinal cell-type specific marker expression normalizes by P28.

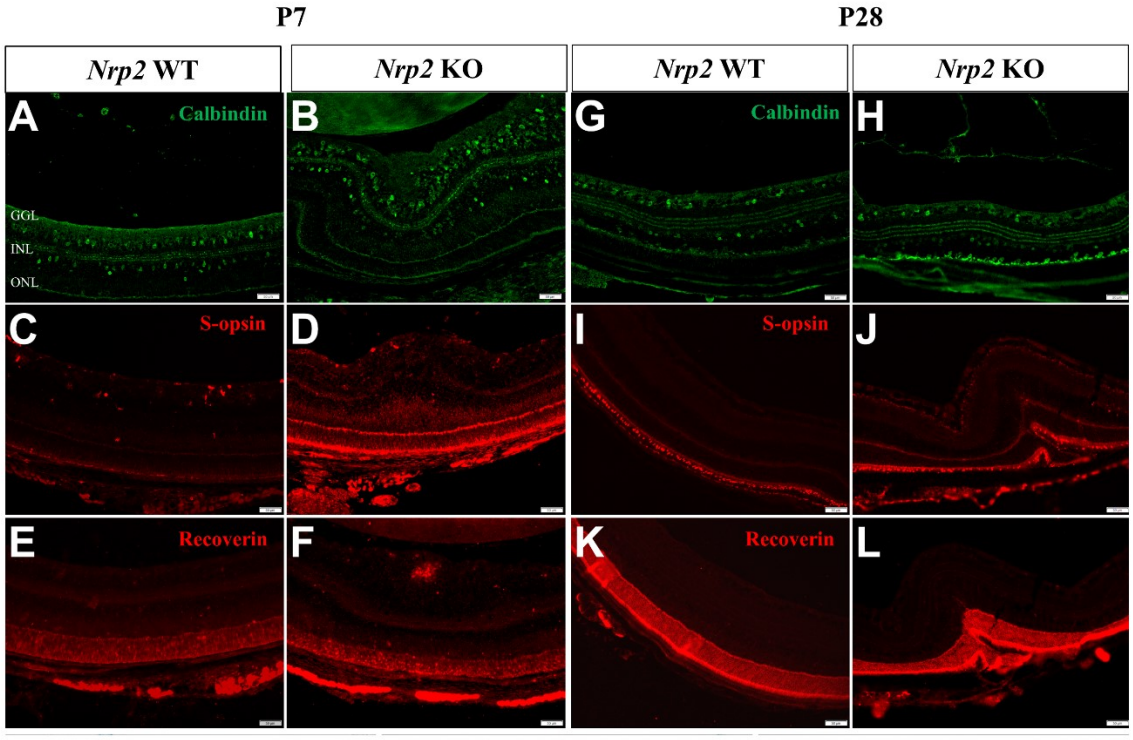

Figure 5.5. Increased expression of Calbindin, S-opsin and Recoverin in P7 *Nrp2* KO retina

(A, B) *Nrp2* WT/KO retina sections labelled with Calbindin at P7. (A) Calbindin expression was evident in the INL in *Nrp2* KO at P7. (B) Calbindin expression appears to be increased in the INL in the *Nrp2* KO retina at P7. (C, D) *Nrp2* WT/KO retina labelled with S-opsin at P7. (C) Low levels of expression of S-opsin were found in the ONL in *Nrp2* WT at P7. (D) S-opsin expression became more evident in the ONL in the *Nrp2* KO at P7. (E, F) *Nrp2* WT/KO retina sections labelled with Recoverin at P7. (E) *Nrp2* WT retina showed Recoverin expression in the OPL at P7. (F) Recoverin expression was increased in the OPL in the *Nrp2* KO at P7. (G, H) *Nrp2* WT/KO retina immunolabelled sections with Calbindin at P28 (G). In collaboration with Pranidhi Baddam. GCL: ganglion cell layer; INL: inner nuclear layer; ONL: outer nuclear layer.

5.3.5 Physiological assessment of the *Nrp2* knockout adult mice

In order to understand the physiological consequences of altered retina development, OCT of *Nrp2* WT, mild and severe *Nrp2* KO mice was performed (Figure 5.6A-C). These scans demonstrated an expansion of the inner plexiform layer and outer nuclear layer as previously seen in the hematoxylin and eosin stain of WT and *Nrp2* KO mice (Figure 5.6D). Electroretinography (ERG) measurements were performed to identify changes in visual function as a result of *Nrp2* deletion in mice; it was conducted under scotopic and photopic conditions (Figure 5.7A-H). The a-wave is a measure of outer retina function and the b-wave is a measure of inner retina function. *Nrp2* KO mice demonstrated reduced a-wave and b-wave under photopic (light adapted) conditions (Figure 5.7E, F), as well as reduced mixed scotopic (dark adapted) a-wave amplitudes (Figure 5.7A). This data suggests that although there is an expansion in the inner retina and outer retina of the *Nrp2* KO mice, neuronal cell function is still reduced in comparison to the WT mice.

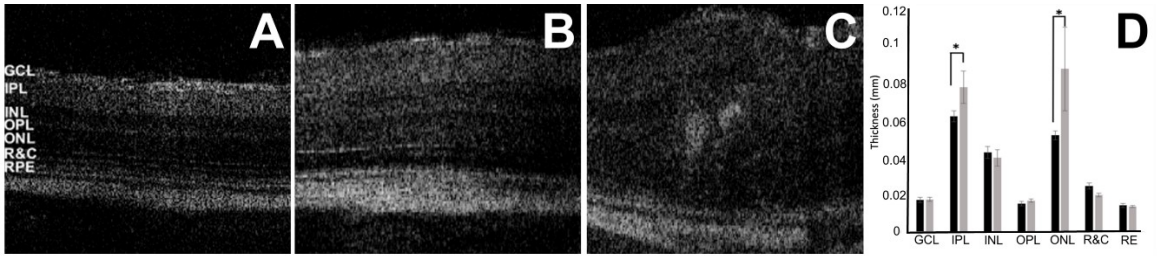

Figure 5.6. Expansion of the IPL and ONL in the *Nrp2* KO retina at P28.

Optical Coherence Tomography of *Nrp2* WT(A), mild *Nrp2* KO (B) and severe *Nrp2* KO (C) in P28 retina suggesting increased thickness of IPL and ONL in the *Nrp2* KO retina. (D) The thickness measurement of retina layers demonstrated significant expansion in the IPL and ONL. Bioptigen software was used to obtain length measurements. GCL, ganglion cell layer; IPL: inner plexiform layer; INL: inner neuroblastic layer; OPL: outer neuroblastic layer; PR: photoreceptor; RE: retina epithelium. In collaboration with Pranidhi Baddam.

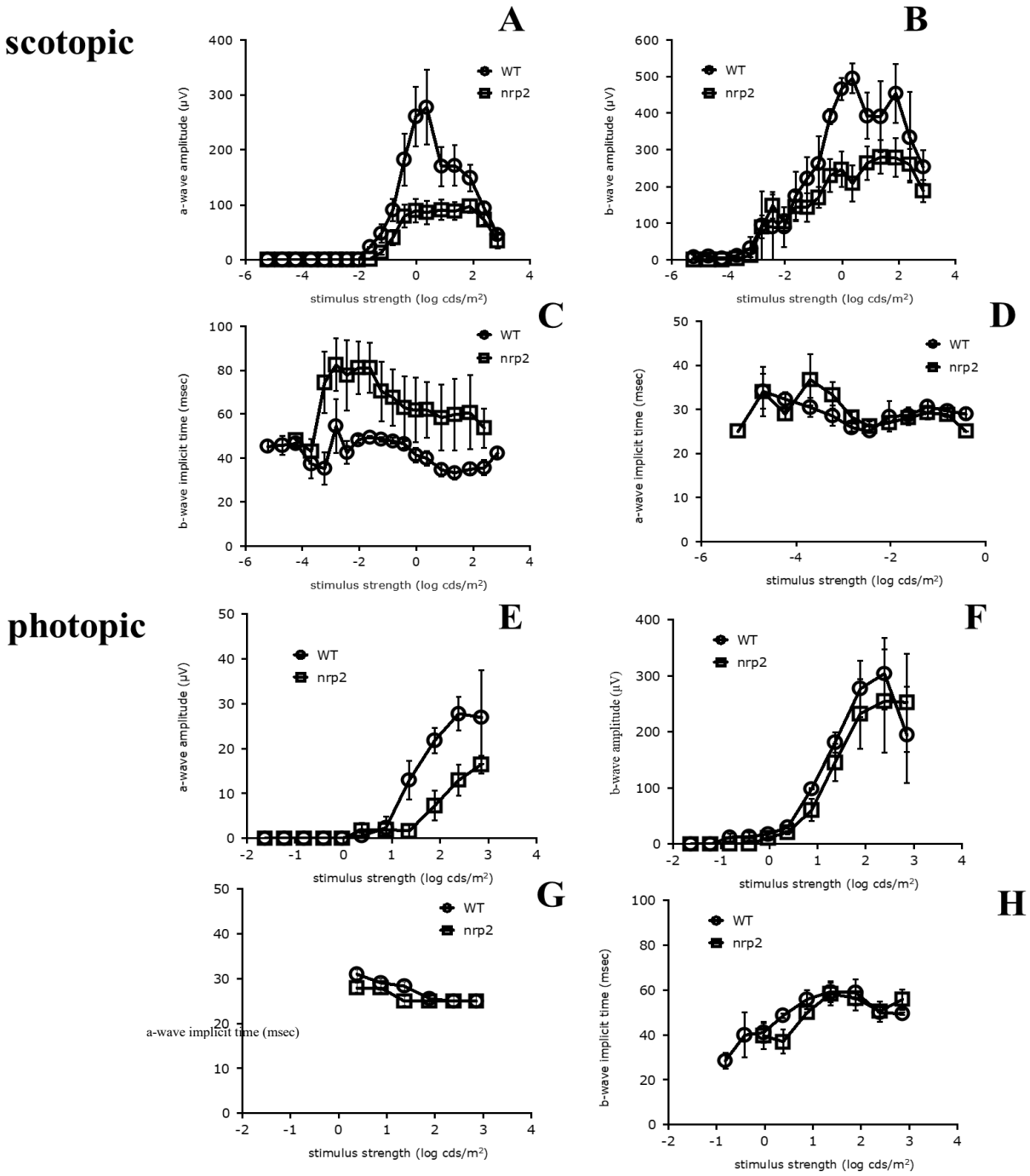

Figure 5.7. Abnormal ERG responses in *Nrp2* KO compared with littermate WT mice

Abnormal ERG responses in *Nrp2* KO (squares) compared with littermate WT (circles) mice. (A-D) reduced mixed scotopic (A) a-wave amplitudes. (E-F) reduced (E) photopic a- and (F) b-wave amplitudes and prolonged a-wave implicit times. n=4, error bars represent SD, scotopic a/b

ratios: 2.0 +/- 0.6 for WT and 2.3 +/- 0.1 for nrp2 (p value > 0.5 with Mann Withney U test), photopic a/b ratios: 10.7 +/- 1.2 for WT and 15.5 +/- 2.6 for nrp2 (p value > 0.5 with Mann Withney U test). In collaboration with Pranidhi Baddam, data analysis was performed by Dr. Yves Sauvé, Departments of Ophthalmology & Vision Sciences and Physiology, University of Alberta.

5.4 Discussion

This study demonstrates for the first time that *Nrp2* is essential for the development and consequent maintenance of vascular and neuronal systems in the retina. Neuropilins are multifunctional co-receptors which are important for neuronal and vascular development, but potentially they may have an additional role in neuronal/vascular diseases. However, many aspects of cellular regulation through NRPs (specially NRP2) are unknown. Based on our findings, there is a strong possibility that *Nrp2* has multiple roles during eye development, such as: hyaloid vasculature, retinal vasculature and retinal neuronal cell development. Unlike *Nrp1* knockout mice which are perinatal lethal (Kawasaki et al., 1999), *Nrp2* knockout mice are viable and fertile during adulthood. This might indicate that *Nrp2* is redundant and that *Nrp1* can compensate for loss of *Nrp2,* but not vice-versa. *Nrp2* KO mice develop a disorganized vasculature in parts of CNS later in adulthood, and *Nrp1* redundancy may compensate for these phenotypes. It has been shown that *Nrp1/Nrp2* act synergistically to guide cranial neural crest cells, but *Nrp2*-null mice present with a less severe phenotype in comparison to *Nrp1*-null mice (Schwarz, Vieira, Howard, Eickholt, & Ruhrberg, 2008). Thus, we have to consider the possible redundant function of *Nrp1* for *Nrp2* since our mice are *Nrp2* single knockouts. There are limited numbers of Sema3 and VEGF ligands that bind to *Nrp2,* not *Nrp1* (Sema3G and VEGF145), and this might be the explanation for the phenotype we describe in *Nrp2* knockout mice. We found that *Nrp2* knockout mice have an average body weight that is lower than littermate control mice (data not shown). *Nrp2* is present in long bones and involved in osteoblast development through the semaphorin family (Verlinden et al., 2013); this may explain in part the weight difference between the *Nrp2* knockout and wild type mice. We also showed that *Nrp2* knockout mice have severely disrupted retina morphology including misfolded and expanded lamination along with

dysplasia in homozygous as well as a heterozygous animal during postnatal angiogenesis and neurogenesis. As mentioned before, VEGF signaling plays an important role in angiogenesis and neurogenesis and its disruption causes severe disruption during embryonic early stages (Raab et al., 2004). *Vegf* endothelial cell transgenic mice develop similar cortical telencephalon morphology when compared with our *Nrp2* knockout mice retinal lamination. The telencephalon cortical lamination is misfolded, cortical dysplasia is evident and the intermediate zone is abnormally expanded (Li et al., 2013). Thus, in the absence of endothelial cell *Vegf,* the telencephalic architecture is perturbed. VGEF-A is one of the ligands which binds to NRP2 receptor; thus, the lack of the receptor may cause disruption in VEGF signaling, and since this process is tightly regulated by VEGF gradients, endothelial cell sprouting could become disoriented. This may explain the phenotypic resemblance between the *Nrp2* knockout and the *Vegf*-endothelial cell knockout (Gerhardt et al., 2003).

NRP2 is a signaling molecule receptor; hence, it may interact with various ligands and co-receptors and these interactions may impact several downstream pathways, which could contribute to the different phenotypes observed in the eye of the *Nrp2* KO mice. Our results show a more severe phenotype at P7 compared to P28. In mice, the primary vasculature plexus forms during the first week after birth where the endothelial cells travel toward the peripheral retina, and by P21 the mature vasculature development is completed (Fruttiger, 2007). Therefore, any disruption during the first week after birth, including an unbalanced VEGF gradient in the absence of *Nrp2* may alter endothelial tip/stalk dynamics. It is probable that the retina morphology slightly recovers by P28 when postnatal eye development is completed. Consistent with our histology staining retinal neuronal cell marker expression increased in *Nrp2* KO mouse

at P7 and recovered at P28, which could be due to delayed retinal programmed cell death (Braunger, Demmer, & Tamm, 2014).

There is a close interaction between endothelial cells and retinal neuronal cells to regulate primary vascular plexus development; thus, any disruption in signaling gradients may contribute to neuronal and vasculature disorientation. During cerebellar development, the distribution of blood vessels affects cortical lamination (Xi et al., 2015). Additionally, VEGF acts as a key stop signal for neuronal proliferation and migration in the cortical cortex, as VEGF endothelial cell deletion leads to increased neuronal proliferation during cortical development (Li et al., 2013).

NRP1 and NRP2 cooperate with each other to regulate Sema3B-mediated division of NPCs in the spinal cord. *Nrp1* endothelial cell null mice not only present disorganized vessel sprouting but also have a premature NPC pool which exited early from the cell cycle (Tata et al., 2016). The loss of *Nrp2* expression may cause a similar premature cell cycle exit of RPC in the retina which induces premature differentiation of retinal neuronal cells. This could explain the higher number of INL and ONL neuronal cell types in the *Nrp2* KO compared to the wild type animals at P7. Additionally, amacrine and horizontal cells interact with the deep/intermediate plexus through Von Hippel-Lindau (VHL)/Hypoxia-inducible factor (HIFα)/VEGF signaling to induce angiogenesis. These retinal cell types build neurovascular units with capillaries in the intraretinal plexuses and develop crosstalk between INL and endothelial cells. Amacrine and horizontal cells are the source of VEGF in an HIFα-dependent manner (H. Y. Park, Kim, & Park, 2014). *Nrp2* is expressed in the INL; thus, its deletion may lead to a VEGF signaling disruption which could change the signaling dynamic in neurovascular units. This could trigger a compensatory signal in capillaries to induce more amacrine/horizontal cell proliferation.

Sema3F is a NRP2 ligand and its expression is found in the outer retina; Sema3F is able to signal an angiorepellent effect (Buehler et al., 2013). In the absence of *Nrp2,* endothelial cells may induce cone proliferation to compensate for the lack of angiorepellent signals. These cells may not be functional due to their early cell cycle exit and incomplete differentiation, which could trigger apoptosis signals later during retina development (H. Y. Park et al., 2014).

Physiological function of the INL and ONL is abnormal in *Nrp2* KO mice compared to controls, as measured with ERG. It is likely that not all neuronal cells are functional since they may be differentiated prematurely from RPCs during retina vasculature development. It is also probable that the *Nrp2* KO mice is presenting with synaptopathy, as *Nrp2* is required for Sema3A binding during the neuronal cell development which interferes with signal transduction (Pellet-Many, Frankel, Jia, & Zachary, 2008). However, to investigate the possible connection between *Nrp2* KO retina disruption and the VEGF signaling pathway, more experiments are required. For instance; the gene expression of *Nrp2* VEGF ligands and their downstream targets can be quantified. Additionally, we can consider applying some vasculature specific markers at various time points of retinal vasculature development.

The *Nrp2* KO mice presents some phenotypic similarities including leukocoria, detached retina, and retinal folding with the human eye disorder Persistent Fetal Vasculature (PFV). Consistent with human PFV, the hyaloid vasculature did not fully regress in the adult mice. Thus, our findings suggest that the *Nrp2* KO could be a novel mouse model for PFV that recapitulates post-natal PFV-like phenotypes and enables us to further understand PFV pathogenesis and prognosis.

6 Chapter 6. Conclusions and Future directions

The animal body consists of a large number of different type of cells, which are the building blocks of various tissues and organs, but all began as a single cell. We can go even further and think of the evolution which began from a single cell, and now here we are as organized multicellular individuals. Thus, we should not underestimate the importance of development, and learning about this complex process. Basic development research not only is a way to uncover the reason behind many genetic diseases but also a way to uncover the secrets of evolution. Development is largely under the control of genes encoding for transcription factors and signalling pathways, where different sets of gene expression contribute to the unique properties and functions of various types of cells and tissues. The retina is one of these tissues which develops as part of the forebrain in a tightly regulated temporal order. The unique neuronal and vascular structure of the retina makes it a great tool to study the developmental complexity of our central nervous system and the key aspects of neurogenesis. My research contributes to uncovering small parts of genetic networks behind retina development. Although these networks are pieces of an immense gene regulatory network puzzle, eventually these little pieces bring the whole image together, and may contribute to answering fundamental questions.

Retinal progenitor cells are one type of multipotent cells which give rise to all the retinal neuronal cells during retinogenesis, regulated by intrinsic and extrinsic factors. My research began with uncovering the role of DLX2 in retinal ganglion cell specification based on our lab's preliminary data. This research showed that there is a genetic regulatory network in which *Dlx2* represses *Crx* and miR-124 transcriptional expression, to promote RGC specification at the expense of PR cells during retinal development. Time and space are determining factors for RPC specification, and they were presented in my model by looking into the DLX2 regulatory

network during late versus early retinal progenitor cell development in the INBL. Part of this GRN focuses on *Otx2's* interaction with *Dlx2* in post-mitotic progenitor cells, which subsequently in coordination with other GRN may lead to one type of neuronal cell specification. Progenitor cells have been receiving considerable attention as potential tools for the restorative treatment of degenerative diseases affecting the retina and visual system. Thus, it is critical to fully understand the mechanism underlying RPC differentiation, and to identify the key regulators of this process.

My research brings us one step closer to understanding *Dlx2* function in retinal progenitor cell specification and RGC maintenance. My model includes multiple key PR regulatory genes such as *Otx2, Crx* and miR-124, which with some added future research could expand our knowledge on PR cell differentiation and maintenance. My research not only used multiple *in-vitro* techniques but also applied two different animal models to study the function of *Dlx* genes in retina. Zebrafish have become a powerful model system to study development (Fadool & Dowling, 2008). Although we could not detect *dlx* gene ortholog expression in the zebrafish eye, we still used that to our advantage to generate *Tg[rx3:Dlx2]* zebrafish. The transgenic fish could become a great tool to further study zebrafish eye development in comparison to mice; moreover, it also could provide evolutionary insights regarding *Dlx* gene function.

Retina vascularization is a critical step during retinal development, which has not been fully understood. The objective of my *Nrp2* collaborative project was to investigate *Nrp2's* role in retinal development, since our *Nrp2* KO mice was characterized with severe eye phenotypes. Our research revealed the possible relationship between retinal neuronal cells and retinal vasculature during development as the retinal neuronal cell layers, numbers and physiology are

affected in the *Nrp2* KO mouse. We discovered phenotypic similarities in *Nrp2* KO mice and the human eye disease Persistent Fetal Vasculature (PFV).

One limitation to my research is that GRNs play various critical roles during development, and they are connected with other GRNs as well as environmental factors to execute their tasks. This makes GRNs a complex, multifactorial phenomenon. Thus, these networks may not be limited to few genes such as *Dlx2* and *Otx2* to regulate retinal progenitor fate, but rather a network of many factors in connection with space and time.

Based on this data, there are numerous possible opportunities which are worth exploring. RNA-sequencing of *Dlx1/Dlx2* DKO/WT retina tissues will provide us with considerable data about possible affected genes at different retinal developmental stages. Analyzing the data may provide us with a bigger picture of *Dlx1/Dlx2's* role during development and give us the opportunity to focus on specific pathways. I proposed a model where *Dlx2/Notch/Otx2* build a network maintaining a retinal progenitor cell pool versus specifying the horizontal cells. Quantifying Notch signaling downstream targets (*Notch1* and *Hes1/Hes5*) in *Dlx1/Dlx2* DKO/WT mice at E13 can provide us with evidence of its possible repression by DLX2. Comparing RPC and horizontal cell specific markers between DKO and WT mice could show possible change in their expression at E13. Retina explant cultures will allow us to study eye development in *ex-vivo* conditions somewhat similar to the animal model. A lentiviral-OTX2 overexpression vector can be used to transfect the retina explant cultures along with empty vector to study possible *Otx2/Dlx2* regulatory relationships. *Otx2*-GFP reporter mice can be obtained and crossbred with *Dlx1/Dlx2* DKO mice to follow *Otx2*-expressing cells in the absence of *Dlx1/Dlx2* gene function.

The miR-124 and *Dlx2* double negative feedback loop was investigated, and some evidence of their reciprocal interaction was provided. However, more evidence is required to clarify the role of miR-124 during retina development. *In-situ hybridization* of *Dlx1/Dlx2* DKO versus WT retina tissues will grant us with additional data on miR-124 expression in the absence of *Dlx1/Dlx2.* Primary retina cell culture can be used to target miR-124 expression by use of the CRISPR/Cas9 system and *Dlx2* expression can be followed in the culture.

We generated a retina-specific *Dlx2*-CKO, in an attempt to study *Dlx2* function in retina after birth. We will cross the *Dkk3-Cre* mouse with *ROSA26* (Dr. Daniel Graf) strain to investigate *Dkk3* expression pattern in retina and brain. We may have to substitute the *Dkk3-Cre* strain with an alternative progenitor *Cre* strain (*Rax* or *Chx10*), based on the *Dkk3* embryonic pattern in the mice.

The expression of mouse *Dlx2* in the zebrafish eye has to be further confirmed by Western Blot in larvae as well as adult fish retina tissues. In order to study RGCs in *Dlx2*-Tg fish, the transgenic adult fish could be crossed with *isl1*-GFP fish. The GFP antibody then will be applied to their progeny to study the GFP-labeled ganglion cells during development in *Tg[rx3:Dlx2]* zebrafish. The photoreceptor cells should also be studied and compared in *Tg[rx3:Dlx2]* and wild type zebrafish eye.

The *Nrp2* KO mouse has various eye abnormalities including neuronal and vasculature defects. Although we found considerable evidence of *Nrp2* KO eye abnormalities, the mechanism underlying these phenotypes has not been investigated. The *Nrp2* KO/WT mice eye can be labelled by various vascular markers to investigate vasculature patterns. We also may cross breed endothelial cell reporter mice (*Tie2*-GFP) to study *Nrp2* in vascular development.

Quantification of *Nrp2* ligands (VEGF or Sema3) or direct downstream targets of these pathways could help us find a possible mechanism underlying *Nrp2* KO eye abnormalities. As previously mentioned, the *Nrp2* KO eyes are phenotypically similar to human PFV patients. Thus, we may be able to obtain some PFV patient blood samples and look for possible germline mutations in the *Nrp2* gene compared to controls.

7 References

Acampora, D., Gulisano, M., Broccoli, V., & Simeone, A. (2001). Otx genes in brain morphogenesis. *Prog Neurobiol, 64*(1), 69-95.

Acampora, D., Merlo, G. R., Paleari, L., Zerega, B., Postiglione, M. P., Mantero, S., . . . Levi, G. (1999). Craniofacial, vestibular and bone defects in mice lacking the Distal-less-related gene Dlx5. *Development, 126*(17), 3795-3809.

Adams, R. H., & Eichmann, A. (2010). Axon guidance molecules in vascular patterning. *Cold Spring Harb Perspect Biol, 2*(5), a001875. doi:10.1101/cshperspect.a001875

Akimoto, M., Cheng, H., Zhu, D., Brzezinski, J. A., Khanna, R., Filippova, E., . . . Swaroop, A. (2006). Targeting of GFP to newborn rods by Nrl promoter and temporal expression profiling of flow-sorted photoreceptors. *Proc Natl Acad Sci U S A, 103*(10), 3890-3895. doi:10.1073/pnas.0508214103

Albaroudi, N., Tijani, M., Lezrek, O., Daoudi, R., & Laghmari, M. (2017). Persistent hyperplastic primary vitreous (PHPV). *J Fr Ophtalmol, 40*(10), e389-e390. doi:10.1016/j.jfo.2016.09.024

Amores, A., Force, A., Yan, Y. L., Joly, L., Amemiya, C., Fritz, A., . . . Postlethwait, J. H. (1998). Zebrafish hox clusters and vertebrate genome evolution. *Science, 282*(5394), 1711-1714.

Anderson, S. A., Eisenstat, D. D., Shi, L., & Rubenstein, J. L. R. (1997). Interneuron migration from basal forebrain to neocortex: Dependence on Dlx genes. *Science, 278*(5337), 474-476. doi:DOI 10.1126/science.278.5337.474

Anderson, S. A., Qiu, M., Bulfone, A., Eisenstat, D. D., Meneses, J., Pedersen, R., & Rubenstein, J. L. (1997). Mutations of the homeobox genes Dlx-1 and Dlx-2 disrupt the striatal subventricular zone and differentiation of late born striatal neurons. *Neuron, 19*(1), 27-37.

Andreeva, K., & Cooper, N. G. (2014). MicroRNAs in the Neural Retina. *Int J Genomics, 2014*, 165897. doi:10.1155/2014/165897

Ang, S. L., Jin, O., Rhinn, M., Daigle, N., Stevenson, L., & Rossant, J. (1996). A targeted mouse Otx2 mutation leads to severe defects in gastrulation and formation of axial mesoderm and to deletion of rostral brain. *Development, 122*(1), 243-252.

Arendt, D. (2003). Evolution of eyes and photoreceptor cell types. *Int J Dev Biol, 47*(7-8), 563-571.

Arendt, D., Tessmar, K., de Campos-Baptista, M. I., Dorresteijn, A., & Wittbrodt, J. (2002). Development of pigment-cup eyes in the polychaete Platynereis dumerilii and evolutionary conservation of larval eyes in Bilateria. *Development, 129*(5), 1143-1154.

Arshavsky, V. Y. (2002). Rhodopsin phosphorylation: from terminating single photon responses to photoreceptor dark adaptation. *Trends Neurosci, 25*(3), 124-126.

Artavanis-Tsakonas, S., Rand, M. D., & Lake, R. J. (1999). Notch signaling: cell fate control and signal integration in development. *Science, 284*(5415), 770-776.

Aspalter, I. M., Gordon, E., Dubrac, A., Ragab, A., Narloch, J., Vizan, P., . . . Gerhardt, H. (2015). Alk1 and Alk5 inhibition by Nrp1 controls vascular sprouting downstream of Notch. *Nat Commun, 6*, 7264. doi:10.1038/ncomms8264

Baas, D., Bumsted, K. M., Martinez, J. A., Vaccarino, F. M., Wikler, K. C., & Barnstable, C. J. (2000). The subcellular localization of OTX2 is cell-type specific and developmentally

regulated in the mouse retina. *Molecular Brain Research, 78*(1-2), 26-37. doi:Doi 10.1016/S0169-328x(00)00060-7
Baden, T., Berens, P., Franke, K., Roman Roson, M., Bethge, M., & Euler, T. (2016). The functional diversity of retinal ganglion cells in the mouse. *Nature, 529*(7586), 345-350. doi:10.1038/nature16468
Benedito, R., Rocha, S. F., Woeste, M., Zamykal, M., Radtke, F., Casanovas, O., . . . Adams, R. H. (2012). Notch-dependent VEGFR3 upregulation allows angiogenesis without VEGF-VEGFR2 signalling. *Nature, 484*(7392), 110-114. doi:10.1038/nature10908
Blackshaw, S., Fraioli, R. E., Furukawa, T., & Cepko, C. L. (2001). Comprehensive analysis of photoreceptor gene expression and the identification of candidate retinal disease genes. *Cell, 107*(5), 579-589.
Blanco, R., & Gerhardt, H. (2013). VEGF and Notch in tip and stalk cell selection. *Cold Spring Harb Perspect Med, 3*(1), a006569. doi:10.1101/cshperspect.a006569
Bobola, N., & Merabet, S. (2017). Homeodomain proteins in action: similar DNA binding preferences, highly variable connectivity. *Curr Opin Genet Dev, 43*, 1-8. doi:10.1016/j.gde.2016.09.008
Boije, H., Shirazi Fard, S., Edqvist, P. H., & Hallbook, F. (2016). Horizontal Cells, the Odd Ones Out in the Retina, Give Insights into Development and Disease. *Front Neuroanat, 10*, 77. doi:10.3389/fnana.2016.00077
Boon, K., Eberhart, C. G., & Riggins, G. J. (2005). Genomic amplification of orthodenticle homologue 2 in medulloblastomas. *Cancer Research, 65*(3), 703-707.
Braunger, B. M., Demmer, C., & Tamm, E. R. (2014). Programmed cell death during retinal development of the mouse eye. *Adv Exp Med Biol, 801*, 9-13. doi:10.1007/978-1-4614-3209-8_2
Buehler, A., Sitaras, N., Favret, S., Bucher, F., Berger, S., Pielen, A., . . . Stahl, A. (2013). Semaphorin 3F forms an anti-angiogenic barrier in outer retina. *FEBS Lett, 587*(11), 1650-1655. doi:10.1016/j.febslet.2013.04.008
Cepko, C. (2014). Intrinsically different retinal progenitor cells produce specific types of progeny. *Nat Rev Neurosci, 15*(9), 615-627. doi:10.1038/nrn3767
Cepko, C. L. (2015). The Determination of Rod and Cone Photoreceptor Fate. *Annu Rev Vis Sci, 1*, 211-234. doi:10.1146/annurev-vision-090814-121657
Cepko, C. L., Austin, C. P., Yang, X., Alexiades, M., & Ezzeddine, D. (1996). Cell fate determination in the vertebrate retina. *Proc Natl Acad Sci U S A, 93*(2), 589-595.
Chang, W. S., & Harris, W. A. (1998). Sequential genesis and determination of cone and rod photoreceptors in Xenopus. *J Neurobiol, 35*(3), 227-244.
Chatelain, G., Fossat, N., Brun, G., & Lamonerie, T. (2006). Molecular dissection reveals decreased activity and not dominant negative effect in human OTX2 mutants. *Journal of Molecular Medicine-Jmm, 84*(7), 604-615. doi:10.1007/s00109-006-0048-2
Chen, H., Bagri, A., Zupicich, J. A., Zou, Y., Stoeckli, E., Pleasure, S. J., . . . Tessier-Lavigne, M. (2000). Neuropilin-2 regulates the development of selective cranial and sensory nerves and hippocampal mossy fiber projections. *Neuron, 25*(1), 43-56.
Cheng, L. C., Pastrana, E., Tavazoie, M., & Doetsch, F. (2009). miR-124 regulates adult neurogenesis in the subventricular zone stem cell niche. *Nature Neuroscience, 12*(4), 399-408. doi:10.1038/nn.2294
Chow, R. L., Volgyi, B., Szilard, R. K., Ng, D., McKerlie, C., Bloomfield, S. A., . . . McInnes, R. R. (2004). Control of late off-center cone bipolar cell differentiation and visual

signaling by the homeobox gene Vsx1. *Proc Natl Acad Sci U S A, 101*(6), 1754-1759. doi:10.1073/pnas.0306520101
Cohen, S. M., & Jurgens, G. (1989). Proximal-distal pattern formation in Drosophila: cell autonomous requirement for Distal-less gene activity in limb development. *EMBO J, 8*(7), 2045-2055.
Conway Morris, S. (2006). Darwin's dilemma: the realities of the Cambrian 'explosion'. *Philos Trans R Soc Lond B Biol Sci, 361*(1470), 1069-1083. doi:10.1098/rstb.2006.1846
Corbo, J. C., Lawrence, K. A., Karlstetter, M., Myers, C. A., Abdelaziz, M., Dirkes, W., . . . Langmann, T. (2010). CRX ChIP-seq reveals the cis-regulatory architecture of mouse photoreceptors. *Genome Res, 20*(11), 1512-1525. doi:10.1101/gr.109405.110
Cruz, M. G. F., & Escobar, A. (2011). Normal neuronal migration. *Salud Mental, 34*(1), 61-66.
Danno, H., Michiue, T., Hitachi, K., Yukita, A., Ishiura, S., & Asashima, M. (2008). Molecular links among the causative genes for ocular malformation: Otx2 and Sox2 coregulate Rax expression. *Proc Natl Acad Sci U S A, 105*(14), 5408-5413. doi:10.1073/pnas.0710954105
Davidson, E. H., Rast, J. P., Oliveri, P., Ransick, A., Calestani, C., Yuh, C. H., . . . Bolouri, H. (2002). A genomic regulatory network for development. *Science, 295*(5560), 1669-1678. doi:10.1126/science.1069883
Davis-Silberman, N., & Ashery-Padan, R. (2008). Iris development in vertebrates; genetic and molecular considerations. *Brain Res, 1192*, 17-28. doi:10.1016/j.brainres.2007.03.043
de Melo, J., Du, G. Y., Fonseca, M., Gillespie, L. A., Turk, W. J., Rubenstein, J. L. R., & Eisenstat, D. D. (2005). Dlx1 and Dlx2 function is necessary for terminal differentiation and survival of late-born retinal ganglion cells in the developing mouse retina. *Development, 132*(2), 311-322. doi:10.1242/dev.01560
de Melo, J., Qiu, X., Du, G., Cristante, L., & Eisenstat, D. D. (2003). Dlx1, Dlx2, Pax6, Brn3b, and Chx10 homeobox gene expression defines the retinal ganglion and inner nuclear layers of the developing and adult mouse retina. *J Comp Neurol, 461*(2), 187-204. doi:10.1002/cne.10674
de Melo, J., Zhou, Q. P., Zhang, Q., Zhang, S., Fonseca, M., Wigle, J. T., & Eisenstat, D. D. (2008). Dlx2 homeobox gene transcriptional regulation of Trkb neurotrophin receptor expression during mouse retinal development. *Nucleic Acids Res, 36*(3), 872-884. doi:10.1093/nar/gkm1099
Debiais-Thibaud, M., Metcalfe, C. J., Pollack, J., Germon, I., Ekker, M., Depew, M., . . . Casane, D. (2013). Heterogeneous conservation of Dlx paralog co-expression in jawed vertebrates. *PLoS One, 8*(6), e68182. doi:10.1371/journal.pone.0068182
den Hollander, A. I., Roepman, R., Koenekoop, R. K., & Cremers, F. P. (2008). Leber congenital amaurosis: genes, proteins and disease mechanisms. *Prog Retin Eye Res, 27*(4), 391-419. doi:10.1016/j.preteyeres.2008.05.003
Deo, M., Yu, J. Y., Chung, K. H., Tippens, M., & Turner, D. L. (2006). Detection of mammalian microRNA expression by in situ hybridization with RNA oligonucleotides. *Dev Dyn, 235*(9), 2538-2548. doi:10.1002/dvdy.20847
Dhawan, R. R., Schoen, T. J., & Beebe, D. C. (1997). Isolation and expression of homeobox genes from the embryonic chicken eye. *Mol Vis, 3*, 7.
Drabkin, H. A., Starkova, J., & Gemmill, R. M. (2017). A triad of NRP2, DLX and p53 proteins in lung cancer metastasis. *Oncotarget, 8*(57), 96464-96465. doi:10.18632/oncotarget.22097

Dror, I., Golan, T., Levy, C., Rohs, R., & Mandel-Gutfreund, Y. (2015). A widespread role of the motif environment in transcription factor binding across diverse protein families. *Genome Res, 25*(9), 1268-1280. doi:10.1101/gr.184671.114

Dyer, M. A., Livesey, F. J., Cepko, C. L., & Oliver, G. (2003). Prox1 function controls progenitor cell proliferation and horizontal cell genesis in the mammalian retina. *Nat Genet, 34*(1), 53-58. doi:10.1038/ng1144

Edwards, M. M., McLeod, D. S., Li, R., Grebe, R., Bhutto, I., Mu, X., & Lutty, G. A. (2012). The deletion of Math5 disrupts retinal blood vessel and glial development in mice. *Exp Eye Res, 96*(1), 147-156. doi:10.1016/j.exer.2011.12.005

Eisenstat, D. D., Liu, J. K., Mione, M., Zhong, W., Yu, G., Anderson, S. A., . . . Rubenstein, J. L. (1999). DLX-1, DLX-2, and DLX-5 expression define distinct stages of basal forebrain differentiation. *J Comp Neurol, 414*(2), 217-237.

Ekker, M., Giroux, G., Zerucha, T., Lewis, A., Gambarotta, A. A., & Schultz, J. R. (1998). Regulation of dlx homeobox gene expression during development of the zebrafish embryo - The potential importance of their genomic organization. *New Developments in Marine Biotechnology*, 109-114.

Ellies, D. L., Stock, D. W., Hatch, G., Giroux, G., Weiss, K. M., & Ekker, M. (1997). Relationship between the genomic organization and the overlapping embryonic expression patterns of the zebrafish dlx genes. *Genomics, 45*(3), 580-590. doi:DOI 10.1006/geno.1997.4978

Elliott, A. M., & Evans, J. A. (2008). The association of split hand foot malformation (SHFM) and congenital heart defects. *Birth Defects Res A Clin Mol Teratol, 82*(6), 425-434. doi:10.1002/bdra.20452

Elshatory, Y., Everhart, D., Deng, M., Xie, X., Barlow, R. B., & Gan, L. (2007). Islet-1 controls the differentiation of retinal bipolar and cholinergic amacrine cells. *J Neurosci, 27*(46), 12707-12720. doi:10.1523/JNEUROSCI.3951-07.2007

Enard, W., Gehre, S., Hammerschmidt, K., Holter, S. M., Blass, T., Somel, M., . . . Paabo, S. (2009). A humanized version of Foxp2 affects cortico-basal ganglia circuits in mice. *Cell, 137*(5), 961-971. doi:10.1016/j.cell.2009.03.041

Erskine, L., Francois, U., Denti, L., Joyce, A., Tillo, M., Bruce, F., . . . Ruhrberg, C. (2017). VEGF-A and neuropilin 1 (NRP1) shape axon projections in the developing CNS via dual roles in neurons and blood vessels. *Development, 144*(13), 2504-2516. doi:10.1242/dev.151621

Erskine, L., Reijntjes, S., Pratt, T., Denti, L., Schwarz, Q., Vieira, J. M., . . . Ruhrberg, C. (2011). VEGF Signaling through Neuropilin 1 Guides Commissural Axon Crossing at the Optic Chiasm. *Neuron, 70*(5), 951-965. doi:10.1016/j.neuron.2011.02.052

Euler, T., Haverkamp, S., Schubert, T., & Baden, T. (2014). Retinal bipolar cells: elementary building blocks of vision. *Nat Rev Neurosci, 15*(8), 507-519.

Fadool, J. M., & Dowling, J. E. (2008). Zebrafish: a model system for the study of eye genetics. *Prog Retin Eye Res, 27*(1), 89-110. doi:10.1016/j.preteyeres.2007.08.002

Fan, W. J., Li, X., Yao, H. L., Deng, J. X., Liu, H. L., Cui, Z. J., . . . Deng, J. B. (2016). Neural differentiation and synaptogenesis in retinal development. *Neural Regen Res, 11*(2), 312-318. doi:10.4103/1673-5374.177743

Fantin, A., Herzog, B., Mahmoud, M., Yamaji, M., Plein, A., Denti, L., . . . Zachary, I. (2014). Neuropilin 1 (NRP1) hypomorphism combined with defective VEGF-A binding reveals

novel roles for NRP1 in developmental and pathological angiogenesis. *Development, 141*(3), 556-562. doi:10.1242/dev.103028
Fernandez-Robredo, P., Selvam, S., Powner, M. B., Sim, D. A., & Fruttiger, M. (2017). Neuropilin 1 Involvement in Choroidal and Retinal Neovascularisation. *PLoS One, 12*(1), e0169865. doi:10.1371/journal.pone.0169865
Fernholm, B., & Holmberg, K. (1975). The eyes in three genera of hagfish (Eptatretus, Paramyxine and Myxine)--a case of degenerative evolution. *Vision Res, 15*(2), 253-259.
Filho, A. B., Souza, J., Faucz, F. R., Sotomaior, V. S., Dupont, B., Bartel, F., . . . Raskin, S. (2011). Somatic/gonadal mosaicism in a syndromic form of ectrodactyly, including eye abnormalities, documented through array-based comparative genomic hybridization. *Am J Med Genet A, 155A*(5), 1152-1156. doi:10.1002/ajmg.a.33942
Fossat, N., Le Greneur, C., Beby, F., Vincent, S., Godement, P., Chatelain, G., & Lamonerie, T. (2007). A new GFP-tagged line reveals unexpected Otx2 protein localization in retinal photoreceptors. *BMC Dev Biol, 7*, 122. doi:10.1186/1471-213X-7-122
Fruttiger, M. (2002). Development of the mouse retinal vasculature: Angiogenesis versus vasculogenesis. *Investigative Ophthalmology & Visual Science, 43*(2), 522-527.
Fruttiger, M. (2007). Development of the retinal vasculature. *Angiogenesis, 10*(2), 77-88. doi:10.1007/s10456-007-9065-1
Fuhrmann, S. (2008). Wnt signaling in eye organogenesis. *Organogenesis, 4*(2), 60-67.
Fujitani, Y., Fujitani, S., Luo, H., Qiu, F., Burlison, J., Long, Q., . . . Wright, C. V. (2006). Ptf1a determines horizontal and amacrine cell fates during mouse retinal development. *Development, 133*(22), 4439-4450. doi:10.1242/dev.02598
Fukushima, Y., Okada, M., Kataoka, H., Hirashima, M., Yoshida, Y., Mann, F., . . . Uemura, A. (2011). Sema3E-PlexinD1 signaling selectively suppresses disoriented angiogenesis in ischemic retinopathy in mice. *J Clin Invest, 121*(5), 1974-1985. doi:10.1172/JCI44900
Furukawa, T., Morrow, E. M., & Cepko, C. L. (1997). Crx, a novel otx-like homeobox gene, shows photoreceptor-specific expression and regulates photoreceptor differentiation. *Cell, 91*(4), 531-541. doi:Doi 10.1016/S0092-8674(00)80439-0
Furukawa, T., Mukherjee, S., Bao, Z. Z., Morrow, E. M., & Cepko, C. L. (2000a). rax, Hes1, and notch1 promote the formation of Muller glia by postnatal retinal progenitor cells. *Neuron, 26*(2), 383-394.
Furukawa, T., Mukherjee, S., Bao, Z. Z., Morrow, E. M., & Cepko, C. L. (2000b). rax, hes1, and notch1 promote the formation of Muller glia by postnatal retinal progenitor cells. *Neuron, 26*(2), 383-394. doi:Doi 10.1016/S0896-6273(00)81171-X
Georgi, S. A., & Reh, T. A. (2010). Dicer Is Required for the Transition from Early to Late Progenitor State in the Developing Mouse Retina. *Journal of Neuroscience, 30*(11), 4048-4061. doi:10.1523/Jneurosci.4982-09.2010
Gerhardt, H., Golding, M., Fruttiger, M., Ruhrberg, C., Lundkvist, A., Abramsson, A., . . . Betsholtz, C. (2003). VEGF guides angiogenic sprouting utilizing endothelial tip cell filopodia. *Journal of Cell Biology, 161*(6), 1163-1177. doi:10.1083/jcb.200302047
Giger, R. J., Cloutier, J. F., Sahay, A., Prinjha, R. K., Levengood, D. V., Moore, S. E., . . . Geppert, M. (2000). Neuropilin-2 is required in vivo for selective axon guidance responses to secreted semaphorins. *Neuron, 25*(1), 29-41. doi:Doi 10.1016/S0896-6273(00)80869-7

Glubrecht, D. D., Kim, J. H., Russell, L., Bamforth, J. S., & Godbout, R. (2009). Differential CRX and OTX2 expression in human retina and retinoblastoma. *J Neurochem, 111*(1), 250-263. doi:10.1111/j.1471-4159.2009.06322.x

Goetz, J. J., Martin, G. M., Chowdhury, R., & Trimarchi, J. M. (2014). Onecut1 and Onecut2 play critical roles in the development of the mouse retina. *PLoS One, 9*(10), e110194. doi:10.1371/journal.pone.0110194

Goto, S., & Hayashi, S. (1997). Specification of the embryonic limb primordium by graded activity of Decapentaplegic. *Development, 124*(1), 125-132.

Gu, C., Rodriguez, E. R., Reimert, D. V., Shu, T., Fritzsch, B., Richards, L. J., . . . Ginty, D. D. (2003). Neuropilin-1 conveys semaphorin and VEGF signaling during neural and cardiovascular development. *Dev Cell, 5*(1), 45-57.

Guido Sanguinetti, Van Anh Huynh-Thu, *Gene Regulatory Networks*: Human Press; 2019 doi: 10.1007/978-1-4939-8882-2

Hackler, L., Jr., Wan, J., Swaroop, A., Qian, J., & Zack, D. J. (2010). MicroRNA profile of the developing mouse retina. *Invest Ophthalmol Vis Sci, 51*(4), 1823-1831. doi:10.1167/iovs.09-4657

Haigh, J. J., Morelli, P. I., Gerhardt, H., Haigh, K., Tsien, J., Damert, A., . . . Nagy, A. (2003). Cortical and retinal defects caused by dosage-dependent reductions in VEGF-A paracrine signaling. *Dev Biol, 262*(2), 225-241.

Hamilton, S. P., Woo, J. M., Carlson, E. J., Ghanem, N., Ekker, M., & Rubenstein, J. L. R. (2005). Analysis of four DLX homeobox genes in autistic probands. *Bmc Genetics, 6*. doi:Artn 5210.1186/1471-2156-6-52

Hart, N. J., Koronyo, Y., Black, K. L., & Koronyo-Hamaoui, M. (2016). Ocular indicators of Alzheimer's: exploring disease in the retina. *Acta Neuropathologica, 132*(6), 767-787. doi:10.1007/s00401-016-1613-6

Hatakeyama, J., Tomita, K., Inoue, T., & Kageyama, R. (2001). Roles of homeobox and bHLH genes in specification of a retinal cell type. *Development, 128*(8), 1313-1322.

Hellstrom, M., Phng, L. K., Hofmann, J. J., Wallgard, E., Coultas, L., Lindblom, P., . . . Betsholtz, C. (2007). Dll4 signalling through Notch1 regulates formation of tip cells during angiogenesis. *Nature, 445*(7129), 776-780. doi:10.1038/nature05571

Hennig, A. K., Peng, G. H., & Chen, S. (2008). Regulation of photoreceptor gene expression by Crx-associated transcription factor network. *Brain Res, 1192*, 114-133. doi:10.1016/j.brainres.2007.06.036

Herzog, Y., Kalcheim, C., Kahane, N., Reshef, R., & Neufeld, G. (2001). Differential expression of neuropilin-1 and neuropilin-2 in arteries and veins. *Mech Dev, 109*(1), 115-119.

Hirota, S., Clements, T. P., Tang, L. K., Morales, J. E., Lee, H. S., Oh, S. P., . . . McCarty, J. H. (2015). Neuropilin 1 balances beta 8 integrin-activated TGF beta signaling to control sprouting angiogenesis in the brain. *Development, 142*(24), 4363-4373. doi:10.1242/dev.113746

Hojo, M., Ohtsuka, T., Hashimoto, N., Gradwohl, G., Guillemot, F., & Kageyama, R. (2000). Glial cell fate specification modulated by the bHLH gene Hes5 in mouse retina. *Development, 127*(12), 2515-2522.

Holland, N. D., Panganiban, G., Henyey, E. L., & Holland, L. Z. (1996). Sequence and developmental expression of AmphiDll, an amphioxus Distal-less gene transcribed in the ectoderm, epidermis and nervous system: insights into evolution of craniate forebrain and neural crest. *Development, 122*(9), 2911-2920.

Holland, P. W., Garcia-Fernandez, J., Williams, N. A., & Sidow, A. (1994). Gene duplications and the origins of vertebrate development. *Dev Suppl*, 125-133.

Huxlin, K. R., Sefton, A. J., & Furby, J. H. (1992). The origin and development of retinal astrocytes in the mouse. *J Neurocytol, 21*(7), 530-544.

Inokuchi, K., Imamura, F., Takeuchi, H., Kim, R., Okuno, H., Nishizumi, H., . . . Sakano, H. (2017). Nrp2 is sufficient to instruct circuit formation of mitral-cells to mediate odour-induced attractive social responses. *Nature Communications, 8*. doi:ARTN 1597710.1038/ncomms15977

Inoue, T., Hojo, M., Bessho, Y., Tano, Y., Lee, J. E., & Kageyama, R. (2002). Math3 and NeuroD regulate amacrine cell fate specification in the retina. *Development, 129*(4), 831-842.

Inukai, S., Kock, K. H., & Bulyk, M. L. (2017). Transcription factor-DNA binding: beyond binding site motifs. *Curr Opin Genet Dev, 43*, 110-119. doi:10.1016/j.gde.2017.02.007

Isshiki, T., Pearson, B., Holbrook, S., & Doe, C. Q. (2001). Drosophila neuroblasts sequentially express transcription factors which specify the temporal identity of their neuronal progeny. *Cell, 106*(4), 511-521.

Jackman, W. R., & Stock, D. W. (2006). Transgenic analysis of Dlx regulation in fish tooth development reveals evolutionary retention of enhancer function despite organ loss. *Proc Natl Acad Sci U S A, 103*(51), 19390-19395. doi:10.1073/pnas.0609575103

Jadhav, A. P., Cho, S. H., & Cepko, C. L. (2006). Notch activity permits retinal cells to progress through multiple progenitor states and acquire a stem cell property. *Proceedings of the National Academy of Sciences of the United States of America, 103*(50), 18998-19003. doi:10.1073/pnas.0608155103

Juan, A. H., Kumar, R. M., Marx, J. G., Young, R. A., & Sartorelli, V. (2009). Mir-214-dependent regulation of the polycomb protein Ezh2 in skeletal muscle and embryonic stem cells. *Mol Cell, 36*(1), 61-74. doi:10.1016/j.molcel.2009.08.008

Jusuf, P. R., Albadri, S., Paolini, A., Currie, P. D., Argenton, F., Higashijima, S., . . . Poggi, L. (2012). Biasing amacrine subtypes in the Atoh7 lineage through expression of Barhl2. *J Neurosci, 32*(40), 13929-13944. doi:10.1523/JNEUROSCI.2073-12.2012

Kautzmann, M. A., Kim, D. S., Felder-Schmittbuhl, M. P., & Swaroop, A. (2011). Combinatorial regulation of photoreceptor differentiation factor, neural retina leucine zipper gene NRL, revealed by in vivo promoter analysis. *J Biol Chem, 286*(32), 28247-28255. doi:10.1074/jbc.M111.257246

Kawasaki, T., Kitsukawa, T., Bekku, Y., Matsuda, Y., Sanbo, M., Yagi, T., & Fujisawa, H. (1999). A requirement for neuropilin-1 in embryonic vessel formation. *Development, 126*(21), 4895-4902.

Kim, J., Oh, W. J., Gaiano, N., Yoshida, Y., & Gu, C. (2011). Semaphorin 3E-Plexin-D1 signaling regulates VEGF function in developmental angiogenesis via a feedback mechanism. *Genes Dev, 25*(13), 1399-1411. doi:10.1101/gad.2042011

Kitsukawa, T., Shimono, A., Kawakami, A., Kondoh, H., & Fujisawa, H. (1995). Overexpression of a membrane protein, neuropilin, in chimeric mice causes anomalies in the cardiovascular system, nervous system and limbs. *Development, 121*(12), 4309-4318.

Kiyama, T., Mao, C. A., Cho, J. H., Fu, X. Y., Pan, P., Mu, X. Q., & Klein, W. H. (2011). Overlapping spatiotemporal patterns of regulatory gene expression are required for neuronal progenitors to specify retinal ganglion cell fate. *Vision Research, 51*(2), 251-259. doi:10.1016/j.visres.2010.10.016

Klagsbrun, M., Takashima, S., & Mamluk, R. (2002). The role of neuropilin in vascular and tumor biology. *Adv Exp Med Biol, 515*, 33-48.
Koike, C., Nishida, A., Ueno, S., Saito, H., Sanuki, R., Sato, S., . . . Furukawa, T. (2007). Functional roles of Otx2 transcription factor in postnatal mouse retinal development. *Mol Cell Biol, 27*(23), 8318-8329. doi:10.1128/MCB.01209-07
Kramer, M. F. (2011). Stem-loop RT-qPCR for miRNAs. *Curr Protoc Mol Biol, Chapter 15*, Unit 15 10. doi:10.1002/0471142727.mb1510s95
Kraus, P., & Lufkin, T. (2006). Dlx homeobox gene control of mammalian limb and craniofacial development. *Am J Med Genet A, 140*(13), 1366-1374. doi:10.1002/ajmg.a.31252
Kwan, K. M., Fujimoto, E., Grabher, C., Mangum, B. D., Hardy, M. E., Campbell, D. S., . . . Chien, C. B. (2007). The Tol2kit: a multisite gateway-based construction kit for Tol2 transposon transgenesis constructs. *Dev Dyn, 236*(11), 3088-3099. doi:10.1002/dvdy.21343
Lagutin, O. V., Zhu, C. C., Kobayashi, D., Topczewski, J., Shimamura, K., Puelles, L., . . . Oliver, G. (2003). Six3 repression of Wnt signaling in the anterior neuroectoderm is essential for vertebrate forebrain development. *Genes Dev, 17*(3), 368-379. doi:10.1101/gad.1059403
Lapan, S. W., & Reddien, P. W. (2011). dlx and sp6-9 Control optic cup regeneration in a prototypic eye. *PLoS Genet, 7*(8), e1002226. doi:10.1371/journal.pgen.1002226
Lauder, G. V. (1997). Early vertebrates - Janvier,P. *Science, 276*(5309), 46-46.
Levi, G., & Gitton, Y. (2014). Dlx genes and the maintenance of bone homeostasis and skeletal integrity. *Cell Death Differ, 21*(9), 1345-1346. doi:10.1038/cdd.2014.94
Levi, G., Puche, A. C., Mantero, S., Barbieri, O., Trombino, S., Paleari, L., . . . Merlo, G. R. (2003). The Dlx5 homeodomain gene is essential for olfactory development and connectivity in the mouse. *Mol Cell Neurosci, 22*(4), 530-543.
Levsky, J. M., & Singer, R. H. (2003). Fluorescence in situ hybridization: past, present and future. *J Cell Sci, 116*(Pt 14), 2833-2838. doi:10.1242/jcs.00633
Li, S., Haigh, K., Haigh, J. J., & Vasudevan, A. (2013). Endothelial VEGF sculpts cortical cytoarchitecture. *J Neurosci, 33*(37), 14809-14815. doi:10.1523/JNEUROSCI.1368-13.2013
Lindsell, C. E., Boulter, J., diSibio, G., Gossler, A., & Weinmaster, G. (1996). Expression patterns of Jagged, Delta1, Notch1, Notch2, and Notch3 genes identify ligand-receptor pairs that may function in neural development. *Mol Cell Neurosci, 8*(1), 14-27. doi:10.1006/mcne.1996.0040
Ling, T. L., & Stone, J. (1988). The development of astrocytes in the cat retina: evidence of migration from the optic nerve. *Brain Res Dev Brain Res, 44*(1), 73-85.
Liu, J. K., Ghattas, I., Liu, S. Y., Chen, S., & Rubenstein, J. L. R. (1997). Dlx genes encode DNA-binding proteins that are expressed in an overlapping and sequential pattern during basal ganglia differentiation. *Developmental Dynamics, 210*(4), 498-512. doi:Doi 10.1002/(Sici)1097-0177(199712)210:4<498::Aid-Aja12>3.0.Co;2-3
Liu, X. S., Chopp, M., Zhang, R. L., Tao, T., Wang, X. L., Kassis, H., . . . Zhang, Z. G. (2011). MicroRNA profiling in subventricular zone after stroke: MiR-124a regulates proliferation of neural progenitor cells through Notch signaling pathway. *PLoS One, 6*(8), e23461. doi:10.1371/journal.pone.0023461
Livesey, F. J., & Cepko, C. L. (2001). Vertebrate neural cell-fate determination: lessons from the retina. *Nat Rev Neurosci, 2*(2), 109-118. doi:10.1038/35053522

Lok, J., Gupta, P., Guo, S., Kim, W. J., Whalen, M. J., van Leyen, K., & Lo, E. H. (2007). Cell-cell signaling in the neurovascular unit. *Neurochem Res, 32*(12), 2032-2045. doi:10.1007/s11064-007-9342-9

Loosli, F., Staub, W., Finger-Baier, K. C., Ober, E. A., Verkade, H., Wittbrodt, J., & Baier, H. (2003). Loss of eyes in zebrafish caused by mutation of chokh/rx3. *EMBO Rep, 4*(9), 894-899. doi:10.1038/sj.embor.embor919

MacDonald, R. B., Debiais-Thibaud, M., Talbot, J. C., & Ekker, M. (2010). The Relationship Between dlx and gad1 Expression Indicates Highly Conserved Genetic Pathways in the Zebrafish Forebrain. *Developmental Dynamics, 239*(8), 2298-2306. doi:10.1002/dvdy.22365

MacDonald, R. B., Pollack, J. N., Debiais-Thibaud, M., Heude, E., Talbot, J. C., & Ekker, M. (2013). The ascl1a and dlx genes have a regulatory role in the development of GABAergic interneurons in the zebrafish diencephalon. *Dev Biol, 381*(1), 276-285. doi:10.1016/j.ydbio.2013.05.025

Mackenzie, F., & Ruhrberg, C. (2012). Diverse roles for VEGF-A in the nervous system. *Development, 139*(8), 1371-1380. doi:10.1242/dev.072348

Mannu, G. S. (2014). Retinal phototransduction. *Neurosciences (Riyadh), 19*(4), 275-280.

Mao, C. A., Cho, J. H., Wang, J., Gao, Z. G., Pan, P., Tsai, W. W., . . . Klein, W. H. (2013). Reprogramming amacrine and photoreceptor progenitors into retinal ganglion cells by replacing Neurod1 with Atoh7. *Development, 140*(3), 541-551. doi:10.1242/dev.085886

Martinez-Morales, J. R., Del Bene, F., Nica, G., Hammerschmidt, M., Bovolenta, P., & Wittbrodt, J. (2005). Differentiation of the vertebrate retina is coordinated by an FGF signaling center. *Developmental Cell, 8*(4), 565-574. doi:DOI 10.1016/j.devcel.2005.01.022

Martinez-Morales, J. R., Dolez, V., Rodrigo, I., Zaccarini, R., Leconte, L., Bovolenta, P., & Saule, S. (2003). OTX2 activates the molecular network underlying retina pigment epithelium differentiation. *J Biol Chem, 278*(24), 21721-21731. doi:10.1074/jbc.M301708200

Masland, R. H. (2012a). The neuronal organization of the retina. *Neuron, 76*(2), 266-280. doi:10.1016/j.neuron.2012.10.002

Masland, R. H. (2012b). The Retina: An Approachable Part of the Brain. *American Journal of Human Biology, 24*(5), 719-719. doi:10.1002/ajhb.22305

Matsushima, D., Heavner, W., & Pevny, L. H. (2011). Combinatorial regulation of optic cup progenitor cell fate by SOX2 and PAX6. *Development, 138*(3), 443-454. doi:10.1242/dev.055178

McDougall, C., Korchagina, N., Tobin, J. L., & Ferrier, D. E. (2011). Annelid Distal-less/Dlx duplications reveal varied post-duplication fates. *BMC Evol Biol, 11*, 241. doi:10.1186/1471-2148-11-241

McGuinness, T., Porteus, M. H., Smiga, S., Bulfone, A., Kingsley, C., Qiu, M., . . . Rubenstein, J. L. (1996). Sequence, organization, and transcription of the Dlx-1 and Dlx-2 locus. *Genomics, 35*(3), 473-485. doi:10.1006/geno.1996.0387

Messina-Baas, O., & Cuevas-Covarrubias, S. A. (2017). Inherited Congenital Cataract: A Guide to Suspect the Genetic Etiology in the Cataract Genesis. *Mol Syndromol, 8*(2), 58-78. doi:10.1159/000455752

Miyama, K., Yamada, G., Yamamoto, T. S., Takagi, C., Miyado, K., Sakai, M., . . . Shibuya, H. (1999). A BMP-inducible gene, dlx5, regulates osteoblast differentiation and mesoderm induction. *Dev Biol, 208*(1), 123-133. doi:10.1006/dbio.1998.9197

Mizeracka, K., DeMaso, C. R., & Cepko, C. L. (2013). Notch1 is required in newly postmitotic cells to inhibit the rod photoreceptor fate. *Development, 140*(15), 3188-3197. doi:10.1242/dev.090696

Morasso, M. I., Grinberg, A., Robinson, G., Sargent, T. D., & Mahon, K. A. (1999). Placental failure in mice lacking the homeobox gene Dlx3. *Proc Natl Acad Sci U S A, 96*(1), 162-167.

Moshiri, A., Gonzalez, E., Tagawa, K., Maeda, H., Wang, M., Frishman, L. J., & Wang, S. W. (2008). Near complete loss of retinal ganglion cells in the math5/brn3b double knockout elicits severe reductions of other cell types during retinal development. *Dev Biol, 316*(2), 214-227. doi:10.1016/j.ydbio.2008.01.015

Muller, B., & Peichl, L. (1993). Horizontal cells in the cone-dominated tree shrew retina: morphology, photoreceptor contacts, and topographical distribution. *J Neurosci, 13*(8), 3628-3646.

Muranishi, Y., Terada, K., Inoue, T., Katoh, K., Tsujii, T., Sanuki, R., . . . Furukawa, T. (2011). An essential role for RAX homeoprotein and NOTCH-HES signaling in Otx2 expression in embryonic retinal photoreceptor cell fate determination. *J Neurosci, 31*(46), 16792-16807. doi:10.1523/JNEUROSCI.3109-11.2011

Neidert, A. H., Virupannavar, V., Hooker, G. W., & Langeland, J. A. (2001). Lamprey Dlx genes and early vertebrate evolution. *Proc Natl Acad Sci U S A, 98*(4), 1665-1670. doi:10.1073/pnas.98.4.1665

Newberry, E. P., Latifi, T., & Towler, D. A. (1998). Reciprocal regulation of osteocalcin transcription by the homeodomain proteins Msx2 and Dlx5. *Biochemistry, 37*(46), 16360-16368. doi:10.1021/bi981878u

Newth, D. R., & Ross, D. M. (1955). On the Reaction to Light of Myxine-Glutinosa L. *Journal of Experimental Biology, 32*(1), 4-21.

Nguyen, M., & Arnheiter, H. (2000). Signaling and transcriptional regulation in early mammalian eye development: a link between FGF and MITF. *Development, 127*(16), 3581-3591.

Ogata, K., Sato, K., & Tahirov, T. H. (2003). Eukaryotic transcriptional regulatory complexes: cooperativity from near and afar. *Curr Opin Struct Biol, 13*(1), 40-48.

Ogunshola, O. O., Stewart, W. B., Mihalcik, V., Solli, T., Madri, J. A., & Ment, L. R. (2000). Neuronal VEGF expression correlates with angiogenesis in postnatal developing rat brain. *Brain Res Dev Brain Res, 119*(1), 139-153.

Okabe, K., Kobayashi, S., Yamada, T., Kurihara, T., Tai-Nagara, I., Miyamoto, T., . . . Kubota, Y. (2014). Neurons limit angiogenesis by titrating VEGF in retina. *Cell, 159*(3), 584-596. doi:10.1016/j.cell.2014.09.025

Omori, Y., Katoh, K., Sato, S., Muranishi, Y., Chaya, T., Onishi, A., . . . Furukawa, T. (2011). Analysis of transcriptional regulatory pathways of photoreceptor genes by expression profiling of the Otx2-deficient retina. *PLoS One, 6*(5), e19685. doi:10.1371/journal.pone.0019685

Otaegi, G., Pollock, A., Hong, J., & Sun, T. (2011). MicroRNA miR-9 modifies motor neuron columns by a tuning regulation of FoxP1 levels in developing spinal cords. *J Neurosci, 31*(3), 809-818. doi:10.1523/JNEUROSCI.4330-10.2011

Pak, W., Hindges, R., Lim, Y. S., Pfaff, S. L., & O'Leary, D. D. (2004). Magnitude of binocular vision controlled by islet-2 repression of a genetic program that specifies laterality of retinal axon pathfinding. *Cell, 119*(4), 567-578. doi:10.1016/j.cell.2004.10.026

Pan, L., Deng, M., Xie, X., & Gan, L. (2008). ISL1 and BRN3B co-regulate the differentiation of murine retinal ganglion cells. *Development, 135*(11), 1981-1990. doi:10.1242/dev.010751

Panganiban, G., & Rubenstein, J. L. (2002). Developmental functions of the Distal-less/Dlx homeobox genes. *Development, 129*(19), 4371-4386.

Pannese, M., Polo, C., Andreazzoli, M., Vignali, R., Kablar, B., Barsacchi, G., & Boncinelli, E. (1995). The Xenopus Homolog of Otx2 Is a Maternal Homeobox Gene That Demarcates and Specifies Anterior Body Regions. *Development, 121*(3), 707-720.

Park, G. T., Denning, M. F., & Morasso, M. I. (2001). Phosphorylation of murine homeodomain protein Dlx3 by protein kinase C. *FEBS Lett, 496*(1), 60-65.

Park, H. Y., Kim, J. H., & Park, C. K. (2014). Neuronal cell death in the inner retina and the influence of vascular endothelial growth factor inhibition in a diabetic rat model. *American Journal of Pathology, 184*(6), 1752-1762. doi:10.1016/j.ajpath.2014.02.016

Pasquier, J., Braasch, I., Batzel, P., Cabau, C., Montfort, J., Nguyen, T., . . . Bobe, J. (2017). Evolution of gene expression after whole-genome duplication: New insights from the spotted gar genome. *J Exp Zool B Mol Dev Evol, 328*(7), 709-721. doi:10.1002/jez.b.22770

Pavlopoulos, A., & Akam, M. (2007). Hox go omics: insights from Drosophila into Hox gene targets. *Genome Biology, 8*(3). doi:ARTN 20810.1186/gb-2007-8-3-208

Pellet-Many, C., Frankel, P., Jia, H., & Zachary, I. (2008). Neuropilins: structure, function and role in disease. *Biochem J, 411*(2), 211-226. doi:10.1042/BJ20071639

Perlmutter, L. S., & Chui, H. C. (1990). Microangiopathy, the Vascular Basement-Membrane and Alzheimers-Disease - a Review. *Brain Research Bulletin, 24*(5), 677-686. doi:Doi 10.1016/0361-9230(90)90007-M

Pinter, R., & Hindges, R. (2010). Perturbations of MicroRNA Function in Mouse Dicer Mutants Produce Retinal Defects and Lead to Aberrant Axon Pathfinding at the Optic Chiasm. *PLoS One, 5*(3). doi:ARTN e1002110.1371/journal.pone.0010021

Plavicki, J. S., Squirrell, J. M., Eliceiri, K. W., & Boekhoff-Falk, G. (2016). Expression of the Drosophila homeobox gene, Distal-less, supports an ancestral role in neural development. *Dev Dyn, 245*(1), 87-95. doi:10.1002/dvdy.24359

Poitras, L., Ghanem, N., Hatch, G., & Ekker, M. (2007). The proneural determinant MASH1 regulates forebrain Dlx1/2 expression through the I12b intergenic enhancer. *Development, 134*(9), 1755-1765. doi:10.1242/dev.02845

Powell, C., Grant, A. R., Cornblath, E., & Goldman, D. (2013). Analysis of DNA methylation reveals a partial reprogramming of the Muller glia genome during retina regeneration. *Proc Natl Acad Sci U S A, 110*(49), 19814-19819. doi:10.1073/pnas.1312009110

Qadir, A. S., Um, S., Lee, H., Baek, K., Seo, B. M., Lee, G., . . . Baek, J. H. (2015). miR-124 negatively regulates osteogenic differentiation and in vivo bone formation of mesenchymal stem cells. *J Cell Biochem, 116*(5), 730-742. doi:10.1002/jcb.25026

Qadir, A. S., Woo, K. M., Ryoo, H. M., Yi, T., Song, S. U., & Baek, J. H. (2014). MiR-124 inhibits myogenic differentiation of mesenchymal stem cells via targeting Dlx5. *J Cell Biochem, 115*(9), 1572-1581. doi:10.1002/jcb.24821

Qiu, F., Jiang, H., & Xiang, M. (2008). A comprehensive negative regulatory program controlled by Brn3b to ensure ganglion cell specification from multipotential retinal precursors. *J Neurosci, 28*(13), 3392-3403. doi:10.1523/JNEUROSCI.0043-08.2008

Qiu, M., Bulfone, A., Ghattas, I., Meneses, J. J., Christensen, L., Sharpe, P. T., . . . Rubenstein, J. L. (1997). Role of the Dlx homeobox genes in proximodistal patterning of the branchial arches: mutations of Dlx-1, Dlx-2, and Dlx-1 and -2 alter morphogenesis of proximal skeletal and soft tissue structures derived from the first and second arches. *Dev Biol, 185*(2), 165-184. doi:10.1006/dbio.1997.8556

Quint, E., Zerucha, T., & Ekker, M. (2000). Differential expression of orthologous Dlx genes in zebrafish and mice: implications for the evolution of the Dlx homeobox gene family. *J Exp Zool, 288*(3), 235-241.

Raab, S., Beck, H., Gaumann, A., Yuce, A., Gerber, H. P., Plate, K., . . . Breier, G. (2004). Impaired brain angiogenesis and neuronal apoptosis induced by conditional homozygous inactivation of vascular endothelial growth factor. *Thromb Haemost, 91*(3), 595-605. doi:10.1160/TH03-09-0582

Raimondi, C., Brash, J. T., Fantin, A., & Ruhrberg, C. (2016). NRP1 function and targeting in neurovascular development and eye disease. *Prog Retin Eye Res, 52*, 64-83. doi:10.1016/j.preteyeres.2016.02.003

Rauskolb, C. (2001). The establishment of segmentation in the Drosophila leg. *Development, 128*(22), 4511-4521.

Raymond, P. A., Colvin, S. M., Jabeen, Z., Nagashima, M., Barthel, L. K., Hadidjojo, J., . . . Lubensky, D. K. (2014). Patterning the cone mosaic array in zebrafish retina requires specification of ultraviolet-sensitive cones. *PLoS One, 9*(1), e85325. doi:10.1371/journal.pone.0085325

Riesenberg, A. N., Le, T. T., Willardsen, M. I., Blackburn, D. C., Vetter, M. L., & Brown, N. L. (2009). Pax6 regulation of Math5 during mouse retinal neurogenesis. *Genesis, 47*(3), 175-187. doi:10.1002/dvg.20479

Robledo, R. F., Rajan, L., Li, X., & Lufkin, T. (2002). The Dlx5 and Dlx6 homeobox genes are essential for craniofacial, axial, and appendicular skeletal development. *Genes Dev, 16*(9), 1089-1101. doi:10.1101/gad.988402

Roy, S., Bag, A. K., Singh, R. K., Talmadge, J. E., Batra, S. K., & Datta, K. (2017). Multifaceted Role of Neuropilins in the Immune System: Potential Targets for Immunotherapy. *Front Immunol, 8*, 1228. doi:10.3389/fimmu.2017.01228

Sakai, K., & Miyazaki, J. (1997). A transgenic mouse line that retains Cre recombinase activity in mature oocytes irrespective of the cre transgene transmission. *Biochem Biophys Res Commun, 237*(2), 318-324.

Samuel, A., Housset, M., Fant, B., & Lamonerie, T. (2014). Otx2 ChIP-seq reveals unique and redundant functions in the mature mouse retina. *PLoS One, 9*(2), e89110. doi:10.1371/journal.pone.0089110

Sanuki, R., Onishi, A., Koike, C., Muramatsu, R., Watanabe, S., Muranishi, Y., . . . Furukawa, T. (2011). miR-124a is required for hippocampal axogenesis and retinal cone survival through Lhx2 suppression. *Nature Neuroscience, 14*(9), 1125-U1177. doi:10.1038/nn.2897

Sapieha, P., Sirinyan, M., Hamel, D., Zaniolo, K., Joyal, J. S., Cho, J. H., . . . Chemtob, S. (2008). The succinate receptor GPR91 in neurons has a major role in retinal angiogenesis. *Nat Med, 14*(10), 1067-1076. doi:10.1038/nm.1873

Sato, S., Inoue, T., Terada, K., Matsuo, I., Aizawa, S., Tano, Y., . . . Furukawa, T. (2007). Dkk3-Cre BAC transgenic mouse line: a tool for highly efficient gene deletion in retinal progenitor cells. *Genesis, 45*(8), 502-507. doi:10.1002/dvg.20318

Scheer, N., Groth, A., Hans, S., & Campos-Ortega, J. A. (2001). An instructive function for Notch in promoting gliogenesis in the zebrafish retina. *Development, 128*(7), 1099-1107.

Schwarz, Q., Vieira, J. M., Howard, B., Eickholt, B. J., & Ruhrberg, C. (2008). Neuropilin 1 and 2 control cranial gangliogenesis and axon guidance through neural crest cells. *Development, 135*(9), 1605-1613. doi:10.1242/dev.015412

Selvam, S., Kumar, T., & Fruttiger, M. (2018). Retinal vasculature development in health and disease. *Prog Retin Eye Res, 63*, 1-19. doi:10.1016/j.preteyeres.2017.11.001

Sernagor, E., Eglen, S. J., & Wong, R. O. (2001). Development of retinal ganglion cell structure and function. *Prog Retin Eye Res, 20*(2), 139-174.

Shea, C. M., Edgar, C. M., Einhorn, T. A., & Gerstenfeld, L. C. (2003). BMP treatment of C3H10T1/2 mesenchymal stem cells induces both chondrogenesis and osteogenesis. *Journal of Cellular Biochemistry, 90*(6), 1112-1127. doi:10.1002/jcb.10734

Shekhar, K., Lapan, S. W., Whitney, I. E., Tran, N. M., Macosko, E. Z., Kowalczyk, M., . . . Sanes, J. R. (2016). Comprehensive Classification of Retinal Bipolar Neurons by Single-Cell Transcriptomics. *Cell, 166*(5), 1308-1323 e1330. doi:10.1016/j.cell.2016.07.054

Simeone, A., Acampora, D., Mallamaci, A., Stornaiuolo, A., D'Apice, M. R., Nigro, V., & Boncinelli, E. (1993). A vertebrate gene related to orthodenticle contains a homeodomain of the bicoid class and demarcates anterior neuroectoderm in the gastrulating mouse embryo. *EMBO J, 12*(7), 2735-2747.

Solek, C. M., Feng, S., Perin, S., Weinschutz Mendes, H., & Ekker, M. (2017). Lineage tracing of dlx1a/2a and dlx5a/6a expressing cells in the developing zebrafish brain. *Dev Biol, 427*(1), 131-147. doi:10.1016/j.ydbio.2017.04.019

Stock, D. W., Ellies, D. L., Zhao, Z. Y., Ekker, M., Ruddle, F. H., & Weiss, K. M. (1996). The evolution of the vertebrate Dlx gene family. *Proceedings of the National Academy of Sciences of the United States of America, 93*(20), 10858-10863. doi:DOI 10.1073/pnas.93.20.10858

Suga, H., Koyanagi, M., Hoshiyama, D., Ono, K., Iwabe, N., Kuma, K., & Miyata, T. (1999). Extensive gene duplication in the early evolution of animals before the parazoan-eumetazoan split demonstrated by G proteins and protein tyrosine kinases from sponge and hydra. *Journal of Molecular Evolution, 48*(6), 646-653. doi:Doi 10.1007/Pl00006508

Sun, Y., Luo, Z. M., Guo, X. M., Su, D. F., & Liu, X. (2015). An updated role of microRNA-124 in central nervous system disorders: a review. *Front Cell Neurosci, 9*, 193. doi:10.3389/fncel.2015.00193

Swaroop, A., Kim, D., & Forrest, D. (2010). Transcriptional regulation of photoreceptor development and homeostasis in the mammalian retina. *Nat Rev Neurosci, 11*(8), 563-576. doi:10.1038/nrn2880

Swift, J., & Coruzzi, G. M. (2017). A matter of time - How transient transcription factor interactions create dynamic gene regulatory networks. *Biochimica Et Biophysica Acta-Gene Regulatory Mechanisms, 1860*(1), 75-83. doi:10.1016/j.bbagrm.2016.08.007

Tahayato, A., Sonneville, R., Pichaud, F., Wernet, M. F., Papatsenko, D., Beaufils, P., . . . Desplan, C. (2003). Otd/Crx, a dual regulator for the specification of ommatidia subtypes in the Drosophila retina. *Dev Cell, 5*(3), 391-402.

Takashima, S., Kitakaze, M., Asakura, M., Asanuma, H., Sanada, S., Tashiro, F., . . . Hori, M. (2002). Targeting of both mouse neuropilin-1 and neuropilin-2 genes severely impairs developmental yolk sac and embryonic angiogenesis. *Proceedings of the National Academy of Sciences of the United States of America, 99*(6), 3657-3662. doi:10.1073/pnas.022017899

Talbot, J. C., Johnson, S. L., & Kimmel, C. B. (2010). hand2 and Dlx genes specify dorsal, intermediate and ventral domains within zebrafish pharyngeal arches. *Development, 137*(15), 2507-2517. doi:10.1242/dev.049700

Tata, M., Wall, I., Joyce, A., Vieira, J. M., Kessaris, N., & Ruhrberg, C. (2016). Regulation of embryonic neurogenesis by germinal zone vasculature. *Proc Natl Acad Sci U S A, 113*(47), 13414-13419. doi:10.1073/pnas.1613113113

Taverna, E., & Huttner, W. B. (2010). Neural Progenitor Nuclei IN Motion. *Neuron, 67*(6), 906-914. doi:10.1016/j.neuron.2010.08.027

Taylor, I. A., McIntosh, P. B., Pala, P., Treiber, M. K., Howell, S., Lane, A. N., & Smerdon, S. J. (2000). Characterization of the DNA-binding domains from the yeast cell-cycle transcription factors Mbp1 and Swi4. *Biochemistry, 39*(14), 3943-3954.

Todeschini, A. L., Georges, A., & Veitia, R. A. (2014). Transcription factors: specific DNA binding and specific gene regulation. *Trends Genet, 30*(6), 211-219. doi:10.1016/j.tig.2014.04.002

Tomita, K., Ishibashi, M., Nakahara, K., Ang, S. L., Nakanishi, S., Guillemot, F., & Kageyama, R. (1996). Mammalian hairy and Enhancer of split homolog 1 regulates differentiation of retinal neurons and is essential for eye morphogenesis. *Neuron, 16*(4), 723-734.

Tomita, K., Moriyoshi, K., Nakanishi, S., Guillemot, F., & Kageyama, R. (2000). Mammalian achaete-scute and atonal homologs regulate neuronal versus glial fate determination in the central nervous system. *EMBO J, 19*(20), 5460-5472. doi:10.1093/emboj/19.20.5460

Tsang, J., Zhu, J., & van Oudenaarden, A. (2007). MicroRNA-mediated feedback and feedforward loops are recurrent network motifs in mammals. *Mol Cell, 26*(5), 753-767. doi:10.1016/j.molcel.2007.05.018

Tsukamoto, Y., & Omi, N. (2017). Classification of Mouse Retinal Bipolar Cells: Type-Specific Connectivity with Special Reference to Rod-Driven AII Amacrine Pathways. *Front Neuroanat, 11*, 92. doi:10.3389/fnana.2017.00092

Turner, D. L., & Cepko, C. L. (1987). A common progenitor for neurons and glia persists in rat retina late in development. *Nature, 328*(6126), 131-136. doi:10.1038/328131a0

Usui, Y., Westenskow, P. D., Kurihara, T., Aguilar, E., Sakimoto, S., Paris, L. P., . . . Friedlander, M. (2015). Neurovascular crosstalk between retinal interneurons and intraretinal capillaries is required for murine visual function. *Investigative Ophthalmology & Visual Science, 56*(7).

Vachon, G., Cohen, B., Pfeifle, C., McGuffin, M. E., Botas, J., & Cohen, S. M. (1992). Homeotic genes of the Bithorax complex repress limb development in the abdomen of the Drosophila embryo through the target gene Distal-less. *Cell, 71*(3), 437-450.

Verlinden, L., Kriebitzsch, C., Beullens, I., Tan, B. K., Carmeliet, G., & Verstuyf, A. (2013). Nrp2 deficiency leads to trabecular bone loss and is accompanied by enhanced osteoclast and reduced osteoblast numbers. *Bone, 55*(2), 465-475. doi:10.1016/j.bone.2013.03.023

Wall, D. S., Mears, A. J., McNeill, B., Mazerolle, C., Thurig, S., Wang, Y. P., . . . Wallace, V. A. (2009). Progenitor cell proliferation in the retina is dependent on Notch-independent

Sonic hedgehog/Hes1 activity. *Journal of Cell Biology, 184*(1), 101-112. doi:10.1083/jcb.200805155
Wang, S., Sengel, C., Emerson, M. M., & Cepko, C. L. (2014). A gene regulatory network controls the binary fate decision of rod and bipolar cells in the vertebrate retina. *Dev Cell, 30*(5), 513-527. doi:10.1016/j.devcel.2014.07.018
Wang, X., Iannaccone, A., & Jablonski, M. M. (2004). Contribution of Muller cells toward the regulation of photoreceptor outer segment assembly. *Neuron Glia Biol, 1*(3), 291-296. doi:10.1017/S1740925X05000049
Wang, X., Xu, S., Rivolta, C., Li, L. Y., Peng, G. H., Swain, P. K., . . . Chen, S. (2002). Barrier to autointegration factor interacts with the cone-rod homeobox and represses its transactivation function. *J Biol Chem, 277*(45), 43288-43300. doi:10.1074/jbc.M207952200
Wawersik, S., Purcell, P., Rauchman, M., Dudley, A. T., Robertson, E. J., & Maas, R. (1999). BMP7 acts in murine lens placode development. *Dev Biol, 207*(1), 176-188. doi:10.1006/dbio.1998.9153
Westerfield, M. (1993). *The zebrafish book : a guide for the laboratory use of zebrafish (Brachydanio rerio)*. Eugene, OR: M. Westerfield.
Wigle, J. T., Chowdhury, K., Gruss, P., & Oliver, G. (1999). Prox1 function is crucial for mouse lens-fibre elongation. *Nature Genetics, 21*(3), 318-322.
Won, K. J., Torihashi, S., Mitsui-Saito, M., Hori, M., Sato, K., Suzuki, T., . . . Karaki, H. (2002). Increased smooth muscle contractility of intestine in the genetic null of the endothelin ETB receptor: a rat model for long segment Hirschsprung's disease. *Gut, 50*(3), 355-360.
Xi, Y., Chen, W. J., Deng, J. X., Cui, Z. J., Liu, H. L., Yan, M. C., . . . Wu, P. (2015). Vasculature-guided neural migration in mouse cerebellum. *Italian Journal of Zoology, 82*(1), 15-24. doi:10.1080/11250003.2014.977359
Xiao, S., McCarthy, J. G., Aster, J. C., & Fletcher, J. A. (2000). ZNF198-FGFR1 transforming activity depends on a novel proline-rich ZNF198 oligomerization domain. *Blood, 96*(2), 699-704.
Xu, S. C., Harris, M. A., Rubenstein, J. L. R., Mundy, G. R., & Harris, S. E. (2001). Bone morphogenetic protein-2 (BMP-2) signaling to the Col2 alpha 1 gene in chondroblasts requires the homeobox gene Dlx-2. *DNA and Cell Biology, 20*(6), 359-365. doi:Doi 10.1089/10445490152122479
Yang, D., Li, T., Wang, Y., Tang, Y., Cui, H., Tang, Y., . . . Le, W. (2012). miR-132 regulates the differentiation of dopamine neurons by directly targeting Nurr1 expression. *J Cell Sci, 125*(Pt 7), 1673-1682. doi:10.1242/jcs.086421
Yesudhas, D., Batool, M., Anwar, M. A., Panneerselvam, S., & Choi, S. (2017). Proteins Recognizing DNA: Structural Uniqueness and Versatility of DNA-Binding Domains in Stem Cell Transcription Factors. *Genes (Basel), 8*(8). doi:10.3390/genes8080192
Yin, J., Morrissey, M. E., Shine, L., Kennedy, C., Higgins, D. G., & Kennedy, B. N. (2014). Genes and signaling networks regulated during zebrafish optic vesicle morphogenesis. *Bmc Genomics, 15*, 825. doi:10.1186/1471-2164-15-825
Yu, C. P., Lin, J. J., & Li, W. H. (2016). Positional distribution of transcription factor binding sites in Arabidopsis thaliana. *Sci Rep, 6*, 25164. doi:10.1038/srep25164
Yuh, C. H., Bolouri, H., & Davidson, E. H. (1998). Genomic cis-regulatory logic: experimental and computational analysis of a sea urchin gene. *Science, 279*(5358), 1896-1902.

Yuh, C. H., Bolouri, H., & Davidson, E. H. (2001). Cis-regulatory logic in the endo16 gene: switching from a specification to a differentiation mode of control. *Development, 128*(5), 617-629.

Yun, S., Saijoh, Y., Hirokawa, K. E., Kopinke, D., Murtaugh, L. C., Monuki, E. S., & Levine, E. M. (2009). Lhx2 links the intrinsic and extrinsic factors that control optic cup formation. *Development, 136*(23), 3895-3906. doi:10.1242/dev.041202

Zaret, K. S., & Mango, S. E. (2016). Pioneer transcription factors, chromatin dynamics, and cell fate control. *Curr Opin Genet Dev, 37*, 76-81. doi:10.1016/j.gde.2015.12.003

Zhang, H., Hu, G., Wang, H., Sciavolino, P., Iler, N., Shen, M. M., & Abate-Shen, C. (1997). Heterodimerization of Msx and Dlx homeoproteins results in functional antagonism. *Mol Cell Biol, 17*(5), 2920-2932.

Zhang, Q., Zagozewski, J., Cheng, S., Dixit, R., Zhang, S., de Melo, J., . . . Eisenstat, D. D. (2017). Regulation of Brn3b by DLX1 and DLX2 is required for retinal ganglion cell differentiation in the vertebrate retina. *Development, 144*(9), 1698-1711. doi:10.1242/dev.142042

Zhou, Q. P., Le, T. N., Qiu, X., Spencer, V., de Melo, J., Du, G., . . . Eisenstat, D. D. (2004). Identification of a direct Dlx homeodomain target in the developing mouse forebrain and retina by optimization of chromatin immunoprecipitation. *Nucleic Acids Res, 32*(3), 884-892. doi:10.1093/nar/gkh233

Zuber, M. E., Gestri, G., Viczian, A. S., Barsacchi, G., & Harris, W. A. (2003). Specification of the vertebrate eye by a network of eye field transcription factors. *Development, 130*(21), 5155-5167. doi:10.1242/dev.00723